

The response of human myeloid cells to  
the infection with *Listeria monocytogenes*

Dissertation

zur

Erlangung des Doktorgrades (Dr. rer. nat.)

der

Mathematisch-Naturwissenschaftlichen Fakultät

der

Rheinischen Friedrich-Wilhelms-Universität Bonn

vorgelegt von

Andrea Niño Castro

aus Bogota, Kolumbien

Bonn, Februar 2013

Angefertigt mit Genehmigung der Mathematisch-Naturwissenschaftlichen Fakultät der Rheinischen Friedrich-Wilhelms-Universität Bonn

1. Gutachter: Prof. Dr. Joachim Schultze
2. Gutachter: Prof. Dr. Percy Knolle

Tag der Promotion: 8. Mai 2013

Erscheinungsjahr: 2013

# Acknowledgements

I would like to express my gratitude to Professor Dr. J. Schultze for allowing me to work in his group and providing me with constant support and constructive guidance during the realization of this thesis

I would like to acknowledge Professor P. Knolle for allowing me to work in the S2 facility at the IMMEI institute. Likewise, I also thank Professor J. Oldenburg for providing us with blood samples from healthy individuals.

I wish to express my gratitude to Dr. Alexey Popov, Dr. Susanne Schmidt, Dr. Marc Beyer and Dr. Zeinab Abdullah for their supervision and support during these years.

I thank my colleagues in the group of Genomics and Immunoregulation of LIMES institute for the nice work environment. Especially, I would like to thank Yasser Thabet, Michael Kraut and Wolfgang Krebs for the interesting academic discussions and technical assistance.

Finally, I owe my deepest gratitude to Blanca, Fideligno, Angela and Manuel. Without your support this thesis would have remained a dream.

This work was financially supported by the German Research Foundation [SFB 670, SFB 704, INST 217/575-1, INST 217/576-1, INST 217/577-1] and the NRW Graduate School Chemical Biology

---

# Contents

<b>Acknowledgements</b> .....	<b>2</b>
<b>Abbreviations</b> .....	<b>8</b>
<b>Summary</b> .....	<b>10</b>
<b>1. Introduction</b> .....	<b>11</b>
1.1 The innate immune system and immune recognition .....	11
1.2 Macrophage heterogeneity.....	12
1.2.1 Macrophage polarization .....	13
1.3 General aspects of dendritic cell immunobiology.....	17
1.3.1 Dendritic cells subsets.....	17
1.3.2 Maturation of dendritic cells.....	18
1.4 Regulatory functions of macrophages and dendritic cells .....	19
1.4.1 Anti-inflammatory mediators in the acquisition of regulatory functions in myeloid cells ..	21
1.4.2 Molecular mechanisms of T cell suppression by macrophages and dendritic cells.....	22
1.5 The pathogenesis of <i>L. monocytogenes</i> .....	23
1.5.1. Innate immune responses against <i>L. monocytogenes</i> .....	24
1.5.2 Human chronic listeriosis .....	26
<b>2. Aim of the study</b> .....	<b>27</b>
<b>3. Materials</b> .....	<b>28</b>
3.1 Chemicals and Reagents.....	28
3.2 Cytokines and TLR agonists .....	30
3.2 Antibodies.....	30
3.3 siRNA oligonucleotides .....	32
3.4 cDNA synthesis and RT-PCR primers .....	32
3.5 Enzyme linked immunosorbent assay .....	33
3.6 Plastic ware.....	34
3.7 Equipment .....	34
3.8 Software .....	35
<b>4. Methods</b> .....	<b>37</b>
4.1 Isolation of monocytes .....	37
4.2 Generation of human monocyte derived macrophages .....	37
4.3 Generation of human monocyte derived dendritic cells .....	38
4.4 Polarization of human macrophages.....	38
4.5 Maturation and stimulation of human dendritic cells .....	39

---

4.6 Generation of murine bone marrow derived dendritic cells and macrophages.....	40
4.7 IDO1 silencing and enzymatic activity inhibition.....	40
4.8 Bacteria culture and FITC labeling.....	41
4.9 Infection of human dendritic cells and macrophages with <i>L. monocytogenes</i> .....	42
4.10 Determination of bacterial burden in infected dendritic cells and macrophages .....	43
4.11 Infection of murine bone marrow derived dendritic cells and macrophages with <i>L. monocytogenes</i> .....	43
4.12 Evaluation of the anti-bacterial and cytotoxic effect of tryptophan catabolites.....	43
4.13 Plaque assay .....	44
4.14 Isolation of human CD4 <sup>+</sup> T cells.....	45
4.15 Generation of artificial antigen presenting cells .....	45
4.16 T cell proliferation assay.....	45
4.17 T cell cytokine production assay .....	46
4.18 Flow cytometry.....	46
4.19 RNA isolation .....	47
4.20 Semi-quantitative real time PCR .....	48
4.21 Microarray analysis .....	49
4.22 Bioinformatic Analysis .....	51
4.23 Cell lysis and western blot.....	51
4.24 Enzyme linked immunosorbent assay .....	52
4.25 Kynurenine and nitrite determination .....	52
4.26 Determination of reactive oxygen species production .....	53
<b>5. Results .....</b>	<b>54</b>
5.1 Macrophages infected with <i>L. monocytogenes</i> present immunostimulatory and immunomodulatory features.....	54
5.2 Soluble factors secreted by macrophages infected with <i>L. monocytogenes</i> modulate the phenotype of bystander macrophages and suppress T cell proliferation .....	59
5.3 The transcriptional response of macrophages to <i>L. monocytogenes</i> infection .....	62
5.4 The transcriptional response of macrophages and dendritic cells to <i>L. monocytogenes</i> infection .....	67
5.5 The transcriptional response of macrophages to infection with wild type <i>L. monocytogenes</i> or hly mutant. ....	71
5.6 Comparative analysis of transcriptional responses in macrophages infected with <i>L. monocytogenes</i> and classical models of macrophage polarization .....	76
5.7 Comparative analysis of transcriptional responses in macrophages infected with <i>L. monocytogenes</i> and regulatory macrophages.....	80

---

5.8 Integration of host factor derived signals and its comparison with the transcriptome of <i>L. monocytogenes</i> infected macrophages .....	84
5.9. IDO1 is expressed in human myeloid cells upon <i>L. monocytogenes</i> infection.....	88
5.10 IDO1 competent myeloid cells efficiently control the intracellular growth of <i>L. monocytogenes</i> .....	90
5.11 Loss of IDO1 function leads to unrestrained bacterial growth .....	93
5.12 IDO1 microbicidal activity is mediated by tryptophan catabolites .....	97
5.13 Exposure to kynurenine does not impair <i>L. monocytogenes</i> invasive capabilities .....	101
5.14 IDO1 is not expressed in murine myeloid cells upon <i>L. monocytogenes</i> infection.....	103
<b>6. Discussion .....</b>	<b>105</b>
6.1 The phenotype of macrophages infected with <i>L. monocytogenes</i> and their regulatory properties .....	105
6.2 Genomic profiling of macrophages infected with <i>L. monocytogenes</i> .....	107
6.3 Comparative analysis of the transcriptional responses of macrophages and dendritic cells to <i>L. monocytogenes</i> infection .....	110
6.4 Transcriptional responses of macrophages to phagosome restricted and cytosolic <i>L. monocytogenes</i> .....	112
6.5 Macrophage polarization upon infection with <i>L. monocytogenes</i> .....	114
6.6 IDO1 plays a role as microbicidal mechanism in human myeloid cells.....	117
<b>Bibliography.....</b>	<b>120</b>
<b>Curriculum Vitae .....</b>	<b>133</b>

## Figures

Figure 1. Models of M $\phi$ activation .....	15
Figure 2. The pathogenesis of <i>L.m.</i> ....	24
Figure 3. Flowchart depicting the experimental procedure followed to generate polarized M $\phi$ .....	39
Figure 4. Flowchart depicting the experimental approach followed to silence IDO1 in DC ....	41
Figure 5. M $\phi$ infected with <i>L.m.</i> express proinflammatory cytokines .....	55
Figure 6. M $\phi$ infected with <i>L.m.</i> secrete proinflammatory cytokines .....	55
Figure 7. M $\phi$ infected with <i>L.m.</i> express immunomodulatory mediators .....	56
Figure 8. M $\phi$ infected with <i>L.m.</i> express CD25 and IDO .....	58
Figure 9. Supernatants of <i>L.m.</i> infected M $\phi$ induce the expression of regulatory factors in uninfected M $\phi$ .....	60
Figure 10. Supernatants of <i>L.m.</i> infected M $\phi$ s are able to suppress T cell proliferation .....	61
Figure 11. Supernatants of M $\phi$ infected with <i>L.m.</i> reduce the production of IFN- $\gamma$ in activated CD4 <sup>+</sup> T cells .....	62
Figure 12. GM-CSF and M-CSF derived M $\phi$ regulate a similar transcriptional profile upon <i>L.m.</i> infection .....	64
Figure 13. GO enrichment analysis of differentially express genes in GM-CSF and M-CSF M $\phi$ s upon <i>L.m.</i> infection .....	66
Figure 14. Heatmap of highly regulated genes in in GM-CSF and M-CSF M $\phi$ infected with <i>L.m.</i> .....	66
Figure 15. DC and M $\phi$ express a common transcriptional signature upon <i>L.m.</i> infection .....	68
Figure 16. DC and M $\phi$ also express cell specific programs upon <i>L.m.</i> infection .....	71
Figure 17. <i>L.m.</i> intracellular fate does not condition the transcriptional response of M $\phi$ .....	72
Figure 18. M $\phi$ infected with <i>L.m.</i> and hly share 85% of DE genes .....	73
Figure 19. GO enrichment analysis of DE present exclusively upon infection of M $\phi$ with <i>L.m. wt.</i> .....	74
Figure 20. M $\phi$ infected with wt <i>L.m.</i> and hly express similar amounts of proinflammatory and immunomodulatory factors .....	75
Figure 21. The transcriptional profile of <i>L.m.</i> -M $\phi$ differs from M1 and M2 polarized M $\phi$ .....	76
Figure 22. The observed IFN- $\gamma$ signature in <i>L.m.</i> infected M $\phi$ represents 30% of DE genes .	78
Figure 23. Hallmark genes of M1 and M2 polarization and their expression in <i>L.m.</i> - M $\phi$ .....	79
Figure 24. M1 M $\phi$ stimulate the production of endogenous TNF- $\alpha$ and IFN- $\beta$ .....	80
Figure 25. <i>L.m.</i> -M $\phi$ and Mreg share a transcriptional signature that represents 50% of the transcriptional response observed upon <i>L.m.</i> infection .....	81
Figure 26. The transcriptional responses of M $\phi$ treated with TNF- $\alpha$ , PGE <sub>2</sub> or Pam <sub>3</sub> do not explain in detail the transcriptome of <i>L.m.</i> -M $\phi$ .....	82
Figure 27. The single stimuli provided by TNF- $\alpha$ , PGE <sub>2</sub> and Pam <sub>3</sub> do not reproduce transcriptional signature common between Mreg and <i>L.m.</i> -M $\phi$ .....	83
Figure 28. Addition of IFN- $\beta$ and IFN- $\gamma$ to TNF- $\alpha$ , PGE <sub>2</sub> and Pam <sub>3</sub> does not lead to major changes in the transcriptome of M $\phi$ .....	85
Figure 29. IFN- $\gamma$ and IFN- $\beta$ addition to TNF- $\alpha$ , PGE <sub>2</sub> and Pam <sub>3</sub> resulted in the regulation of 200 new genes in common with <i>L.m.</i> -M $\phi$ .....	87

---

Figure 30. The genes in TPP-I-I and <i>L.m.</i> infected M $\phi$ are related mainly to Type I interferon mediated signaling.....	88
Figure 34. ROS and nitrite production in <i>L.m.</i> infected DC and M $\phi$ .....	92
Figure 35. Knock-down of IDO1 in DC.....	93
Figure 36. IDO1 mediates the control of <i>L.m.</i> infection in DCreg .....	94
Figure 37. IDO1 but not IDO2 is essential for Trp catabolism in human DC.....	95
Figure 38. IDO1 enzymatic activity is important for the control of <i>L.m.</i> infection in IDO competent cells .....	96
Figure 39. Tryptophan starvation does not mediate the anti-bacterial activity of DCreg.....	98
Figure 43. The sensitivity of bacteria against Trp catabolites varies between species .....	101
Figure 44. Kynurenine exposure to <i>L.m.</i> does not affect infective capabilities .....	102
Figure 45. IDO1 expression is not induced in murine myeloid cells upon <i>L.m.</i> infection .....	104



## Abbreviations

1-methyl-tryptophan	1-MT
Actin assembly-inducing protein	ActA
3-hydroxy-anthranilic acid	HA
3-hydroxy-L-kynurenine	3HK
Activation protein-1	AP-1
Anthranilic acid	AA
Antigen presenting cells	APC
Artificial antigen presenting cells	aAPC
Aryl hydrocarbon receptor	AHR
Brain heart infusion	BHI
Carboxyfluorescein diacetate succinimidyl ester	CFSE
Colony forming unit	CFU
Cyclooxygenase 2	COX-2
Dendritic cells	DC
Differential expressed	DE
Fetal calf serum	FCS
Fluorescence activated cell sorting	FACS
Fold of change	FC
Hours post-infection	hpi
IL-1R activated kinase	IRAK
Immature DC	immDC
Indoleamine 2,3-dioxygenase	IDO1
Interferon response factor	IRF
Kynurenine	Kyn
<i>L.m.</i> -M $\phi$	macrophages infected with <i>L. monocytogenes</i>
Lipopolysaccharide	LPS
Listeria innocua	<i>L.i.</i>
Listeria monocytogenes	<i>L.m.</i>
Listeriolysin	LLO
Macrophages	M $\phi$
Magnetic assorted cell sorting	MACS
Mature DC	matDC
Mixed leukocyte reaction	MLR
Multiplicity of infection	MOI
Murine dendritic cells	mDC
Myeloid primary response protein 88	MyD88
Murine macrophages	mM $\phi$
Nitric oxide	NO
Nucleotide binding domain and leucine rich-repeat containing receptors	NLR
Pam3CSK4	Pam <sub>3</sub>
Pathogen- associated molecular patterns	PAMPs
Pathogen recognition receptors	PPR
Peripheral blood mononuclear cells	PBMCs
Phorbolmyristate acetate	PMA
phosphatidylcholine phospholipase C	PC-PLC

phosphatidylinositol-specific phospholipase C	PI-PLC
Picolinic acid	PA
Principal component analysis	PCA
Propidium iodide	PI
Prostaglandin E2	PGE <sub>2</sub>
Quinolinic acid	QA
Reactive oxygen species	ROS
Recombinant human	rh
Recombinant murine	rm
Regulatory DC	DCreg
Regulatory macrophages	Mreg
Regulatory T cells	Treg
Relative expression	RE
Retinoic acid-inducible gene I	RIG-I
sCD25	soluble CD25
Semi quantitative real time PCR	qRT-PCR
Small interfering RNA	siRNA
Streptococcus piogenes	<i>S.p</i>
T helper 1	T <sub>H</sub> 1
T helper 17	T <sub>H</sub> 17
Toll like receptor	TLR
Toll/ interleukin-1 receptor	TIR
Tryptohan	Trp
Wild type	wt

## Summary

Macrophages (M $\phi$ ) and dendritic cells (DC) constitute the first line of defense against invading microorganisms. These myeloid cells have been identified as the major components of the outer ringwall of suppurative granulomas present in patients with chronic listeriosis. M $\phi$  and DC acquire diverse pro-inflammatory features in response to bacteria. However, using infection of in vitro generated professional phagocytes with *Listeria monocytogenes* (*L.m.*) as a model, it has been shown that M $\phi$  like DC express a set of regulatory molecules in response to *L.m.* infection. This regulatory program comprises the expression of indoleamine 2,3-dioxygenase (IDO1), CD25 and IL-10. Moreover, the data indicated that this program has functional relevance since supernatants of infected M $\phi$  suppressed T cell proliferation. In addition, whole transcriptome analysis has shown that M $\phi$  and DC react to *Listeria* infection by inducing a common transcriptional program that includes proinflammatory and immunomodulatory mediators. Moreover, the data suggest that an important part of the transcriptional response of M $\phi$  after *L.m.* infection is not tuned according to the level of threat represented by phagosome-restricted or fully competent bacteria. In line with these findings, I could show that around half of the transcriptional changes induced upon *L.m.* infection in M $\phi$  are dependent on host factors mainly TNF- $\alpha$  and IFN- $\gamma$ , while the remaining 50% might be attributed to interactions between the host cell and viable invading bacteria.

IDO1 has been recognized as an antimicrobial effector, essential in the defense against numerous pathogens. Herein I present data demonstrating that IDO1 is amongst the highest expressed genes and proteins after *L.m.* infection in human myeloid cells, including DC and M $\phi$ . Several mechanisms such as IDO1-mediated tryptophan (Trp) depletion, but also accumulation of tryptophan catabolites have been associated with the antimicrobial effects of IDO1 expressing cells. The results obtained via IDO1 specific knockdown and enzymatic activity inhibition, have shown that human M $\phi$  and DC use IDO1 to control the growth of cytosolic *L.m.* Furthermore, accumulation of tryptophan catabolites, but not Trp depletion has been identified as the main anti-bacterial mechanism in human myeloid cells against *L.m.* infection. In contrast to the important role exerted by IDO1 in human DC and M $\phi$ , this protein was not induced in murine myeloid cells highlighting the specificity of host-pathogen interactions amongst species.

# 1. Introduction

## 1.1 The innate immune system and immune recognition

Individuals are constantly exposed to microorganisms and environmental agents that can be beneficial or represent a hazard for the host. In order to respond to this challenge, vertebrates possess two mechanisms that recognize and defend against potential threats: the innate and the adaptive immune system. The innate immune system is considered as an ancient tool in evolution since its basic molecular modules are present in plants and animals. This evidence indicates that this defense system emerged for the first time before the split of these two kingdoms (Hoffmann, Kafatos et al. 1999; Janeway and Medzhitov 2002). Innate and adaptive immunity differ fundamentally in the way they perform recognition of danger signals. Adaptive immunity relies on a set of non-germ line encoded receptors generated *de novo* in each organism providing high specificity (Iwasaki and Medzhitov 2010). In contrast, innate immune cells recognize a broad range of invariant microbial components, known as pathogen-associated molecular patterns (PAMPs), but also abnormal self-antigens, using a defined set of germ line encoded pathogen recognition receptors (PPR). Innate immune cells include M $\phi$ , DC, neutrophils, granulocytes and mast cells amongst others. Upon a challenge, they respond rapidly and in most of the cases their actions are sufficient to clear the invaders. However, when the innate immune system is overwhelmed T and B cells as cellular mediators of adaptive immunity are activated providing specific recognition and immune memory (Janeway and Medzhitov 2000).

PPRs can be classified as secreted, transmembrane and cytosolic receptors. Secreted PPRs comprise collectins, ficolins and pentraxins. These molecules bind to microbial surfaces and are able to activate the complement response. In addition, they can act as opsonins promoting phagocytosis of microorganisms by M $\phi$ . Transmembrane receptors include the Toll like receptor family (TLR), which in humans is composed of ten members. TLR1, 2, 4, 5 and 6 are located in the extracellular membrane and recognize microbial products at the surface like lipoteichoic acid (TLR1/2), lipoproteins (TLR2/6), lipopolysaccharide (LPS) (TLR4), and flagelin (TLR5). Intracellular TLR receptors, including TLR3, 7 and 9 localize in the membrane of phagocytic compartments and recognize nucleic acids (Kawai and Akira 2006). All TLRs elicit pathways that culminate with the activation of the nuclear factor (NF)  $\kappa$ B and the activation protein-1 (AP-1). The activation of these transcription factors is mediated by signaling events occurred after PAMP recognition. TLRs contain two domains, the leucine rich and the Toll/ interleukin-1 receptor (TIR) (Takeda and Akira 2004). Whereas the first one is involved in PAMPs recognition, the second one is involved in signal

transduction via its interaction with cytosolic adapters like the myeloid primary response protein 88 (MyD88), the TIR domain-containing protein (TRAP) and the TIR domain-containing inducing IFN $\beta$  (Trif) protein. Once the signal is detected, MyD88 recruits signaling molecules that activate the IL-1R activated kinase (IRAK) family leading to activation of tumor necrosis receptor-associated factor 6 (TRAF6) and finally to NF $\kappa$ B activation and nuclear translocation. Nevertheless, TLRs can also signal through a MyD88 independent pathway using TRIF as adapter. This pathway is essential to induce IFN $\beta$  expression, since Trif-deficient mice show a deficiency in type I interferon production upon stimulation with LPS (Takeda, Kaisho et al. 2003; Takeda and Akira 2004). Cytosolic PRRs include the retinoic acid-inducible gene I (RIG-I) like receptors and the nucleotide binding domain and leucine rich-repeat containing receptors (NLRs). RLRs are important to respond against virus since they recognize viral nucleic acids in the cytoplasm leading to the production of type I interferon and antiviral effector proteins (Pichlmair and Reis e Sousa 2007). RLRs use the common adaptor mitochondrial antiviral signaling protein (MAVS) to drive activation of NF $\kappa$ B and proteins from the interferon response factor (IRF) family (Takeuchi and Akira 2009). The NLR family is diverse and is comprised of 22 members in humans. They are involved not only in recognition of PAMPs, but also in the response to endogenous stress and danger signals (Chen, Shaw et al. 2009).

M $\phi$  and DC are key components of the innate immune system and drive nearly all inflammatory processes (Janeway and Medzhitov 2002). M $\phi$  and DC recognize and clear pathogens as well as present hazardous antigens to T cells leading to a productive immune response. Nonetheless, M $\phi$  and DC are highly plastic cells, able to integrate a broad range of signals from the microenvironment, leading to changes in their phenotype and function which enable these cells to shape adaptive immune responses and influence the balance between immunity and tolerance (Gordon and Taylor 2005; Mosser and Edwards 2008; Schmidt, Nino-Castro et al. 2012).

## **1.2 Macrophage heterogeneity**

M $\phi$  were first described by Elie Metchnikoff, who observed their outstanding capacity to phagocytize foreign particles (Cavaillon 2011). Besides their well-known capability to clear invading microorganisms, M $\phi$  play a fundamental role in organ homeostasis, tissue remodeling, ontogenesis, response to tissue injury and orchestrate metabolic functions (Mosser and Edwards 2008). M $\phi$  like DC are a diverse population; they are found in the vast majority of tissues and have been divided in different subpopulations according to their anatomical location and expression of surface markers (Murray and Wynn 2011). In mice,

tissue resident M $\phi$  originate mainly from monocytes that circulate in the bloodstream and enter the tissues to differentiate via the action of macrophage-colony stimulating factor (M-CSF) (Gordon and Taylor 2005). However in murine models, it has been recently reported that M $\phi$  can develop at the yolk sac, before the development of hematopoietic stem cells. Furthermore, this population might act as precursor of a myeloid cell lineage that does not depend on hematopoietic stem cells for its replenishment (Schulz, Gomez Perdiguero et al. 2012). Interestingly, the yolk sac lineage comprises M $\phi$  subpopulations that have been previously described as able of self-renewal directly at the tissues, including Kupffer cells (Klein, Cornejo et al. 2007), microglia (Ajami, Bennett et al. 2007), pleural macrophages (Jenkins, Ruckerl et al. 2011), but also epidermal Langerhans cells (Merad, Manz et al. 2002). Despite their heterogeneity, M $\phi$  keep an essential transcriptional program that preserves their identity. Probably the transcription factor PU.1 plays a key role in this matter since it is a genome wide modifier which enables the formation and accessibility of macrophage-specific regulatory genomic regions (Natoli 2010).

### **1.2.1 Macrophage polarization**

M $\phi$  are plastic cells and their interactions with other components of the immune system in vivo are versatile and complex. In order to approach the intricate network of M $\phi$  responses, a useful strategy has been to stimulate them in vitro with microbial agonists or cytokines that mimic an in vivo situation. This approach, in combination with evidence obtained in murine models has enabled the characterization of two distinct phenotypic and functional profiles, known as classical and alternative activation, or by mirroring the T cell nomenclature M1 and M2 respectively.

#### *Classical M1 activated macrophages*

Mackness showed for the first time in 1962, that M $\phi$  extracted from mice which overcame a prior infection with *L.m.*, were more efficient in the control of this bacterium, than their counterparts isolated from mice that were not previously infected (Mackness 1962). After this seminal work, Bloom and Bennet established lymphocytes as main activators of M $\phi$  (Bloom and Bennett 1970) and IFN- $\gamma$  emerged as the obligatory cytokine leading classical M $\phi$  activation (Nathan, Murray et al. 1983; Adams and Hamilton 1984; Mosser 2003). In vitro, the phenotype of M1 macrophages has been characterized via stimulation with IFN- $\gamma$  alone or in concert with TNF $\alpha$  and / or TLR agonists (Mosser and Edwards 2008). Classically activated M1 M $\phi$  are potent antigen presenting cells that secrete high levels of pro-inflammatory cytokines like IL-12, IL-6, TNF- $\alpha$  and IL-15. All of these immune modulators are involved in

the promotion of T helper 1 (T<sub>H</sub>1) and T helper 17 (T<sub>H</sub>17) responses (Krausgruber, Blazek et al. 2011). In contrast, they only express low levels of the immunosuppressive cytokine IL-10 (Sica and Mantovani 2012). M1 also express a wide variety of pro-inflammatory chemokines and chemokine receptors like CCL3, CCL2, CCL4, CCL5, IL-8 and CCR7 amongst others, that promote the recruitment of NK and T<sub>H</sub>1 cells at the sites of infection (Mantovani, Sica et al. 2004). Consistent with their microbicidal properties, M1 are efficient in the production of reactive oxygen species (ROS). In mice M1 M $\phi$  express inducible nitric oxide (iNOS) leading to the production of nitric oxide (NO) and reactive nitrogen intermediaries that play an important role in the control of diverse intracellular pathogens (Chakravorty and Hensel 2003).

In the last years, a significant effort has been made to identify the transcription factors that direct M $\phi$  polarization. The canonical IRF/STAT pathway is involved in shaping the M1 phenotype via STAT1 transcriptional activity (Lawrence and Natoli 2011). Similarly, IRF5 is responsible for the induction of genes encoding the different subunits of IL-12, but also for the repression of IL-10 transcription. Furthermore, adding exogenous IRF5 led to the expression of M1 phenotypic markers (Krausgruber, Blazek et al. 2011). NF $\kappa$ B is strongly induced upon TLR activation and leads to the production of pro-inflammatory mediators related to a M1 phenotype (Bonizzi and Karin 2004). At the same time, NF $\kappa$ B activity mediates the transcriptional program necessary for the resolution of inflammation (Lawrence and Gilroy 2007) making it less likely that this transcription factor is specific for a particular polarization (Figure1).

Functionally M1 have been associated with a protective response against infection including, *L.m.* (Shaughnessy and Swanson 2007), *Salmonella typhimurium* and the acute phase of *Mycobacterium tuberculosis* (Benoit, Desnues et al. 2008). However, an uncontrolled M1 activation can lead to tissue damage and multiple organ failure. In septic patients high production of M1-type cytokines is associated with a high mortality rate (Bozza, Salluh et al. 2007).

## M1 classical activation

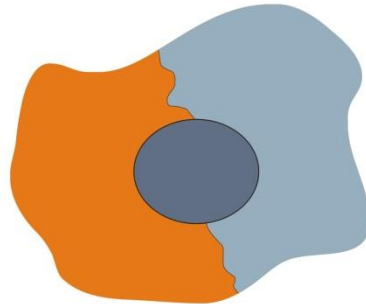
### Transcription factors:

IRF5, STAT1, NF $\kappa$ B

### Chemokines:

CCL2, CCL3, CCL4, CCL5,  
CCL8, CCL15,  
CCL19, CCL20, IL-8  
CXCL9, CXCL10, CXCL11,  
CXCL13

**Cytokines:** IL-6, IL-12,  
IL-15, TNF $\alpha$



## M2 alternative activation

**Transcription factors:** STAT3,  
STAT6, IRF4, PPAR $\gamma$ , CREB

### Chemokines:

CCL13, CCL14, CCL17,  
CCL18, CCL23, CCL26,  
CXCL1, CXCL2, CXCL3

**Cytokines:** IL-10, TGF $\beta$

**Figure 1. Models of M $\phi$  activation**

Activation of M $\phi$  has been traditionally assessed by the expression of hallmark molecules, including cytokines, chemokines and more recently transcription factors. M1 classical activation is characterized by the expression of proinflammatory cytokines (TNF- $\alpha$ , IL-6, IL-12, and IL-15) and chemokines that recruit monocytes, natural killer and T<sub>H</sub>1 cells, including CCL2, CCL4 and CCL8. Several transcription factors mediate the acquisition of an M1 phenotype including IRF5, STAT1 and NF $\kappa$ B. Hallmarks of M2 alternative activation is the expression of the anti-inflammatory mediators IL-10 and TGF- $\beta$ . Several transcription factors have been suggested for the acquisition of a M2 phenotype including STAT3, STAT6, IRF4, PPAR $\gamma$  and CREB (Mantovani, Sica et al. 2004; Martinez, Gordon et al. 2006; Sica and Mantovani 2012).

### *Alternatively M2 activated macrophages*

Alternative activation of M $\phi$  emerged after the description of IL-4 (Howard and Paul 1983) and IL-13 (Minty, Chalon et al. 1993) as the immunological counterparts of IFN- $\gamma$  and key drivers of T<sub>H</sub>2 responses (Wynn 2003). Abramson and Gallin, demonstrated for the first time, that IL-4 impaired the respiratory burst and decreased production of IL-1 $\beta$  and IL-8 on M $\phi$  (Abramson and Gallin 1990). The discovery of the mannose receptor as a surrogate marker expressed on IL-4 treated M $\phi$ , together with the important role of these cells in the control of *Trypanosoma cruzi*, led to the concept of alternative activation of M $\phi$  (Martinez, Helming et al. 2009). More recently, other factors have been described to shape M $\phi$  phenotype and function, amongst them IL-10, glucocorticoid receptor ligands and, TLR ligands e.g. bacterial LPS in concert with immune complexes. Therefore, a new classification of alternative M2 activation has been proposed as follows: M2a comprises M $\phi$  induced by IL-4 and/or IL-13, M2b macrophages induced by TLR ligands and immune complexes and finally M2c induced by glucocorticoids and IL-10 (Benoit, Desnues et al. 2008).

M2 are characterized by the expression of surface receptors like CD23, MCR1, scavenger receptors, but also by the secretion of high levels of IL-10 concomitant with low or no IL-12



secretion (Sica and Mantovani 2012). However, the expression of other hallmark genes varies between human and mice. In murine models, M2 macrophages express the proteins Ym1 and Fizz1 and the enzyme Arginase-I that shift the metabolism from NO production to accumulation of ornithine and polyamines through induction of L-arginine metabolism (Raes, Van den Bergh et al. 2005). Regarding chemokine production in murine M2, CCL2 and CCL7 promote the recruitment of basophils and eosinophils. In contrast, human alternatively activated M $\phi$  express the chemokines CCL13, 14 and 17, although they recruit the same cell types at sites of inflammation (Martinez, Helming et al. 2009).

Transcription factors driving alternative activation in M $\phi$  have not been completely elucidated yet. However, studies performed in murine models have contributed to the discovery of several interesting candidates. STAT6 as downstream transcription factor of the signaling pathway initiated by IL-4 and IL-13 has been involved in this process. Another transcription factor activated after IL-4 stimulation is the peroxisome proliferator-activated receptor gamma (PPAR $\gamma$ ) (Huang, Welch et al. 1999). This transcription factor has an important role in M $\phi$  metabolic functions, particularly in lipid metabolism and has been found constitutively expressed in adipose tissue M $\phi$ , where it promotes anti-inflammatory processes (Lawrence and Natoli 2011). Interestingly, it was shown that PPAR $\gamma$  can act in concert with STAT6 to regulate gene expression (Szanto, Balint et al. 2010). Similarly, in human and mice STAT3 acts as an effector transcription factor of IL-10 and mediates the transcription of some of the hallmark genes of M2 polarization, like IL-10, TGF $\beta$  and MRC1 (Takeda, Clausen et al. 1999; Lang, Patel et al. 2002; Williams, Bradley et al. 2004). Finally, epigenetic changes induced by the jumonji domain containing-3 demethylase (Jmjd3) in concert with the transcription factor IRF4 promote the transcription of M2 related genes in mice (Satoh, Takeuchi et al. 2010) (Figure 1).

Traditionally M2 have been associated with tissue repair and successful immune responses against helminthes. M $\phi$  of p50NF $\kappa$  $\beta$  deficient mice are unable to acquire M1-related characteristics. These animals showed a strong M2 polarization in response to the chronic infection with the nematocystode *Taenia crassiceps* associated with a decrease in the parasitic burden (Porta, Rimoldi et al. 2009). Along the same lines, mice holding a M $\phi$ /neutrophil selective lineage knock-out of the IL-4 receptor  $\alpha$  (IL-4R $\alpha$ ) chain were highly susceptible to *Schistosoma mansoni* infection (Herbert, Holscher et al. 2004). Nevertheless, alternative activation of M $\phi$  can be deleterious for the organism and has been associated with the promotion of a broad range of chronic pathological conditions, including asthma, atherosclerosis, cancer and obesity (Sica and Mantovani 2012).

## 1.3 General aspects of dendritic cell immunobiology

DC were first described in the mouse spleen as an unusual “stellate” cell, morphologically distinct from M $\phi$  by Steinman and Cohn (Steinman and Cohn 1973). Soon after this discovery, Steinman and Witmer showed that DC were potent stimulators of T cells in mixed leukocyte reaction (MLR) assays (Steinman and Witmer 1978). This pioneering work enabled the characterization of DC as the main antigen presenting cells (APC) in the immune system. DC constitute the bridge between the innate and the adaptive immune system due to their remarkable capacity to capture, process and present antigens to T cells via major histocompatibility complexes (MHC) (Banchereau and Steinman 1998). In general, these cells originate from bone marrow precursor cells (Banchereau and Steinman 1998; Geissmann, et al. 2010), with the exception of Langerhans cells, which have the capacity of self-renewal directly in the tissues (Merad, et al. 2002) and seem to be generated from yolk sac M $\phi$  in the embryo (Schulz, Gomez Perdiguero et al. 2012). In mice, DC develop from CD34+ stem cells that give rise to two main branches, known as the common lymphoid progenitor and the common myeloid progenitor. The common myeloid progenitor will differentiate into a M $\phi$  common precursor followed by a common DC precursor giving origin to DC, M $\phi$  and monocytes (Fogg, et al. 2006). However, in humans the common DC precursor has not been identified yet and it seems that DC can originate from a granulocyte-macrophage precursor as well as from precursor cells with combined lymphoid and myeloid potential known as multi-lymphoid progenitors (Doulatov, et al. 2010).

### 1.3.1 Dendritic cells subsets

DC are a heterogeneous cell population. Classically, they have been divided into different subtypes primarily based on phenotypic markers, migratory capabilities, and functional status (Kushwah and Hu 2011). DC classification is complex, and it has been difficult to unify between human and mouse models, mainly because some of the hallmark genes of mice are absent in human and because of ethical constraints associated with the study of human tissues (Collin, et al. 2011). Broadly, DC have been divided into myeloid cells that can be considered equivalent to conventional DC in mice, plasmacytoid DC, which are functionally equivalent in both species, and monocyte derived DC. Monocyte derived DC have been described only in mice, although they are commonly used in vitro to study the biology of human DC (Sallusto and Lanzavecchia 1994). Conventional DC are specialized in antigen processing and presentation. They have been subdivided according to their migratory capacity and the tissue of residence. In mice, migratory DC are generally characterized by the expression of CD11b. However, they can be further subdivided into CD11b+ and CD11b-CD103+ DC. They sample constantly their microenvironment and upon antigen encounter

migrate to lymph nodes (Banchereau, et al. 2000). In contrast, resident lymphoid DC do not traffic between organs and they are likely generated directly in the lymph node.

Human and murine plasmacytoid DC (pDC) are a rare cell population that can be found in lymphoid and non-lymphoid organs and in humans also as circulating cells in the blood (Reizis, et al. 2011). Despite molecular differences and the expression of certain markers, the overall phenotype and function of pDC seems to be conserved between mouse and human (Croizat, et al. 2010). In contrast to myeloid DC, immature pDC seem to be only weak APC due to their low expression of MHC class II or co-stimulatory molecules on the cell surface (Reizis, et al. 2011). One of the most outstanding features of pDC is their ability to produce high amounts of type I interferons in response to viral infections (Fitzgerald-Bocarsly, et al. 2008; Liu 2005). Consistently with this role pDC express preferentially TLR7 and TLR9, both implicated in recognition of viral RNA and DNA (Ito, et al. 2005).

In murine models, it has been described that under inflammatory conditions fully differentiated DC characterized by CD209 expression can be originated from circulating monocytes (Cheong, et al. 2010). Furthermore, in vivo after cutaneous infection with *Leishmania major* a population of monocytes is recruited to the dermis and differentiates into dermal monocyte-derived DC, which subsequently can migrate into draining lymph nodes (Leon, et al. 2007). Along the same lines, Serbina et al. have identified a subtype of inflammatory DC that emerge in response to *L.m.* infection via CCR2 mediated recruitment of monocytes to the spleen (Serbina, et al. 2003). Although the differentiation of human monocytes driven by GM-CSF and IL-4 in vitro (Sallusto and Lanzavecchia 1994) is one of the most extended procedures to study DC biology, in vivo it has not been proven yet that monocytes can give rise to DC in humans. Interestingly, a subset of CD209+ CD14+ cells sharing some of the characteristics of monocyte derived DC from mouse, have been found in human dermis (Angel, et al. 2007).

### **1.3.2 Maturation of dendritic cells**

The process of DC maturation can be considered as a continuum of closely linked events. This process starts in the periphery, where DC capture antigens, and finalizes upon T cell encounter in the lymph node (Banchereau, Briere et al. 2000). Immature DC are highly phagocytic and can take up a wide range of antigens under steady state conditions via several mechanisms, like macropinocytosis, receptor mediated endocytosis and phagocytosis (Sallusto, Cella et al. 1995). Upon encounter with pathogens, but also after stimulation with cytokines like TNF $\alpha$ , IL-1 and IL-6, DC undergo phenotypic and functional changes. For example, they lose their phagocytic capacity, start to secrete cytokines and

increase the expression of MHCII and co-stimulatory molecules like CD40, CD80 and CD86 (Gallucci and Matzinger 2001). The stimuli that induce DC maturation trigger also the process of migration from peripheral tissues to lymphoid organs. In order to guarantee the efficiency of this process, maturation implies drastic changes in the repertoire of chemokine receptors present on the surface of DC. On the one hand, CCR7 expression is up-regulated enabling DC to respond to gradients of CCL19 and CCL21 that are produced abundantly in the lymph node. On the other hand, the expression of CCR1, CCR2 and CCR5 is decreased, avoiding the interaction with their ligands, which are mainly produced at sites of injury and inflammation (Sanchez-Sanchez, Riol-Blanco et al. 2006; Randolph, Ochoa et al. 2008).

DC present antigen to T cells in the context of MHC I and II molecules triggering CD8<sup>+</sup> and CD4<sup>+</sup> T cell responses respectively. Exogenous antigens are presented via MHCII molecules that are located in the endocytic compartment, where they encounter antigens. Subsequently, the loaded complexes are translocated to the cell surface and remain stable and available for recognition by CD4<sup>+</sup> T cells (Cella, Engering et al. 1997). In contrast, MHCI molecules present antigens from endogenous and exogenous nature. DC are crucial in priming CD8<sup>+</sup> T cell cytotoxic as well as CD4<sup>+</sup> T cells mediated responses. In this process, recognition of MHC molecules via TCR receptors constitutes the first signal to prime T cell clonal expansion and activation. The second signal is provided by the interaction between co-stimulatory molecules on the DC surface and their counterparts in T cells, whereas the microenvironment constitute a third signal that further shapes the nature of T cell responses (Banchereau, Briere et al. 2000). The outcome of these complex interactions can be an effective immune response, but can also lead to tolerance or immunosuppression.

## **1.4 Regulatory functions of macrophages and dendritic cells**

The immune system exists in a delicate balance between immunity and tolerance that allows the development of effective but limited responses, avoiding a destructive uncontrolled reaction against host tissues. Classically, T cells have been recognized as the main players in immunoregulation and tolerance. Nevertheless, there is an enlarged body of evidence which suggests the relevance of DC as key modulators of the immune response in the periphery (Schmidt, Nino-Castro et al. 2012). More recently, it has been proposed that a subset of regulatory M $\phi$  might also play a role in inducing tolerance in different pathological conditions including transplantation (Wood, Bushell et al. 2012) and models of septic shock (Fleming and Mosser 2011).

While activation of M $\phi$  (classical and alternative) and the maturation of immunogenic DC have been linked to a defined set of phenotypic characteristics, there is not a clear set of hallmark molecules for myeloid cells that exert regulatory functions. For instance, it has been the common view that only immature DC can induce tolerance. This concept was developed on the basis of early experiments, which demonstrated that antigen presentation in the absence of co-stimulation, leads to T cell anergy and T cell deletion (Jonuleit, Schmitt et al. 2000; Lutz, Kukutsch et al. 2000; Reis e Sousa 2006; Manicassamy and Pulendran 2011). However, in more recent years, this concept has changed and there is increasing evidence showing that mature DC can have a regulatory function. For example, in a murine asthma model fully matured DC expressing high levels of co-stimulatory molecules promoted the development of regulatory T cells (T<sub>reg</sub>) via an IL-10 depending mechanism (Akbari, DeKruyff et al. 2001). In humans, monocyte-derived DC stimulated with prostaglandin E<sub>2</sub> (PGE<sub>2</sub>), Pam<sub>3</sub>CSK<sub>4</sub> (Pam<sub>3</sub>) and TNF $\alpha$  (named DCreg) exhibit a fully mature phenotype characterized by high expression levels of co-stimulatory molecules and proinflammatory cytokines, yet they suppress T cell activation via an effective combination of factors like IDO1, CD25, and IL-10 (Popov, Abdullah et al. 2006; von Bergwelt-Baildon, Popov et al. 2006; Popov, Driesen et al. 2008). Along the same lines, the presence of IDO<sup>+</sup> DC has been documented in different malignancies, including melanoma (Vermi, Bonocchi et al. 2003) and head and neck cancers (Hartmann, Wollenberg et al. 2003). Moreover, IDO<sup>+</sup> pDC present in tumor draining lymph nodes of human and mice, were described to induce anergy towards tumor antigens (Baban, Hansen et al. 2005). Finally, DC with intermediate features between the immature and mature state expressing co-stimulatory molecules, but only low levels of inflammatory cytokines, such as IL-12, IL-6 and TNF- $\alpha$ , are also characterized by regulatory function (Lutz and Schuler 2002).

Activation of M $\phi$  has been classified in classical and alternative. However, experimental evidence suggests that M $\phi$  can also exert regulatory functions that differ from the tasks accomplished by alternative activated M $\phi$  in tissue remodeling, parasitical infections or response to injury (Fleming and Mosser 2011). Although, stable phenotypic markers have not yet been defined, it has been shown recently that human monocyte derived M $\phi$  cultured in presence of human AB serum and treated with IFN- $\gamma$  were able to suppress T cell proliferation in vitro. Moreover, when these regulatory M $\phi$  were transferred to recipients of kidney transplant, they reduced the need for immunosuppressive medication, suggesting their tolerogenic activity in vivo (Hutchinson, Riquelme et al. 2011). Similarly, it has been shown in mice that the treatment of bone marrow derived M $\phi$  with immune complexes in concert with LPS leads to an increased production of IL-10 concomitant with low levels of IL-12 secretion; these cells were able to suppress T cell proliferation in vitro. Furthermore, in vivo M $\phi$  treated with immune complexes and LPS were able to increase the survival of mice

treated with lethal doses of LPS (Gerber and Mosser 2001). More recently, it has been shown that the interaction between B cells and M $\phi$  confers the later with a unique phenotype characterized by the simultaneous expression of pro-inflammatory cytokines and chemokines, but also IL-10 production (Wong, Puaux et al. 2010). Moreover, Schaefer et al. demonstrated in vitro that human monocyte derived M $\phi$ , treated with TNF- $\alpha$  in concert with PGE<sub>2</sub> and Pam<sub>3</sub> suppress T cell proliferation MLR in assays. These regulatory M $\phi$  (named Mreg) exhibit a similar phenotype to DC treated under the same conditions and do also express IDO1, IL-10 and CD25. However, they have a unique transcriptional program probably reflecting their common functions in regulation of immune responses (Schaefer 2009).

#### **1.4.1 Anti-inflammatory mediators in the acquisition of regulatory functions in myeloid cells**

The microenvironment plays a decisive role in the generation of regulatory M $\phi$  and DC. Several immunomodulatory factors including IL-10 and PGE<sub>2</sub> have a crucial influence on the differentiation of regulatory myeloid cells. During inflammatory immune responses PGE<sub>2</sub> is expressed by epithelial cells, fibroblasts and proinflammatory infiltrating cells (Kalinski 2012). PGE<sub>2</sub> increases CCR7 expression in monocyte-derived DC and is often used as an immunogenic factor to promote DC maturation (Scandella, Men et al. 2002; Legler, Krause et al. 2006). Nevertheless, PGE<sub>2</sub> treated DC show only a transient expression of CCR7 and reduced levels of secreted CCL19, which is the key chemokine attracting naïve and central memory T cells (Muthuswamy, Mueller-Berghaus et al. 2010). Along the same lines, PGE<sub>2</sub> treated monocyte derived DC have shown an enhanced IL-12p40 secretion which is not accompanied by production of IL-12p35 leading to an overall diminished production of the bioactive IL-12 heterodimer (Kalinski, Vieira et al. 2001). Furthermore, PGE<sub>2</sub> induces the expression of immunomodulatory molecules on DC such as thrombospondin-1 (TBS-1) (Doyen, Rubio et al. 2003), IL-10 (Kalinski, Hilkens et al. 1997) and in combination with TNF- $\alpha$ , IDO1 (von Bergwelt-Baildon, Popov et al. 2006). Similarly, PGE<sub>2</sub> might also promote the acquisition of an anti-inflammatory function on M $\phi$ . Recently, it has been shown in vitro that PGE<sub>2</sub> secreted by human mesenchymal stem cells inhibited the secretion of IL-12, IL-6 and TNF- $\alpha$  by LPS treated M $\phi$ , and increased IL-10 secretion (Ylostalo, Bartosh et al. 2012). Similarly, high levels of PGE<sub>2</sub> in the lung have been associated with low phagocytic and microbicidal activity in mouse alveolar M $\phi$  (Ballinger, Aronoff et al. 2006). IL-10 has a well-recognized immunoregulatory role on myeloid cells. DC exposed to IL-10 fail to induce IL-12 (De Smedt, Van Mechelen et al. 1997) and TNF- $\alpha$ . This loss of chemokine production is associated with a poor surface expression of MHC class II molecules and CD86, resulting in an impaired ability of IL-10 primed DC to induce T cell allogeneic responses (Moore, de Waal

Malefyt et al. 2001). Similarly, it has been demonstrated that IL-10 secreted by M $\phi$  in response to different infections, but also TLR agonists has a modulatory effect on bystander M $\phi$ , avoiding the production of pro-inflammatory cytokines associated with classical activation including TNF- $\alpha$ , IL-6, IL-12 amongst others, via a STAT3 mediated mechanism (Bode, Ehling et al. 2012).

#### **1.4.2 Molecular mechanisms of T cell suppression by macrophages and dendritic cells**

M $\phi$  and DC exposed to an immunosuppressive environment acquire a set of molecular mechanisms able to suppress T cells responses (Popov, Driesen et al. 2008). These mechanisms include IDO1, CD25, Cyclooxygenase 2 (COX-2) and IL-10. IDO1 catalyzes the first rate-limiting step in Trp degradation (Yamamoto and Hayaishi 1967), leading to Trp depletion and accumulation of Trp catabolites, collectively known as kynurenines (Sugimoto, Oda et al. 2006). IDO1 was first described as a potent inhibitor of the growth of intracellular pathogens via a mechanism that involves Trp depletion (Pfefferkorn 1984; MacKenzie, Worku et al. 2003; Oberdorfer, Adams et al. 2003). However, later it was found that besides their microbicidal effect, IDO1 was responsible for the maintenance of the maternal T cell tolerance to fetal tissues and by this action is proposed as a natural immunoregulatory mechanism (Munn, Zhou et al. 1998). More recently it has been found that IDO-mediated Trp starvation and accumulation of Trp catabolites can lead to T cell proliferation arrest and apoptosis (Terness, Bauer et al. 2002; von Bergwelt-Baildon, Popov et al. 2006). Furthermore, DC can induce the expansion of autologous T<sub>reg</sub> via an IDO-dependent mechanism (Chung, Rossi et al. 2009). In addition, it has been reported that the Trp catabolite kynurenine (Kyn) can bind and activate the aryl hydrocarbon receptor (AHR) on T cells leading to AHR-dependent T<sub>reg</sub> generation in mice (Mezrich, Fehner et al. 2010). CD25 ( $\alpha$  chain of the IL-2 receptor) has been proposed as a marker of DC maturation that mediates strong stimulatory signals upon ligand binding. However, in human and mouse DC the  $\beta$ -chain of the IL-2 receptor which is required for signal transduction is not expressed (Velten, Rambow et al. 2007) and it has been proposed that CD25, in particular its soluble form, acts as a decoy receptor for IL-2 leading to an impaired T cell activation and proliferation (Driesen, Popov et al. 2008). COX-2 catalyzes the synthesis of PGE<sub>2</sub>. This mediator has a strong effect, on phenotype and function of myeloid cells but also modifies T cell mediated responses. PGE<sub>2</sub> inhibits T cell proliferation and dampens the production of IFN- $\gamma$  and IL-2 by T<sub>H1</sub> activated cells (Hilkens, Snijders et al. 1996; Harris and Phipps 2002). Similarly, it has been reported that PGE<sub>2</sub> inhibits T<sub>H17</sub> cell differentiation in vitro (Duffy, Pindjakova et al. 2011). Finally, IL-10 is a well-known suppressor of T cell responses and can inhibit IL-2, IL-5

and TNF- $\alpha$  secretion as well as the expression of CXCR4 and chemotaxis in response to its ligand SDF1 (Moore, de Waal Malefyt et al. 2001). It has also been shown that IL-10 in concert with TGF- $\beta$  and retinoic acid are involved in the development of induced T<sub>reg</sub> cells in the periphery which is a mechanism crucial for gut homeostasis (Murai, Krause et al. 2010).

## 1.5 The pathogenesis of *L. monocytogenes*

*L.m.* is a gram positive bacterium that can survive as a saprophyte in a broad range of environmental conditions (Freitag, Port et al. 2009). Upon encounter with a potential host, *L.m.* activates different molecular mechanisms to guarantee its internalization, as well as, its replication inside the cytoplasm of mammalian cells. In humans *L.m.* causes listeriosis, a food borne disease that is characterized in healthy individuals by a self-limited gastroenteritis. However, in the elderly population, but also newborns, pregnant women and immunocompromised individuals, *L.m.* can cause a potentially life threatening disease and can lead to chronic meningoencephalitis and sepsis with the presence of suppurative granulomas in multiple organs (Swaminathan and Gerner-Smidt 2007; Allerberger and Wagner 2010; Mook, Patel et al. 2011; Silk and Mahon 2011).

Extensive studies in a mouse model of systemic *L.m.* infection are the foundation for the characterization of *L.m.* pathogenesis (Unanue and Carrero 2012) in mice (Figure 2). For example, it was determined that *L.m.* can infect a wide variety of cell types. In the gastrointestinal epithelium, *L.m.* triggers its own phagocytosis via interactions of internalins A (InIA) and B (InIB) with E-cadherin and the hepatocyte growth factor receptor, respectively (Seveau, Pizarro-Cerda et al. 2007). Once *L.m.* is internalized, it escapes from the phagocytic compartment via the action of listeriolysin O (LLO) (Schnupf and Portnoy 2007), phosphatidylinositol-specific phospholipase C (PI-PLC) and phosphatidylcholine phospholipase C (PC-PLC) (Mengaud, Braun-Breton et al. 1991). These molecules allow *L.m.* to disrupt the phagosomal compartment and reach the cytoplasm, where it replicates using the nutrients provided by the host cell. Once in the cytoplasm it uses the actin assembly-inducing protein (ActA) to exploit host actin as a molecular motor to propel itself to the next cell (Domann, Wehland et al. 1992). Finally, *L.m.* spreads through the next cell via the actions of LLO, PI-PLC and PC-PLC. It is important to note that nearly all genes that mediate *L.m.* virulence are under the control of the transcriptional regulator PrfA. Mutants that lack the functional expression of this protein are unable to replicate in infected cells and are 100.000 fold less virulent than wild type bacteria (Freitag, Rong et al. 1993).



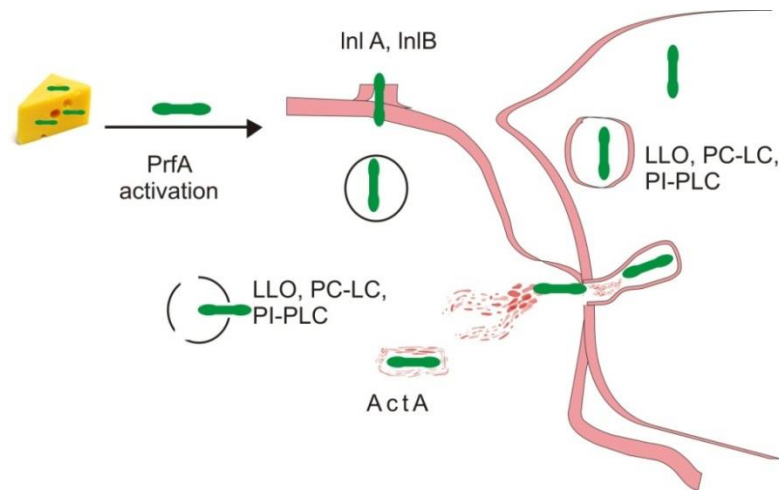


**Figure 2. The pathogenesis of *L.m.***

Microenvironmental cues trigger PrfA expression in *L.m.* PrfA acts as a transcriptional regulator that controls the expression of virulence factors, including InlA and InlB which guarantees the bacterial entry into the host cell. LLO and phospholipases facilitate the escape from the phagosomal compartment. Finally, the expression of ActA results in invasion of a new cell via a host actin propulsion mechanism.

### 1.5.1. Innate immune responses against *L. monocytogenes*

The important role of innate immunity in the response against *L.m.* was first appreciated in mice suffering from severe combined immunodeficiency syndrome. Surprisingly, these mice were highly resistant to *L.m.* infection, although they were unable to clear the bacteria in the long term (Nickol and Bonventre 1977; Bancroft, Schreiber et al. 1991). Several components of the innate immune system have shown to be crucial for the development of a successful immune response against *L.m.* including PRR receptors, cytokines and myeloid cells.

TLR2 senses PAMPs of gram positive bacteria, including lipoproteins and lipoteichoic acid. Therefore, it was proposed as a key mediator in the recognition and triggering of the innate immune response against *L.m.* infection. Although, M $\phi$  lacking TLR2 showed a diminished capability to internalize *L.m.* via phagocytosis (Shen, Kawamura et al. 2010), TLR2 deficient mice did not show any disadvantage in the clearance of *L.m.* infection (Edelson and Unanue 2002). On the contrary, mice deficient for the protein adaptor MyD88 were extremely susceptible to *L.m.* infection and showed low production of pro-inflammatory cytokines (Edelson and Unanue 2002; Seki, Tsutsui et al. 2002). Once *L.m.* escapes from phagosomal compartments, it enters the cytoplasm where it encounters intracellular PPRs. Mice deficient for the nod like receptor NOD-2 showed an increased sensibility upon *L.m.* intragastric infection associated with higher bacterial burdens, suggesting the importance of this receptor during the intestinal immune response to *L.m.* (Kobayashi, Chamaillard et al. 2005).

Cytokines produced by cells of the innate immunity are relevant in the control of *L.m.* For example, IL-12 blockade in mice results in high bacterial burden. This effect is abrogated upon IFN- $\gamma$  administration (Tripp, Gately et al. 1994). Similarly, IFN- $\gamma$  knockout mice showed high susceptibility and early lethality upon *L.m.* infection (Harty and Bevan 1995). More recently Kernbauer et al. showed that a M $\phi$  restricted ablation of STAT1 leads to an increased bacterial burden in *L.m.* infected mice, corroborating the importance of IFN- $\gamma$  in the early response against this pathogen (Kernbauer, Maier et al. 2012). Another important cytokine for the early control of *L.m.* infection is TNF- $\alpha$  since mice lacking the TNF- $\alpha$  receptor are highly prone to the infection (Rothe, Lesslauer et al. 1993). Moreover, mice expressing a functional mutant form of the TNF- $\alpha$  receptor that is constitutively active during infection are significantly more resistant to *L.m.* than their wild type counterparts (Xanthoulea, Pasparakis et al. 2004).

In mice, it has been demonstrated that DC, M $\phi$  and neutrophils play a role in the clearance of *L.m.* after the injection into the blood stream. However, the extent of their cooperation, as well as, the overall effect for the host remains controversial. For instance, it has been proposed that Kupffer cells, resident M $\phi$  of the liver, are responsible for clearing *L.m.* in the first stages of infection (Gregory, Cousens et al. 2002). Nevertheless, it has also been suggested that neutrophils and monocytes recruited to sites of infection might play a crucial role in this process. On the one hand, neutrophil depletion led to an increment in the bacterial load of 10-10.000 fold in the liver (Carr, Sieve et al. 2011). On the other hand, mice deficient for the chemokine receptor CCR2 were unable to clear *L.m.* (Kurihara, Warr et al. 1997), suggesting the relevance of monocyte recruitment in this process (Pamer 2004). On the contrary, the uptake of *L.m.* by splenic DC seems to have a deleterious effect for the host and promotes bacterial dissemination. Mice temporarily depleted of DC show a decrease of 50-500 folds in the bacterial burden of the spleen and were less prone to systemic infection. Additionally it was shown that CD8 $\alpha^+$ , but not CD8 $\alpha^-$  DC were heavily infected suggesting their predominant role in the establishment of the infection (Neuenhahn, Kerksiek et al. 2006). Furthermore, mice deficient for expression of the basic leucine rich zipper transcription factor ATF-like 3 lack functional CD8 $^+$  DC and were resistant to lethal doses of *L.m.* (Edelson, Bradstreet et al. 2011). In contrast, it has been shown that a DC population emerging upon recruitment of monocytes is characterized by the production of high amounts of TNF- $\alpha$  and NO both essential for the control of *L.m.* in vivo (Serbina, Salazar-Mather et al. 2003).

### **1.5.2 Human chronic listeriosis**

The immune response to *L.m.* has been well characterized in murine models. However, much less is known about the events involved in human chronic listeriosis, a rare, but life threatening condition associated with impairment of the adaptive immune response (Popov, Abdullah et al. 2006). Patients in advanced stages of chronic listeriosis present granuloma formation in lymph node tissues (Gray and Killinger 1966). These structures are organized immune cell aggregates that form in response to persistent stimuli of infectious or non-infectious nature (Ramakrishnan 2012). Traditionally it has been considered that once the immune system has failed to eradicate pathogens, granulomas act as a containment strategy, avoiding the dissemination of the pathogenic agents (Ehlers 2005). Recently, it has been found that M $\phi$  and DC are the main constitutive elements of *L.m.* suppurative granulomas, whereas cells from the adaptive immune system like B and T cells are excluded from these structures (Popov, Abdullah et al. 2006). Furthermore, transcriptome profiling revealed that DC infected with *L.m.* present a distinctive signature characterized by the expression of pro-inflammatory and immunomodulatory mediators, including TNF- $\alpha$ , IFN- $\gamma$ , IL-10, COX-2, IDO1 and CD25. The expression of these factors confers these cells with regulatory properties, including the capacity to suppress activated T cell proliferation (Popov, Abdullah et al. 2006; Popov, Driesen et al. 2008).

## 2. Aim of the study

The pathogenesis of *L.m.* has been extensively studied in mice. However, immunological processes involved in the development of human chronic listeriosis have been barely studied. Previously it has been demonstrated that M $\phi$  along with DC are the major components of the outer ringwall of suppurative granulomas present in patients with chronic listeriosis (Popov, Abdullah et al. 2006). Similarly, it has been demonstrated that human monocyte derived DC acquire regulatory properties upon *L.m.* infection, including the expression of IDO1, an enzyme that can exert microbicidal, as well as, regulatory functions (Popov et al., 2006; Popov et al., 2008). Moreover, it was established that IDO1 expressing DCreg, are capable to control more efficiently the intracellular growth of *L.m.* in comparison to their immature and mature counterparts (Popov, Driesen et al. 2008). In contrast, infection of M $\phi$  with bacteria, including *L.m.*, has been associated with a strong proinflammatory phenotype, displaying characteristics for classically activated M1 M $\phi$  (Benoit et al., 2008). This observations triggered several questions: first, are M $\phi$  in granuloma counteracting the regulatory function of DC in chronic *L.m.* infection? Second, how are M $\phi$  infected with *L.m.* related to the current model of M $\phi$  polarization? Third, is IDO1 expression a key mechanism that allows DCreg to control the intracellular growth of *L.m.*? And fourth, is IDO1 also relevant in defense mechanisms in M $\phi$  against *L.m.* infection? These questions were approached on different levels using an in vitro model of infection of M $\phi$  and DC. The host-pathogen interaction was studied via unbiased whole transcriptome analysis, as well as, by hypothesis driven in vitro assays.

## 3. Materials

### 3.1 Chemicals and Reagents

1-methyl-DL-tryptophan	Sigma Aldrich, Taufkirchen, DE
Anthranilic acid	Sigma Aldrich, Taufkirchen, DE
3- Hydroxy-L-Kynurenine	Sigma Aldrich, Taufkirchen, DE
3- Hydroxyanthranilic acid	Sigma Aldrich, Taufkirchen, DE
BCA protein assay kit	Thermo Scientific, Rockford, USA
BHI agar	Roth, Karlsruhe, DE
BHI broth	Applichem, Gatersleben, DE
Boric acid	Merck, Darmstadt, DE
Brefeldin A Sigma	Aldrich, Taufkirchen, DE
BSA	Sigma, St Louis, USA
Cell-Gro	Cellgenix, Freiburg, DE
CFSE	Sigma-Aldrich, München, DE
Cytofix/Cytoperm kit	BD Biosciences, Heidelberg, DE
Dimethylsulfoxid (DMSO)	Sigma-Aldrich, München, DE
Dithiothreitol (DTT)	Sigma Aldrich, München, DE
Dynabeads <sup>®</sup> M-450	InvitrogenLifeTechnologies, Karlsruhe, DE
Ethylendiamintetraacetat (EDTA)	Sigma, St Louis, USA
Ethanol	Roth, Karlsruhe, DE
Fetal calf serum (FCS)	Invitrogen LifeTechnologies, Karlsruhe, DE
Glacial acetic acid	Roth, Karlsruhe, DE
Gentamycin	Sigma-Aldrich, DE
Glacial acetic acid	Roth, Karlsruhe, DE
Glutamax	Invitrogen Life Technologies, Karlsruhe, DE
Griess reagent system	Promega, Fitchburg, Winsconsin, USA
Ionomycin	Sigma Aldrich, Taufkirchen, DE
L-kynurenine	Sigma Aldrich, Taufkirchen, DE
Luminol	Sigma Aldrich, Taufkirchen, DE
Methanol	Roth, Karlsruhe, DE
MicroBeads CD14 <sup>+</sup>	MiltenyiBiotec, Bergisch Gladbach, DE
miRNAeasy Mini Kit	Qiagen, Hilden, DE

---

Sodium chloride (NaCl)	Roth, Karlsruhe, DE
Naïve CD4+ T cell isolationKit II	MiltenyiBiotec, Bergisch Gladbach, DE
NuPAGE®Transferpuffer 20x	Invitrogen Life Technologies, Karlsruhe, DE
Odyssey® Blocking Buffer	Licor Biosciences, Bad Homburg, DE
Odyssey® Two-Color molecular weight marker (10-250 kDa)	Licor Biosciences, Bad Homburg, DE
OptimemReduced Serum Medium	InvitrogenLifeTechnologies,Karlsruhe, DE
PBS	PAA Laboratories GmbH, Pasching, AT
Pancoll	PAA Laboratories GmbH, Pasching, AT
P-dimethylbenzaldehyde	Roth, Karlsruhe, DE
Penicillin	PAA Laboratories GmbH, Pasching, AT
Phorbol 12- myristate 13-acetate	Sigma Aldrich, Taufkirchen, DE
Picolinicacid	Sigma Aldrich, Taufkirchen, DE
Propidium Iodide	Sigma Aldrich, Taufkirchen, DE
Prostaglandin E <sub>2</sub>	Sigma Aldrich, Taufkirchen, DE
QIAzol <sup>®</sup>	Qiagen, Hilden, DE
Quinolinicacid	Sigma Aldrich, Taufkirchen, DE
Re-Blot plus mild solution	Merck-Millipore, Darmstadt, DE
RosetteSep CD4 <sup>+</sup> T cell enrichment kit	Stem Cell Technologies, London, GB
RPMI	PAA Laboratories GmbH, Pasching, AT
Running buffer 20x	Invitrogen Life Technologies, Karlsruhe, DE
SDS	AppliChem, Darmstadt, DE
Sodium chloride (NaCl)	Roth, Karlsruhe, DE
Sodium hydroxide (NaOH) (32 %)	Merck, Darmstadt, DE
Streptomycin	PAA Laboratories GmbH, Pasching, AT
Targetamp-Nanolabeling kit	
for IlluminaBeadChip	Epicentre, Madison, Wisconsin, USA
Trichloroaceticacid	Merck, Darmstadt, DE
TRIS (hydroxymethyl)-aminomethane	Roth, Karlsruhe, DE
Tryptophan	Sigma Aldrich, Taufkirchen, DE
Triton X-100	Promega Corporation, Madison, USA
Trypanblue	Merck, Darmstadt, DE
Tween 20	Merck, Darmstadt, DE
Trypanblue	Merck, Darmstadt, DE

## 3.2 Cytokines and TLR agonists

Human recombinant GM-CSF, IL-4, IFN- $\gamma$ , TNF- $\alpha$ , mouse recombinant GM-CSF and M-CSF were purchased from Immunotools, Friesoythe, DE. Pam<sub>3</sub>Cysk4 was purchased from Invivogen, San Francisco California, USA.

## 3.2 Antibodies

### Western blot and functional assays

Antigen	Species	Distributor
$\alpha$ -actin	Mouse anti-human	Merck- Millipore, Darmstadt, DE
CD3	Mouse anti-human	Janssen-Cilag, NeUSAs, DE
CD28	Mouse anti-human	a kind gift of Dr. Carl June, Abramson Cancer Research Center, University of Pennsylvania, Philadelphia
COX-2	rabbit	Caymanchemicals, Ann Arbor, Michigan USA
IDO1	Mouse anti-human	Oriental yeast
IDO1	Rat anti-mouse	Biolegend, San Diego, California USA
iNOS	Rabbit	Caymanchemicals, Ann Arbor, Michigan USA
IgG, IRDye 680	Anti-mouse	Licor Biosciences, Bad Homburg, DE
IgG, IRDye 800CW	Anti-mouse	Licor Biosciences, Bad Homburg, DE
IgG, IRDye 680	Anti-rabbit	Licor Biosciences, Bad Homburg, DE
IgG, IRDye 800CW	Anti -rabbit	Licor Biosciences, Bad Homburg, DE

### Flow cytometry

Antigen	Conjugate	Distributor
CD11c	PE	BD Biosciences, Heidelberg, DE
CD25	PE	BD Biosciences, Heidelberg, DE
CD80	FITC, PE	BD Biosciences, Heidelberg, DE
CD83	FITC, APC	BD Biosciences, Heidelberg, DE
CD86	APC	BD Biosciences, Heidelberg, DE
CD206	FITC	BD Biosciences, Heidelberg, DE
CD163	APC	RandD systems, Minneapolis, Minnesota, USA
CD 23	FITC	Biolegend, San Diego, California, USA
CD 14	APC	BD Biosciences, Heidelberg, DE
CD 64	PE	BD Biosciences, Heidelberg, DE
CD4	PE	BD Biosciences, Heidelberg, DE
CD45RA	FITC	BD Biosciences, Heidelberg, DE
CD3	APC-Cy7	BD Biosciences, Heidelberg, DE
IL-4	Alexafluor 488	BD Biosciences, Heidelberg, DE
IFN- $\gamma$	PE-Cy7	Biolegend, San Diego, California, USA
IL-17	Pacific blue	Biolegend, San Diego, California, USA
IL-2	Alexafluor 647	Biolegend, San Diego, California, USA
Anti-mouse IgG1 $\kappa$	APC, APC-Cy7, PE, PE-Cy7, Pacific blue	BD Biosciences, Heidelberg, DE Biolegend, San Diego, California, USA
Anti.mouse IgG2b	APC, PE, FITC	BD Biosciences, Heidelberg, DE Biolegend, San Diego, California, USA
Anti-rat IgG2 $\kappa$ b	Alexafluor 647	Biolegend, San Diego, California, USA
Anti-rat IgG2 $\kappa$ b	Alexafluor 647	Biolegend, San Diego, California, USA



### 3.3 siRNA oligonucleotides

Target Gene	Description	Target Sequence 5'-3'	Distributor
INDO	IDO siRNA - 1	UCACCAAUCCACGAUCAU	Thermo Scientific, Rockford, USA
INDO	IDO siRNA - 2	UUUCAGUGUUCUUCGCAUA	Thermo Scientific, Rockford, USA
INDO	IDO siRNA - 3	GUAUGAAGGGUUCUGGGAA	Thermo Scientific, Rockford, USA
INDO	IDO siRNA - 4	GAACGGGACACUUUGCUAA	Thermo Scientific, Rockford, USA
Renilla	control siRNA	AAAAACATGCAGAAAATGCTGTT	Biomers.net, Ulm, DE

### 3.4 cDNA synthesis and RT-PCR primers

The Transcriptor first strand cDNA synthesis kit as well as the universal probe library system for semi-quantitative real time PCR were purchased from Roche applied sciences, Switzerland. The primers were designed using the ProbeFinder software. The corresponding oligonucleotides were purchased from Sigma-Aldrich, Taufkirchen, DE.

Target Gene	Sequence5'-3'
IL6	gaggagcccagctatgaact gaaggcagcaggcaacac
IL1B	tacctgtcctgcgtgttgaa tcttgggtaattttgggatct
IL8	ctagagccgaactcaagttcc atggtccttccgggtgt
IFNG	ggcattttgaagaattggaag tttggatgctctggtcatctt
IL10	tgggggagaacctgaagac ccttgctctgtttcacagg
PTGES2	cttcacgcatcagttttcaag tcaccgtaaataatgatttaagtccac
GADPH	agccacatcgctcagacac gccaatacgaacaaatcc
IDO2	gaaatgaagcttgacacttcacc tctgtggggctccattattt

### 3.5 Enzyme linked immunosorbent assay

Human IL-10, IL-6 and TNF- $\alpha$  ELISA MAX standard kit were purchased from Biolegend, San Diego California, USA. The human IL-12 (p70) OptEIA kit was purchased from DB, Heidelberg, DE. Human soluble CD25 and IFN- $\gamma$  Eli-pair kit were purchased from Diaclone, Besancon, Fr. Human interferon- $\alpha$  ELISA kit was purchased from Pbl interferon source, Piscataway, USA and human IFN- $\beta$  was purchased from USACNK, Wuhan, China.

### 3.6 Plastic ware

96-well tissue culture plate	Greiner bio-one, Frickenhausen, DE
0,2 - 2 ml Eppendorf tubes	Eppendorf GmbH, Hamburg, DE
Hyperfilm™ ECL	GE healthcare, Piscataway, US
LS columns	Miltenyi Biotech, Bergisch Gladbach, DE
Nitrocellulose-Membrane, Hybond-C Extra	GE healthcare, Piscataway, US
Nunclon™ 6-well tissue culture plate	Thermo Scientific, Rockford, US
Nunclon™ 24-well tissue culture plate	Thermo Scientific, Rockford, US
Nunclon™ 48-well tissue culture plate	Thermo Scientific, Rockford, US
NuPAGE® Novex Bis-Tris Gels, 10 %	Invitrogen, Carlsbad, US
Parafilm	Pechiney, Chicago, US
Pipettes 2, 5, 10 and 25 ml	Greiner bio-one, Frickenhausen, DE
Pipette tips, 10, 200, 1000 µl	Greiner bio-one, Frickenhausen, DE
Pre-Separation Filters	MiltenyiBiotech, Bergisch-Gladbach, DE
Safe Seal Tips	BIOzym Diagnostik GmbH, DE
SentrixBeadChips V3	Illumina, Eindhoven, NL
Falcon 15 ml	Greiner bio-one, Frickenhausen, DE
Falcon 50 ml	Greiner bio-one, Frickenhausen, DE
Syringe 50 ml	Braun, Melsungen, DE
Sterile filter 22 µm	Sartorius, Hannover, DE

### 3.7 Equipment

Centrifuges	
Type 5810R	Eppendorf GmbH, Hamburg, DE
Type 5415	Eppendorf GmbH, Hamburg, DE
Type 5424	Eppendorf GmbH, Hamburg, DE
Incubators	
Binder C series	Binder, Tuttlingen, DE
Binder B series	Binder, Tuttlingen, DE

---

Orbital shaking incubator	Stuart, Staffordshire, UK
BD LSR II Flow cytometer	BD Biosciences, Heidelberg, DE
Gene pulserXcell™	BioRad Laboratories, München, DE
HiScanSQ system	Illumina, Eindhoven, NL
LightCycler 480 PCR system	Roche diagnostics, Basel, Switzerland
Magnet MPC-S	DynalBiotech, Oslo, NO
Magnet MACS Multi Stand	MiltenyiBiotech, Bergisch Gladbach, DE
Auto MACS pro separator	MiltenyiBiotech, Bergisch Gladbach, DE
Medgenix 400 AT microplate reader	SLT Instruments, Salzburg, AT
Mikroskope SM-LUX	Leitz, Wetzlar, DE
Mini-Protean Electrophoresis System	Bio-Rad Laboratories, München, DE
NanoDrop	Thermo Scientific, Rockford, USA
Neubauer chamber	Carl Roth Karlsruhe, DE
Odyssey® Infrared Imaging System	LI-COR Biosciences, Bad Homburg, DE
pH-meter	Knick, Berlin DE
Pipette boy	IBS Integra Biosciences, CH
PowerPac HC Power Supply	Bio-Rad Laboratories, München, DE
Roller Mixer SRT 1	Stuart, Staffordshire, UKMettler-Toledo, Zwingenberg, DE
Scale	GFL, Burgwedel, DE
Shaker (type 3011)	Bio-Rad Laboratories, München, DE
Trans-Blot Semi-Dry Transfer Cell	Bender&Hobein AG, Zürich, CH
Vortex Genie2	

### 3.8 Software

Mayday	Integrative Transcriptomics. Center for Bioinformatics Tuebingen, University of Tuebingen
CorelDRAW X4	Corel Corporation, Ontario, CA
FACS Diva	BD Biosciences, Heidelberg, DE
Flowjo 7.6.1	Tree Star, Ashland, Oregon, USA
GenomeStudio	Illumina, Eindhoven, NL

LightCycler 480 SW 1.5	Roche applied sciences, Basel, CH
Microsoft Office	Microsoft GmbH, Unterschleissheim, DE
ImageJ	free license, <a href="http://rsb.info.nih.gov/ij/">http://rsb.info.nih.gov/ij/</a>
Odyssey V3.0	Licor Biosciences, Bad Homburg, DE
Partek genomics suite	Partek, Saint Louis, Missouri, USA
ProbeFinder	Roche applied science, CH
SigmaPlot 10.0	Systat Software GmbH, Erkrath, DE

## 4. Methods

Blood samples from healthy blood donors were collected at the Institute for Experimental Hematology and Transfusion Medicine of the University Hospital Bonn, after written consent was obtained. The blood samples in form of buffy coats were provided immediately after processing.

### 4.1 Isolation of monocytes

Monocytes were isolated from human blood by CD14 positive selection using the magnetic assorted cell sorting (MACS) technique. In the first step, peripheral blood mononuclear cells (PBMCs) were isolated by centrifugation at 250g for 25 minutes in a Pancol density gradient. After the centrifugation step, the interface containing the PBMCs was collected and washed twice with PBS. The fraction of white blood cells was resuspended in 3 ml of MACS buffer (BSA 0.5%, 20mM EDTA in PBS) and incubated with 200  $\mu$ l of CD14<sup>+</sup> magnetic beads for 20 minutes. During this incubation time, LS columns were assembled in a midi-MACS separation magnet. In addition, a pre-separation filter was used to avoid the transfer of cell aggregates. Subsequently, the cells were washed once and applied directly onto the separation filter. The column was washed three times with 3 ml of MACS buffer, after magnet removal the CD14<sup>+</sup> fraction was eluted and counted. The purity was assessed via staining with CD14 and CD11c antibodies coupled to fluorochromes, followed by fluorescence activated cell sorting (FACS) analysis. Only monocyte fractions with purity above 95% were used for subsequent analysis.

### 4.2 Generation of human monocyte derived macrophages

Freshly isolated monocytes were cultured in RPMI supplemented with 10% fetal calf serum (FCS) in the presence of 500U/ml of recombinant human (rh) granulocyte macrophage colony-stimulating factor (rhGM-CSF) or 50U/ml macrophage colony-stimulating factor (rhM-CSF) at a cell density of  $2 \times 10^6$  cells/ml. The cells were seeded in 6 well- plates (5ml/well) and maintained for 72 h at 37°C 5%CO<sub>2</sub>. M $\phi$  were harvested after this time, and the purity of the cell culture was tested through staining with CD206 and CD14 fluorochrome coupled antibodies followed by FACS analysis. Depending on the

experiments to perform, M $\phi$  were harvested directly at day three or culture for additional 3 days with maturation stimuli for polarization experiments (Figure 1).

### 4.3 Generation of human monocyte derived dendritic cells

Freshly isolated monocytes were cultured in Cell-Gro serum free media, supplemented with 1% glutamine and 800U/ml of rhGM-CSF and 500U/ml rhIL-4 at a cell density of  $2 \times 10^6$  cells/ml. The cells were seeded in 6 -well tissue culture plates (5ml/well) and maintained for 72 h at 37°C and 5%CO<sub>2</sub>. DC were harvested after this time, and the purity of the cell culture was tested through staining with CD209 fluorochrome coupled antibody followed by FACS analysis.

### 4.4 Polarization of human macrophages

After 72 h, M $\phi$  were counted and resuspended in RPMI supplemented with 10% FCS and 500U/ml rhGM-CSF. In addition to obtain M $\phi$  populations with different polarization status, M $\phi$  cultures were treated with soluble factors and cytokines as described in Table 1. The M $\phi$  polarization experiments were carried out with the kind support of Dr. Susanne Schmidt and other members of the group of Genomics and Immunoregulation from the Life and Medical Sciences (LIMES) Institute.

Polarization	Factor	Dose
M1	rhIFN- $\gamma$	200U/ml
M2	rhIL-4	500U/ml
Mreg	rhTNF- $\alpha$	800U/ml
	PGE <sub>2</sub>	1 $\mu$ g/ml
	Pam <sub>3</sub> CSK4	1 $\mu$ g/ml
M1	rhTNF- $\alpha$	800U/ml
other	PGE <sub>2</sub>	1 $\mu$ g/ml
other	Pam <sub>3</sub> CSK4	1 $\mu$ g/ml
other	rhIFN $\beta$	100U/ml
other	rhIFN- $\gamma$ , rhIFN $\beta$ , PGE <sub>2</sub> Pam <sub>3</sub>	200, 100U/ml, 1 $\mu$ g/ml

**Table 1. Cytokines and soluble factors used to stimulate M $\phi$**

Stimulated M $\phi$  were kept in culture for further 24 h. A minimum of  $1 \times 10^6$  cells were lysed in QIAzol<sup>®</sup> after the stimulation period. RNA extraction for microarray and qRT-PCR validation was performed with the miRNeasy mini kit, according to manufacturer's advice. Alternatively, supernatants of at least  $5 \times 10^6$  cells were collected to perform western blot, and ELISA assays. Additionally, for T cell polarization experiments, 24h post-stimulation M $\phi$  were washed three times with 10ml PBS and further cultured in RPMI supplemented with 10% FCS and rhGM-CSF (500 U/ml) during 24h at 37°C and 5%CO<sub>2</sub> (Figure 3).

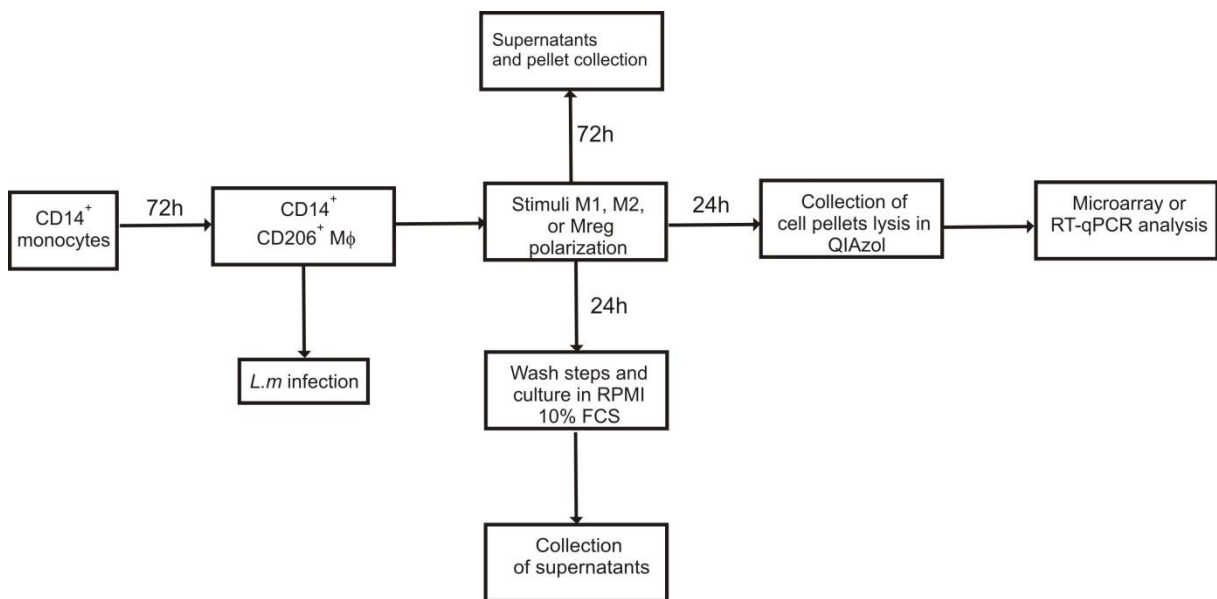


**Figure 3. Flowchart depicting the experimental procedure followed to generate polarized M $\phi$**

Freshly isolated monocytes were cultured in the presence of rhGM-CSF during 72 h. After this time, differentiated M $\phi$  were cultured in the presence of different cytokines and factors to generate cells with different polarization status.

#### 4.5 Maturation and stimulation of human dendritic cells

Immature monocyte derived DC (immDC) were counted and cultured in Cell-Gro medium supplemented with rhGM-CSF (800 U/ml) and rhIL-4 (500 U/ml). In addition, immDC were either left untreated or stimulated with rhTNF- $\alpha$  (800U/ml) alone or in concert with PGE<sub>2</sub> and Pam<sub>3</sub> to originate mature DC (matDC) or regulatory DC (DCreg) respectively. DC were harvested after 48 h and were stained with fluorochrome coupled antibodies against CD86, CD83 and CD25 for FACS analysis, in order to corroborate the success of the stimulation process, or collected to perform infection with *L.m*. After this period of incubation, DC viability was assessed via propidium iodide (PI) staining followed by FACS analysis.



## 4.6 Generation of murine bone marrow derived dendritic cells and macrophages

Murine DC and M $\phi$  were generated from the bone marrow of 10-16 week old C57BL/6 mice. Briefly, mice were sacrificed by exposure to Isofluran, followed by cervical dislocation. Immediately after the sacrifice, the tibiae and femur of hind legs were released, and the soft tissue was removed. Subsequently, the bones were cut on the extremes and the bone marrow was flushed out using a 27G syringe. After one washing step, the recovered cells were cultured for 7 days in IMDM medium supplemented with 10% FCS, 100 U/ml penicillin and 0.1 mg/ml streptomycin. To drive the differentiation of bone marrow cells towards DC or M $\phi$  10ng/ml (200U/ml) of recombinant murine (rm) GM-CSF or rmM-CSF, respectively, were added to the cell culture medium.

## 4.7 IDO1 silencing and enzymatic activity inhibition

IDO1 was silenced using small interfering RNA (siRNA) technique, a method that allows the post-transcriptional targeting of genes based on the principle of RNA interference. By this mechanism, short double strand RNAs (20-25 bp) target the degradation of complementary and usually fully processed mRNAs mediated by the RNA induced silencing complex (RISC) (Moss 2001). ImmDC were collected, counted and washed twice with PBS. Finally, cells were resuspended in Opti-MEM<sup>®</sup> medium at a cell density of  $4 \times 10^7$  cells/ml. In the next step, four different pre-designed artificial siRNA sequences targeting IDO1 were prepared in 1X siRNA dilution buffer at a final concentration of 20 $\mu$ M. In total 10 $\mu$ g of siRNA (2.5  $\mu$ g/each sequence) were placed on the bottom of 4 mm electroporation cuvettes. 100  $\mu$ l of the cell suspension were added gently to the mixture. After 3 minutes of incubation at room temperature, the cells were electroporated using a wave square protocol composed of two pulses of 1000 V with a pulse length of 0.5ms. Immediately after the procedure, the cells were transferred to fresh culture media supplemented with rhGM-CSF and rhIL-4 and incubated for further 48 h. ImmDC transfected with 10 $\mu$ g of renilla control siRNA under the same conditions described above were used as controls. IDO1 and control siRNA transfected DC were stimulated with TNF- $\alpha$  together with PGE<sub>2</sub> and Pam<sub>3</sub> or left untreated. After 24 h the cells were collected and infected with *L.m.* as described in chapter 4.9. Approximately  $2 \times 10^6$  cells were used to evaluate the bacterial burden during 6 hpi. Additionally,  $2 \times 10^6$  infected cells were kept in

culture for 24h in order to evaluate IDO1 silencing efficiency via western blot and determination of Kyn by Ehrlich colorimetric reaction (Figure 4).

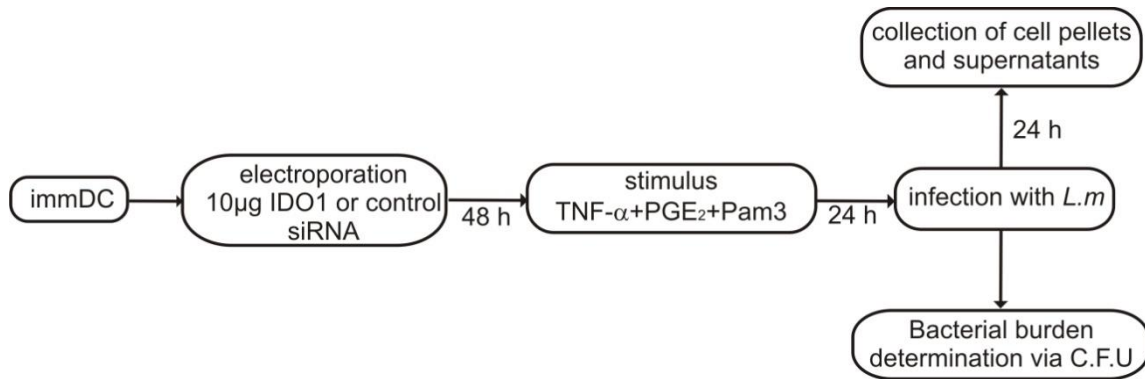


**Figure 4. Flowchart depicting the experimental approach followed to silence IDO1 in DC**

immDC were transfected with 10µg of control or IDO1 specific siRNA via electroporation. After 48 h of incubation immDC transfected with IDO1 or control siRNA were stimulated with TNF- $\alpha$  in combination with PGE<sub>2</sub> and Pam<sub>3</sub> and incubated for 24h. Pretreated DC were infected with *L.m.* and the bacterial burden was assessed. IDO1 silencing efficiency was determined via western blot and Ehrlich colorimetric reaction.

The enzymatic activity of IDO1 was inhibited in DC and M $\phi$  with the competitive inhibitor 1-methyl-tryptophan (1-MT). Prior to infection with *L.m.*, myeloid cells were treated with 150 µM 1-MT. To evaluate the bacterial burden after IDO1 enzymatic inhibition DC and M $\phi$  were kept during 6h in HBSS supplemented with 150 µM of 1-MT and 24 µM of Trp. The cell viability was assessed via PI staining followed by FACS analysis. The efficiency of IDO1 enzymatic inhibition was evaluated by measuring of Kyn accumulation in supernatants of treated cells.

## 4.8 Bacteria culture and FITC labeling

*Listeria innocua* (*L.i.*), *L.m.* strain EGD-e wild type and hly mutant were kindly provided by Professor Doctor Trinad Chakraborty, Institute for Medical Microbiology, Justus-Liebig-University of Giessen, Germany. The bacteria were cultured overnight in brain heart infusion (BHI) broth at 37°C. The next day, the cultures were diluted 1:50 in fresh BHI broth and cultured under the same conditions until the optical density at 600nm (OD600) reached 1. At this point, the bacteria were centrifuged at 4000xg for 30 minutes at 4°C.

Approximately half of the total recovered bacteria were mixed in 10% DMSO in PBS and were frozen immediately at  $-80^{\circ}\text{C}$ . The rest of the culture was resuspended in a solution of fluorescein isothiocyanate (FITC) 0.1 mg/ml in 0.1M  $\text{NaHCO}_3$  (pH 9.0) and incubated for 1 h at  $25^{\circ}\text{C}$ . After this incubation, the bacteria were washed extensively and frozen as described previously. 24h after the procedure, the viability of the bacteria in the frozen aliquots was determined via colony forming unit assay (CFU). Briefly, serial dilutions of bacteria suspensions ( $10^{-4}$ - $10^{-7}$ ) were performed and plated on BHI agar. The plates were incubated at  $37^{\circ}\text{C}$  overnight and counted the next day. *Streptococcus piogenes* (*S.p*) was cultured in sheep blood agar during 24 h. The next day the bacteria were transferred in BHI broth and frozen aliquots were prepared in 10% DMSO.

#### **4.9 Infection of human dendritic cells and macrophages with *L. monocytogenes***

DC and  $\text{M}\phi$  were counted and washed twice with PBS. After the last wash step, the cells were resuspended in HBSS at a cell density of  $4 \times 10^6$  cells /ml. Meanwhile, the suspension of FITC labeled *L.m.* was prepared in HBSS supplemented with 10% of human serum, to achieve a multiplicity of infection (MOI) of 1:10. Subsequently, 500 $\mu\text{l}$  of the bacterial suspension were mixed 1 to 1 with the cell suspension. The bacteria-cell mixture was placed during 30 minutes at  $37^{\circ}\text{C}$  under constant rotation. As a control, the cells were resuspended in PBS supplemented with 10% of human serum. After this incubation time, the cells were chilled immediately on ice and washed extensively four times. To avoid the transference of free bacteria to further cell cultures, the cell suspension was passed through a density gradient of 30% glucose. Finally, the cells were counted and cultured either in RPMI ( $\text{M}\phi$ ) or Cell-Gro (DC) supplemented with 50 $\mu\text{g}$  of gentamycin and the percentage of infection was assessed via FACS analysis. Additionally, DC and  $\text{M}\phi$  were placed on HBSS, to evaluate their microbicidal capabilities by determining *L.m.* viability via CFU as described under section 4.10. Cell pellets and supernatants of infected cells were collected at 24hpi and kept at  $-80^{\circ}\text{C}$ . For some experiments, freshly collected supernatants were passed through a 0.22  $\mu\text{m}$  membrane, to avoid the transference of extracellular bacteria. Experiments of  $\text{M}\phi$  and DC infection were performed with the kind support of Dr. Zeinab Abdullah (Institutes of Molecular Medicine and Experimental Immunology, University of Bonn, Bonn, Germany).

#### **4.10 Determination of bacterial burden in infected dendritic cells and macrophages**

The bacterial burden of infected cells was evaluated by CFU analysis. Immediately after infection,  $2 \times 10^6$  DC or M $\phi$  were resuspended in 1ml HBSS. To establish the initial number of bacteria that entered the cells, 100 $\mu$ l of the cell suspension were added to a solution of triton 0.001% in water during 5 minutes, to lyse eukaryotic cells without affecting the viability of bacteria (Campbell, Canono et al. 2001). After the lysis, 1:10 dilutions were performed sequentially ( $10^{-2}$ - $10^{-5}$ ) and seeded on BHI agar. The remaining cell suspension was placed at 37°C under constant rotation. To establish *L.m.* viability in a time course 100  $\mu$ l aliquots of the cell suspension were taken at 0.5, 1, 2, and 6 hours post infection (hpi) and treated as described for the determination of initial bacterial burden. The inoculated plates were kept overnight at 37°C for counting on the next day. Dependent on the experiment HBSS was supplemented with Kyn 50-100  $\mu$ g/ml or Trp (98  $\mu$ M). In order to calculate the bacterial burden of infected cells at different time points, the initial number of colonies was set to 100% and the fraction of surviving colonies for the following time points was calculated on this basis.

#### **4.11 Infection of murine bone marrow derived dendritic cells and macrophages with *L. monocytogenes***

Bone marrow derived M $\phi$  (BMM) and DC (BMDC) were harvested and counted. 24h prior to the infection with *L.m.* BMM and BMDC cells were washed three times and seeded on six-well culture plates at a cell density of  $3 \times 10^5$  cells/ml in RPMI medium supplemented with 10% FCS, without any further additives. Immediately before the infection, *L.m.* suspension was prepared in HBSS supplemented with 5% of mouse serum and added to the cell monolayer to obtain a MOI of 1:5. The plates were incubated for 30 minutes at 37°C. After this incubation time the plates were chilled on ice and washed four times with cold HBSS. The cells were cultured for 24h in RPMI supplemented with 50 $\mu$ g/ml of gentamycin.

#### **4.12 Evaluation of the anti-bacterial and cytotoxic effect of tryptophan catabolites**

Stable intermediaries of the kynurenine pathway including Kyn, 3-hydroxy-L-kynurenine (3HK), anthranilic (AA), 3-hydroxy-anthranilic (HA), picolinic (PA) and quinolinic acid (QA)

were dissolved in water (100°C) at concentrations between 1-5 g/ml. To evaluate the anti-bacterial effect of Trp catabolites the stock solutions were filtered (0.22µM) and added to RPMI medium to obtain final concentrations between 48 and 200µM. Meanwhile, *L.m.*, *L.i.* and *S.p.* frozen aliquots were thawed and resuspended in RPMI to a final OD600 of 0.100. The bacterial suspension was mixed 1:1 with the solutions of Trp catabolites or RPMI alone in 48 well-plates and the resultant cultures were incubated during 24 h at 37°C. In the next step, serial dilutions of the bacterial cultures were performed ( $10^{-2}$ - $10^{-5}$ ) and plated on BHI agar for *L.m.* and *L.i.* or sheep blood agar for *S.p.* The plates were incubated overnight, and the colonies were counted the next day. The number of colonies observed in RPMI alone was set as 100%. The fraction of colonies counted in RPMI supplemented with the different concentrations of Trp catabolites was estimated according to this.

To establish the potential cytotoxic effect of Trp catabolites on DC the stock solutions of Trp catabolites were diluted in Cell-Gro at a final concentration of 100µM. Subsequently, immDC and DCreg were resuspended in Cell-Gro alone or supplemented with Trp catabolites. The cell cultures were incubated during 48 h at 37°C, and the cell viability was assessed by PI staining, followed by FACS analysis.

### 4.13 Plaque assay

*L.m.* was grown overnight in BHI broth at 37°C with shaking (150 rpm). On the next day bacterial cultures were diluted and further incubated during 3 h alone or in the presence of Kyn at concentrations of 12.5 µM, 25µM and 50µM. 3T3 fibroblast monolayers were cultured in RPMI supplemented with 10% FCS without antibiotics prior to infection the cells were seeded in 6-well plates and plaque assay was performed as follows. Confluent cell monolayers of 3T3 fibroblast were infected with an MOI of 0.1 or alternatively with serial dilutions ( $10^{-2}$ - $10^{-5}$ ) obtained after lysis of immDC or DCreg 6 hpi. After the infection cells were overlaid with 0.5% low melting point agarose supplemented with 10µg/ml of gentamycin and incubated during 72 h at 37°C. Plaques were visualized by addition of agarose 0.5% supplemented with 0.1% of neutral red and 10µg/ml of gentamicin. After 6 h the plates were scanned on a HP precision scanner. The plaque diameter was determined using image J (U. S. National Institutes of Health, Bethesda, Maryland, USA, <http://imagej.nih.gov/ij/>, 1997-2012).

#### 4.14 Isolation of human CD4<sup>+</sup> T cells

The population of CD4<sup>+</sup> T cell was enriched from human blood via Rosettesep method. Briefly, 50 µl of enrichment cocktail were added per ml of blood. After 20 minutes of incubation at room temperature, the cells were overlaid carefully on Pancol density media and centrifuged at 250xg during 20 minutes with the brake off. The enriched CD4<sup>+</sup>Tcell population was recovered from the interface and stained with carboxyfluorescein diacetate succinimidyl ester (CFSE). Alternatively, CD4<sup>+</sup> naïve T cells were isolated via MACS technique, according to the protocol provided by the manufacturer. PBMCs were isolated as described under section 4.1. After the procedure,  $10 \times 10^6$  cells were incubated during 10 minutes with 10µl of the biotin antibody cocktail II at 4°C. Next, the cells were washed twice and incubated for 15 minutes with the anti-biotin magnetic beads at 4°C. In the final step, the cells were washed and resuspended in 500 µl of MACS buffer, to perform magnetic separation using the auto MACS pro separator under the sensitive depletion program. The purity of T cells was evaluated via FACS analysis after staining with fluorochrome coupled antibodies against CD4 respectively CD3. For naïve T cells, a third anti-CD45RA antibody was added to the staining panel.

#### 4.15 Generation of artificial antigen presenting cells

Artificial antigen presenting cells (aAPCs) were generated via coating of magnetic beads with a solution of antibodies as follows; anti-CD3 (5%), anti-CD28 (13%) and anti MHC-1 (81%) prepared in 0.1M of boric acid. The magnetic beads were incubated overnight with the antibody solution at 4°C under constant rotation. In the next step, the beads were washed three times using bead wash buffer (PBS 3% BSA and 0.1% NaN<sub>3</sub>) by placing the containing vials on a magnet and replacing the buffer. Each wash step was followed by incubations of 30 minutes in a rotator, and the last incubation step was performed overnight. The washed beads were counted and resuspended to a density of  $50 \times 10^6$  beads/ml. Alternatively, control beads coated only with CD3 and MHC-1 antibody were prepared following the same process described above.

#### 4.16 T cell proliferation assay

Freshly isolated CD4<sup>+</sup>T cells were stained with CFSE as follows. Immediately after the isolation procedure,  $10 \times 10^6$  CD4<sup>+</sup>T cells were washed twice and resuspended in a CFSE solution (0.5 µM in PBS). The cells were incubated at room temperature during 8 minutes with constant shaking. After this incubation, two wash steps were performed, and the cells

were counted. Next, the stained CD4<sup>+</sup>T cells were resuspended in fresh RPMI medium supplemented with 10% FCS at a cell density of  $1 \times 10^6$  cells/ml and were co-cultured with aAPCs at a 1:1 ratio. For some experimental conditions, the RPMI medium was supplemented with 50% of supernatants conditioned previously by M $\phi$  with different status of polarization, including untreated control, M1, and *L.m.*-infected. After 72 h, the cell proliferation was assessed by detecting the dilution of the CFSE dye via FACS analysis. The percentages of proliferating cells, as well as the division index were calculated with the tool for cell proliferation of the Flowjo 7.6.1 software.

#### 4.17 T cell cytokine production assay

Freshly isolated naïve CD4<sup>+</sup>T cells were co-cultured with aAPCs (1:1 ratio) in RPMI supplemented 10% FCS alone or with 50% of supernatants conditioned previously by M $\phi$  with different status of polarization. After 72 h, T cells were stimulated during 2 h with phorbolmyristate acetate (PMA) and ionomycin. The cells were washed once, and treated with brefeldin A during 2 h. After this incubation time, the cells were washed twice and stained during 30 minutes with a solution 1:3000 of the Invitrogen live/dead AmCyan ® coupled dye, in order to identify the population of viable cells. Subsequently, intracellular staining with fluorochrome coupled antibodies against the cytokines, IFN- $\gamma$ , IL-10, IL-17, IL-4 and IL-2 was performed followed by FACS analysis.

#### 4.18 Flow cytometry

Flow cytometry is a versatile technique that uses light scattering, light excitation and emission of fluorochromes to generate multi-parameter information of cells (Macey 2007). To assess the expression of surface molecules in M $\phi$  and DC, between  $1$  and  $2 \times 10^5$  cells per treatment were resuspended in 300 $\mu$ l of blocking buffer (PBS 10% FCS) and incubated during 20 minutes on ice. After this incubation period, 1-5  $\mu$ l of antibodies coupled to fluorochromes (see materials section) were added to the cells and incubated at 4°C for 20 minutes. Next, the cells were washed with 2ml of PBS and centrifuged at 300g during 8 minutes. The supernatants were discarded, and 200 $\mu$ l of fresh PBS were added. To control the unspecific binding of antibodies,  $2 \times 10^5$  cells per each treatment were stained with matching isotype controls for each one of the antibodies used for the staining. Simultaneously, the compensation controls were prepared by performing single stainings on anti-IgG1 $\kappa$  coated polystyrene beads using antibodies coupled to the complete panel

of fluorochromes used on each assay. To control the viability of the analyzed populations, the cells were stained with PI at a final concentration of 1µg /ml added immediately before the acquisition of the events in the flow cytometer.

To evaluate the expression of intracellular molecules, the cells were collected after treatment with the Invitrogen live/dead AmCyan dye<sup>®</sup>. Subsequently, the cells were incubated during 20 minutes in the dark with 1ml of the fix/perm buffer. Immune cells were washed once and incubated with 1ml of permeabilization buffer for 15 minutes at room temperature in the dark followed by a wash step. After this procedure, the cells were incubated with 5 µl of the selected antibodies or their correspondent isotype antibodies during 30 minutes at room temperature followed by a wash step with PBS. Finally, the cell pellets were resuspended in 200 µl of fresh PBS. The compensation controls were prepared as described for surface staining.

The data were acquired within a maximum of 2 h after sample preparation using a flow cytometer (BD LSRII) and the FACS Diva software. The cells were gated according to the expected size and granularity. Subsequently the population of viable cells was set based on the information provided by staining with PI (surface staining) or live/dead dye <sup>®</sup> (intracellular staining). After suitable gates were fixed, 10.000-50.000 were acquired and the results were analyzed using the FlowJo7.6.1 software.

#### **4.19 RNA isolation**

Cell lysates prepared in 1ml of QIAzol<sup>®</sup> reagent were thawed and 200 µl of chloroform were added by mixing vigorously. Next, the samples were centrifuged at 12.000 g at 4°C for 15 minutes and the aqueous phase was transferred to a new tube. The aqueous phase was applied immediately to a miRNeasy mini kit<sup>®</sup> column. After 3 wash steps with the buffers provided by the supplier, the RNA was eluted in RNase free water. The quantity and quality of the isolated RNA was evaluated by measuring the absorption of the samples at 260 and 280 nm in a NanoDrop spectrophotometer. A ratio OD260/OD280 equal to 2 was considered as optimal. For microarray experiments, an additional quality control was carried out by analyzing the electrophoretic mobility of the RNA samples on a denaturing agarose gel.



## 4.20 Semi-quantitative real time PCR

The first strand cDNA synthesis kit<sup>®</sup> (Roche applied systems) was used to obtain cDNA starting from 500-1000 ng of RNA following the instructions provided by the manufacturer. In the first step, the RNA was annealed to the Anchored-oligo (dT)<sub>18</sub> primer by heating the mixture at 65°C. Next, the solution was chilled on ice and a master mix containing transcriptor reverse transcriptase enzyme, deoxynucleotides mix and RNase inhibitor was added. After 1 hour of incubation at 50°C, the reaction was inactivated by a heating step at 85°C for 5 minutes. The method is described in detail on table 2.

The semi quantitative real time (qRT-PCR) reaction was performed using the universal probe library system. The specific primers for every gene of interest were designed with the ProbeFinder software and were used together with the dye suggested by the program. The data were acquired with a Light Cycler 1.3 instrument and the analysis was performed using LightCycler<sup>®</sup> 4.05 software. In all cases, the expression of target genes was normalized by the expression of the house keeping gene glyceraldehyde-3-phosphate dehydrogenase (GAPDH). The composition of the qRT-PCR reaction, as well as, the program used for amplification are described in table 3.

Component	Amount
RNA	500-1000 ng
Anchored oligo (dT) <sub>18</sub> 50pmol/μl	1μl
H <sub>2</sub> O	Up to 13 μl
Incubate for 10 minutes at 65°C, immediately chill on ice	
Reverse Transcription buffer 5X	4μl
Deoxynucleotide mix (10mM each)	2μl
Transcriptor reverse transcriptase 20U/μl	0.5 μl
Incubate 50°C for 1 h the inactivate 85°C for 5 minutes	

**Table 2. cDNA synthesis procedure**

The cDNA was synthesized with the first strand cDNA synthesis kit from Roche applied systems following the instructions of the manufacturer.

RT-PCR master mix Component	amount
Universal ProbeLibrary probe	0.1 μl
Primer for 10uM	0.2 μl
Primer rev 10uM	0.2 μl
ddH <sub>2</sub> O	0.5 μl
Probe master mix: Reaction buffer, Hot start Taq polymerase, and dNTPs	5 μl
cDNA	4 μl
RT-PCR Programm	Temperature°C/ time/ number of cycles
Initial denaturation	95/10 min/1
Denaturation	95 /10s
Annealing	60/ 30s
Extension	72/ 5s
cooling	40/10s/1

**Table 3. Composition of qRT-PCR reaction and amplification program**

4μl of cDNA were seeded onto 96 well-plates and 6μl of the RT-PCR master mix were added. Every sample was assessed by triplicate.

## 4.21 Microarray analysis

The sample preparation for microarray analysis was carried out by Mr. Michael Kraut and Mrs. Laura Bohmman in the laboratory of genomics and immunoregulation at the LIMES Institute (Bonn, Germany). Briefly, biotin labeled cRNA was generated using the TargetAmp™-Nano Labeling Kit for Illumina® Expression BeadChip®. The biotin labeled

cRNA samples (1.5 µg) were hybridized on SentrixBeadChips V3 (Illumina) and scanned on an IlluminaHiScanSQ system<sup>®</sup>, following the instructions provided by the manufacturer. Suitable reports for further analysis were generated from raw data with the GenomeStudio software (Illumina). Subsequent data analysis was performed with Partek<sup>®</sup> genomics suite software. Quality of array data was assessed using pairwise scatterplots whereby the correlation coefficient should account to  $r^2 \geq 0.95$  (Beyer, Mallmann et al. 2012). The experiments included in the microarray analysis are summarized in table 4.

Cell type	stimulus	Time after stimulus (h)	Donors (n>3)
immDC	rhGM-CSF, rhIL-4	72	3
<i>L.m.</i> -DC	<i>L.m.</i> infection	24	3
Mφ	rhGM-CSF	72	6
GM-CSF <i>L.m.</i> -Mφ	<i>L.m.</i> infection	72	6
Mφ	rhM-CSF	24	3
M-CSF <i>L.m.</i> -Mφ	<i>L.m.</i> infection	24	3
M1	rhGM-CSF, rhIFN-γ	24	3
M2	rhGM-CSF, rh IL-4	24	3
Mreg	rhGM-CSF, rhTNF-α, PGE <sub>2</sub> , Pam <sub>3</sub>	24	5
Mφ	rhTNF-α	24	3
Mφ	PGE <sub>2</sub>	24	3
Mφ	Pam <sub>3</sub>	24	3
Mφ	IFN-β	24	3
Mφ	rhTNF-α, PGE <sub>2</sub> , Pam <sub>3</sub> IFN-β IFN-γ	24	3

**Table 4. Summary of experiments included for microarray analysis**

## 4.22 Bioinformatic Analysis

After passing the quality control, the data were normalized via the quantile normalization method and further bioinformatic analysis was conducted using the genomics suite of Partek<sup>®</sup> software. As first approach to study the relationship between the experimental groups, principal component (PCA) and hierarchical cluster analysis on variable genes were performed. Subsequently, the determination of differential expressed (DE) genes between the experimental groups was performed via ANOVA analysis. For all the data sets, the genes with a fold of change (FC) between 2 and -2 and a FDR corrected p-value <0.05 were defined as DE genes. To confirm that the variance between the experimental groups was dependent mainly on the treatment, and was not associated to random factors, like experimental error or donor-dependent variation, a two way ANOVA was conducted and the sources of variation were identified. Only data sets in which the treatment explained more than 60% of the variability were used. Additionally, in cases in which factors like donor intrinsic properties, or the variation associated to the beadchip used in the experiment explained over 10% of the variation between the groups, a batch removal correction was implemented. To compare the set of DE genes between groups, gene lists were generated and plotted as Venn diagrams. In order to determine whether the DE genes common between two groups presented similar tendencies, the relationship between FC was represented in a scatter FC vs FC (FC/FC) plots. To visualize the levels of gene expression in different experimental groups, the average expression values of target genes, were obtained from microarray experiments and were standardized using z-score transformation. The visualization of the data was obtained using Mayday software. Finally, to establish the biological meaning of DE genes observed in the experimental groups, gene ontology (GO) analysis was performed.

## 4.23 Cell lysis and western blot

Cell pellets were lysed in 30  $\mu$ l per  $2 \times 10^6$  of lysis buffer (20mM Tris-HCl, 10% Triton X-100, 100mM NaCl, 1mM EDTA, 1M DTT) and 1 miniTab of Roche protease cocktail inhibitor. The samples were incubated on ice for 30 minutes and centrifuged at 12.000 g for 10 minutes. The soluble phase was recovered, and the protein determination was performed by the bicinchoninic acid method. Between 20-50 $\mu$ g of total protein were loaded on a sodium dodecylsulfate-polyacrylamide (SDS) gel and the electrophoresis was run at 150 V for about 1.5 h. The protein transference from the gel to a nitrocellulose membrane was conducted at 100V for 20 min. Subsequently, the membranes were soaked in blocking buffer for 1 h. Immediately after blocking step, the membranes were

incubated overnight at 4°C, with primary antibodies at the concentrations recommended by the manufacturer. The next day, the membranes were washed four times with 0.1% Tween in PBS, and were incubated for 1 h with suitable secondary antibodies coupled to infrared dyes (IRDye 700<sup>®</sup> or IRDye800<sup>®</sup>) at a concentration of 1 to 5000. After four washing steps, the membranes were scanned in an Odyssey imager. In all cases,  $\beta$ -Actin was used as a loading control and the acquired images were analyzed using ImageJ software.

#### **4.24 Enzyme linked immunosorbent assay**

Enzyme linked immunosorbent (ELISA) assays were performed to determine the concentration of the cytokines IL-6, TNF- $\alpha$ , IL-10, IFN- $\gamma$ , IFN- $\alpha$ , IFN- $\beta$  and the soluble receptor CD25 in supernatants of DC and M $\phi$  from different experimental groups. In all cases, the instructions provided by the supplier were followed precisely. Briefly, supernatants from treated DC and M $\phi$  were incubated for 2 h in 96 well-plates previously coated with suitable capture antibodies. The plates were washed extensively with the solution recommended by the supplier. Subsequently the plates were incubated with suitable biotinylated detection antibodies. After extensive washing steps, the plates were incubated with streptavidin coupled horseradish peroxidase. For signal detection, the ready-to-use tetramethylbenzidine substrate was used. The reaction was stopped by the addition of 1 M H<sub>2</sub>SO<sub>4</sub>, and the absorbance was read at 450 nm with a microplate reader.

#### **4.25 Kynurenine and nitrite determination**

The Kyn amount in DC supernatants was determined by Ehrlich colorimetric reaction assay (Braun et al., 2005). Briefly, cell supernatants were mixed with 30% of trichloroacetic acid in a ratio of 2:1, vortexed and centrifuged at 10,000 rpm for 5 minutes. 75  $\mu$ l of the upper phase were removed and added to an equal volume of Ehrlich reagent (100 mg P-dimethylbenzaldehyde and 5 ml glacial acetic acid) in a 96-well plate. Samples were assessed by triplicate against a standard curve of Kyn (0-100  $\mu$ g/ml). Optical density was measured with a microplate reader at 492 nm.

The nitrite detection was carried out via Griess colorimetric reaction. The cell supernatants were incubated for 10 min with Griess reagent A (1% Sulfanilamide solution) in 96-well plates. Next, the Griess reagent B (0.1% of N-(1-naphthyl) ethylene-diamine-dihydrochloride) was added to the mixture and incubated for further 10 minutes protected

from light. The absorbance was determined within 30 minutes after the reaction in a microplate reader.

#### **4.26 Determination of reactive oxygen species production**

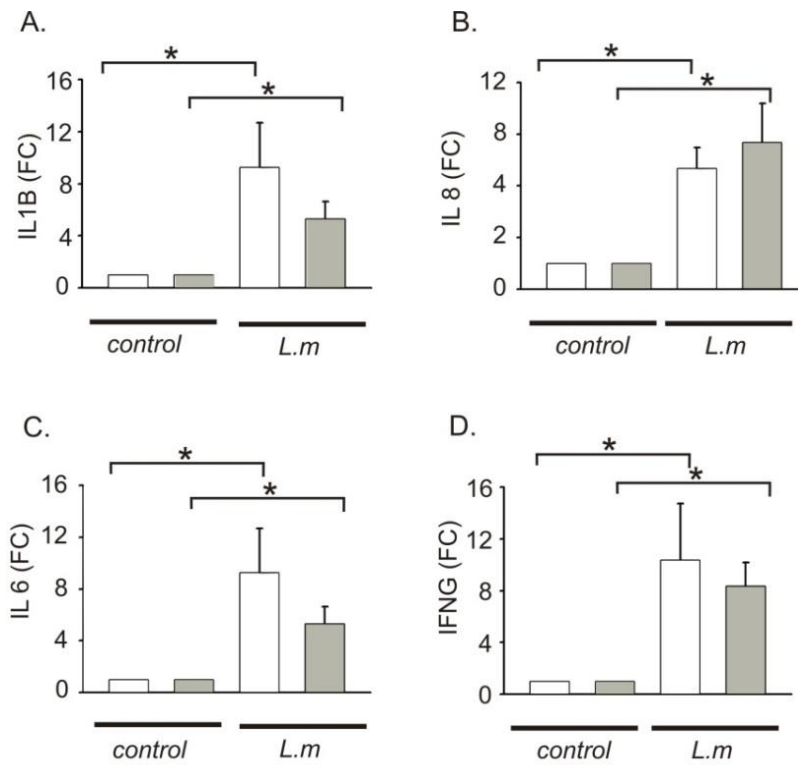
ROS production was assessed via the luminol amplified chemiluminescence method. DC and M $\phi$  infected with *L.m.* were seeded in dark 96 well-plates ( $2 \times 10^5$  cells/well). Next, 50  $\mu$ l of a solution containing luminol (250 $\mu$ M) and horseradish peroxidase (16U/ml) were added. Subsequently, the plates were transferred to a luminometer provided with temperature control. Measurements of light intensity were taken every 8 minutes during 6 h at 37°C.

## 5. Results

### 5.1 Macrophages infected with *L. monocytogenes* present immunostimulatory and immunomodulatory features

M $\phi$  and DC are the main constitutive elements of the outer ring wall of granuloma in patients chronically infected with *L.m.* (Popov, Abdullah et al. 2006; Popov, Driesen et al. 2008). Whereas previous studies have shown that human monocyte derived DC acquire regulatory properties upon *L.m.* infection (Popov, Abdullah et al. 2006; Popov, Driesen et al. 2008), bacterial infection of M $\phi$  including *L.m.* has been associated with a strong proinflammatory phenotype characteristic for M1 polarization (Benoit, Desnues et al. 2008). In order to gain insights about the function that M $\phi$  can accomplish in granuloma, an in vitro model of infection was used. Briefly, M $\phi$  differentiated from human blood monocytes in the presence of either GM-CSF (GM-CSF M $\phi$ ) or M-CSF (M-CSF M $\phi$ ) were exposed to *L.m.* using an MOI of 1:10. 24 hpi supernatants and cell pellets were collected to assess mRNA and protein expression of some distinctive markers for M1 polarization as well as immunomodulatory markers previously observed on DC infected with *L.m.*, but also in regulatory myeloid cells, including DCreg and Mreg.

In agreement with previous reports, GM-CSF and M-CSF M $\phi$  infected with *L.m.* increased significantly the mRNA expression of proinflammatory mediators, including the cytokines IL1B, IL6, IFNG and the chemokine IL8 when compared to uninfected M $\phi$  (Figure 5). Furthermore, a strong accumulation of the proinflammatory cytokines IL-6, IFN- $\gamma$ , TNF- $\alpha$  and IL-12 was detected via ELISA in supernatants of *L.m.* infected M $\phi$  whereas supernatants from control M $\phi$  contained low or non-detectable levels of these cytokines (Figure 6). Although, M-CSF M $\phi$  tend to produce lower amounts proinflammatory cytokines when compared to GM-CSF M $\phi$ , these differences were only statistically significant for IL-12 production suggesting that in general terms the pro-inflammatory response against *L.m.* is common for both subtypes. Together, this data suggest that the in vitro model of infection herein established reflects the features of *L.m.* infected M $\phi$  (*L.m.*-M $\phi$ ) described in the literature including the acquisition of properties associated to a M1 phenotype.



independent experiments \* $p < 0.05$  (student's  $t$  test) non detected (n.d).

### Figure 5. Mφ infected with *L.m.* express proinflammatory cytokines

The fold of change (FC) in mRNA expression of **A.** IL1B, **B.** IL8, **C.** IL6 and **D.** IFNG was assessed via q RT-PCR in GM-CSF (white bars) and M-CSF derived Mφ (grey bars) either infected with *L.m.* or untreated at 24 hpi. The expression of the target mRNA was normalized by GAPDH expression. The FC was calculated in respect to the control. The results represent the mean  $\pm$  sd of four

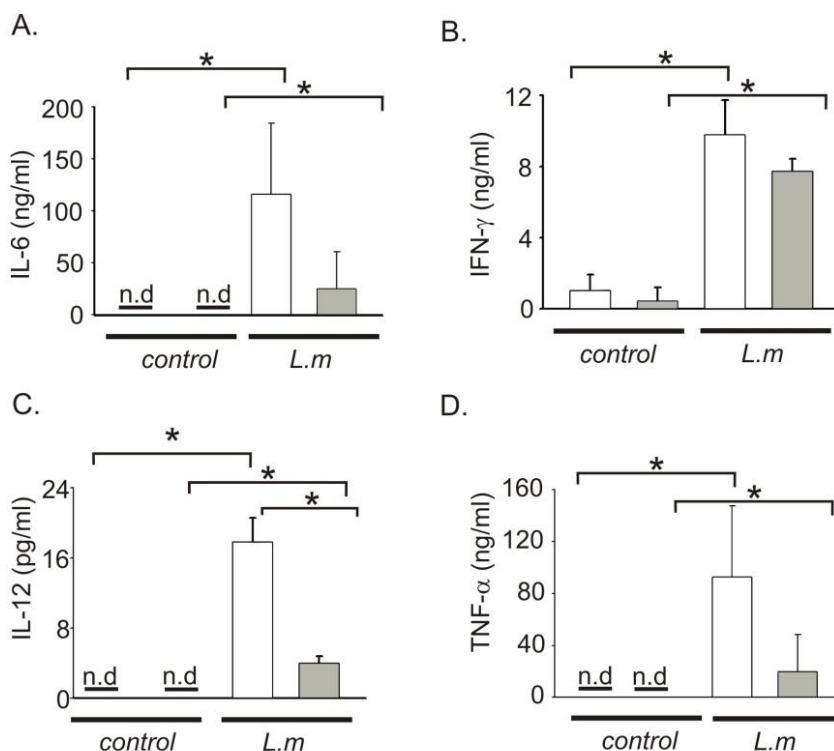


### Figure 6. Mφ infected with *L.m.* secrete proinflammatory cytokines

The secretion of **A.** IL-6, **B.** IFN- $\gamma$ , **C.** IL-12 and **D.** TNF- $\alpha$  was evaluated via ELISA in supernatants of GM-CSF (white bars) and M-CSF (grey bars) derived Mφ control or infected with *L.m.* at 24 hpi. The results are presented as the mean  $\pm$  sd of four independent experiments \* $p < 0.05$  (student's  $t$  test), non detected (n.d).

Despite the prominent proinflammatory properties exhibited by *L.m.*-Mφ, these cells also expressed molecules associated with regulatory function. For instance, the mRNA



expression of IL10, a hallmark cytokine for M2 polarized M $\phi$  (Sica and Mantovani 2012) was upregulated between 6 and 10 fold in *L.m.*-M $\phi$  when compared to control cells (Figure 7A). Moreover, the increase in IL10 mRNA transcripts was concomitant with a robust accumulation of IL-10 protein in the supernatants of GM-CSF and M-CSF infected M $\phi$  (60-65 ng/ml), but it was not detectable in supernatants of control cells (Figure 7B). Similarly, the expression of PTGS2 mRNA increased around 10 fold in the infection model of *L.m.*-M $\phi$  (Figure 7C). In addition, the product of the PTGS2 gene, the enzyme COX-2, which acts in concert with several prostaglandin synthases to produce the anti-inflammatory mediator PGE<sub>2</sub> (Kalinski 2012) was also detected via western blot in *L.m.* infected, but not in control M $\phi$  (Figure 7D).

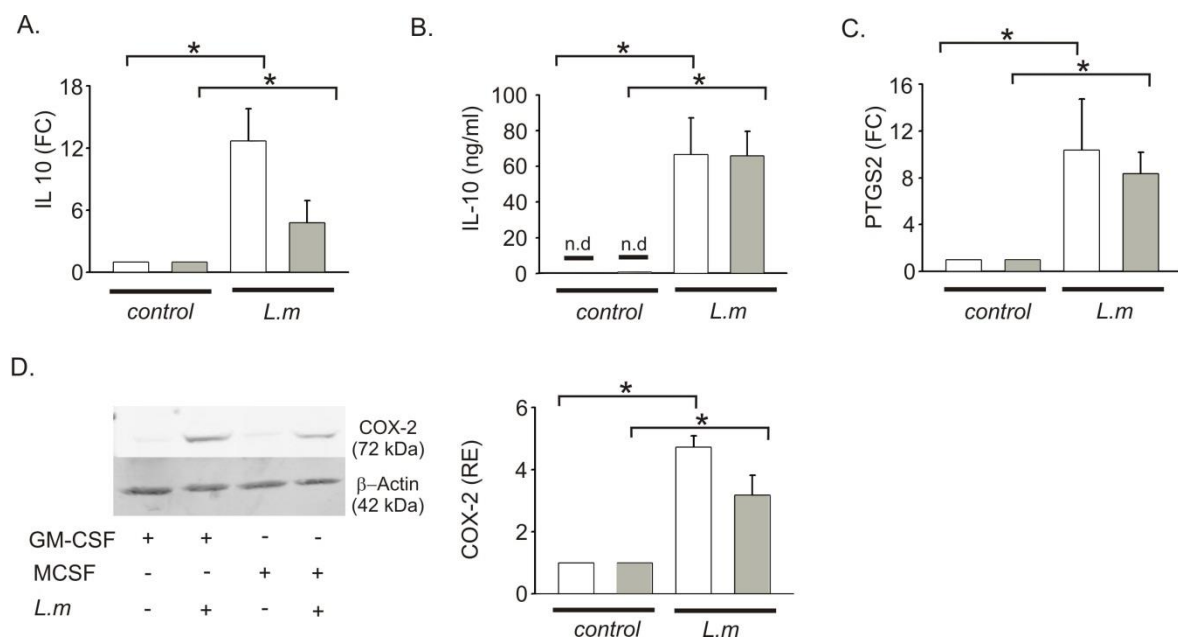


**Figure 7. M $\phi$  infected with *L.m.* express immunomodulatory mediators**

**A.** The expression of IL10 was evaluated via qRT-PCR in GM-CSF (white bars) and M-CSF (gray bars) M $\phi$  infected with *L.m.* or untreated cells at 24 hpi. **B.** IL-10 secretion was evaluated via ELISA in supernatants of GM-CSF M $\phi$  (white bars) and M-CSF M $\phi$  (grey bars) infected with *L.m.* or untreated control at 24 hpi. **C.** PTGS2 expression was evaluated by qRT-PCR in GM-CSF (white bars) and M-CSF (gray bars) M $\phi$  infected with *L.m.* or untreated M $\phi$  at 24 hpi. **D.** COX-2 protein expression was evaluated by western blot. Protein levels of the housekeeping gene  $\beta$ -actin were used as loading control. The relative expression (RE) of COX-2 was estimated by analyzing the intensity of each band normalized by  $\beta$ -actin. The results represent the mean  $\pm$  sd of at least 3 independent experiments \* $p$  < 0.05 (student's  $t$ -test), non-detected (n.d).

---

Along the same lines, CD25, a hallmark molecule of regulatory myeloid cells, was present in  $78\pm 19\%$  of the *L.m.*-M $\phi$ , but absent in the control population (Figure 8A). Interestingly, CD25 can be excised from the cell membrane giving rise to a soluble form (sCD25) (Robb and Kutny 1987). This soluble form binds to IL-2 with an affinity similar to its membrane bound counterpart. Thereby, sCD25 acts as a decoy receptor for IL-2, leading to impaired T cell activation (Driesen, Popov et al. 2008; Popov, Driesen et al. 2008; Lindqvist, Christiansson et al. 2010). An accumulation of sCD25 was determined in supernatants of infected and control M $\phi$ . Whereas supernatants of control M $\phi$  did not show any detectable levels of sCD25, supernatants from *L.m.*-M $\phi$  contained between 16 to  $19\pm 3$  ng/ml of this soluble receptor (Figure 8 B).

Finally, a second marker for regulatory myeloid cells, namely IDO1, was induced strongly upon *L.m.* infection in both GM-CSF and M-CSF M $\phi$  reaching a fold change of 12 when compared to controls (Figure 8 C). Interestingly, IDO1 has been classified as a typical marker for M1 (Benoit, Desnues et al. 2008), but also as a hallmark for M2 activation (Lawrence and Natoli 2011). This divergence in the literature can be explained by the apparently contradictory role that IDO1 plays as a microbicidal mediator and as a modulator of T cell responses (Mellor and Munn 2004).

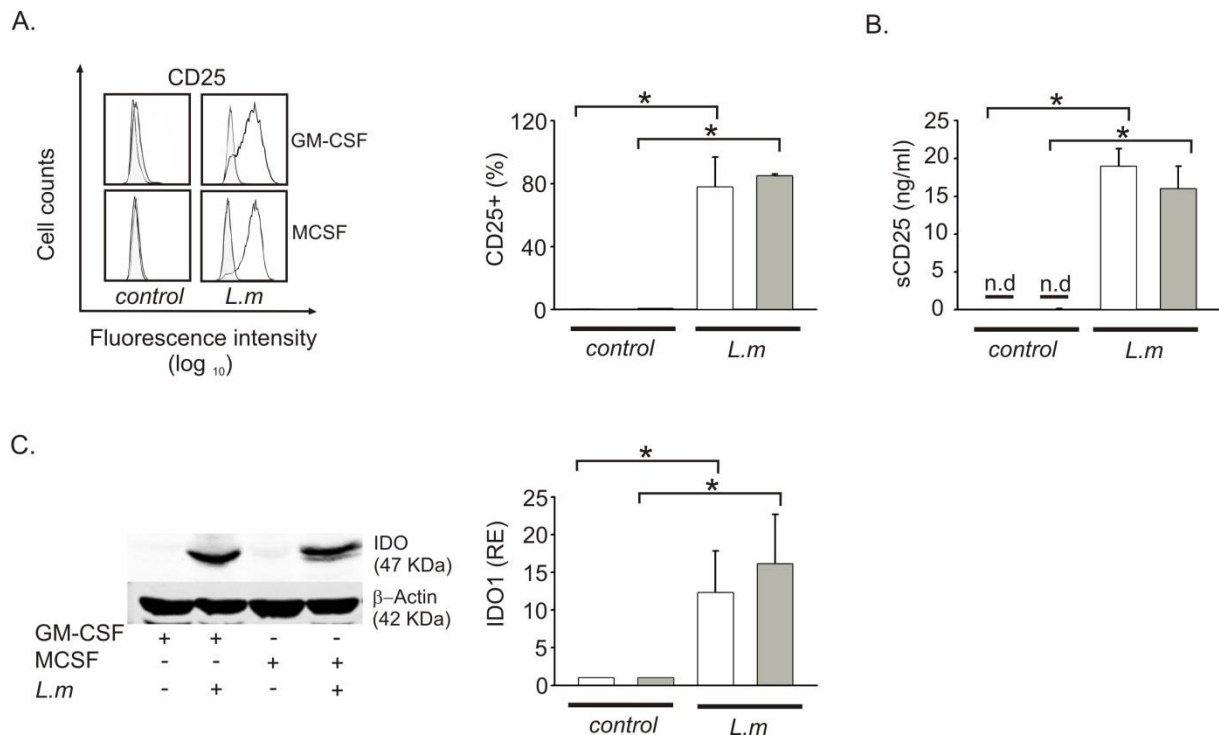


**Figure 8. M $\phi$  infected with *L.m.* express CD25 and IDO**

**A.** CD25 expression was evaluated by flow cytometry in GM-CSF (white bars) and M-CSF (grey bars) M $\phi$  either infected with *L.m.* or untreated at 24 hpi. The results are presented as percentage of positive cells. **B.** sCD25 secretion was assessed via ELISA in supernatants of GM-CSF (white bars) and M-CSF (grey bars) derived M $\phi$  either infected with *L.m.* or untreated at 24 hpi. **C.** IDO1 protein expression was evaluated via western blot in GM-CSF (white bars) and M-CSF (grey bars) M $\phi$  either infected with *L.m.* or untreated at 24 hpi. IDO1 RE (relative expression) was estimated by analyzing the intensity of each band normalized by  $\beta$ -actin. The results represent the mean  $\pm$  sd of at least three independent experiments, \* $p$  < 0.05 (student's *t* test), non-detected (n.d.).

In summary, the presented data suggest that independently from GM-CSF or M-CSF human monocyte derived M $\phi$  infected with *L.m.* present characteristics from a proinflammatory M1 phenotype, but also exhibit features previously associated to a regulatory function including, secretion of IL-10, expression of surface and soluble CD25, IDO1 and COX-2.

---

## 5.2 Soluble factors secreted by macrophages infected with *L. monocytogenes* modulate the phenotype of bystander macrophages and suppress T cell proliferation

To assess the impact of soluble factors secreted by *L.m.* infected M $\phi$  on uninfected bystander cells, the cell culture medium of untreated GM-CSF M $\phi$  was supplemented with increasing percentages (10, 25 and 50% v/v) of supernatants from *L.m.* infected M $\phi$  previously filtered to avoid the transference of bacteria to the new culture. As control, M $\phi$  treated with supernatants from control cells were used. Additionally, M $\phi$  with regulatory properties (Mreg), were generated via stimulation with TNF- $\alpha$  in concert with PGE<sub>2</sub> and Pam<sub>3</sub>. M $\phi$  were treated under these conditions for 48 h. After this period, the expression of surface CD25, COX-2 and IDO1 was evaluated and compared to the expression of these markers in Mreg generated from the same donors. Interestingly, the treatment with 10% v/v of supernatants from *L.m.*-M $\phi$  was sufficient to induce the expression of CD25 in 46 $\pm$ 8% of the M $\phi$  population. The induction of CD25 expression was dose dependent since the treatment with 50% of *L.m.*-M $\phi$  supernatants induced CD25 expression in 80 $\pm$ 10% of the M $\phi$  population. This level of expression is comparable to the observed levels in Mreg (Figure 9 A). Along the same lines, the treatment of M $\phi$  with supernatants from infected cells led to a significant induction in the protein expression of COX-2 and IDO1, but only upon treatment with 50% of the supernatants of *L.m.*-M $\phi$ . For both IDO1 and COX-2 the relative expression of the protein reached similar values to those observed in Mreg (Figure 9 B-D).

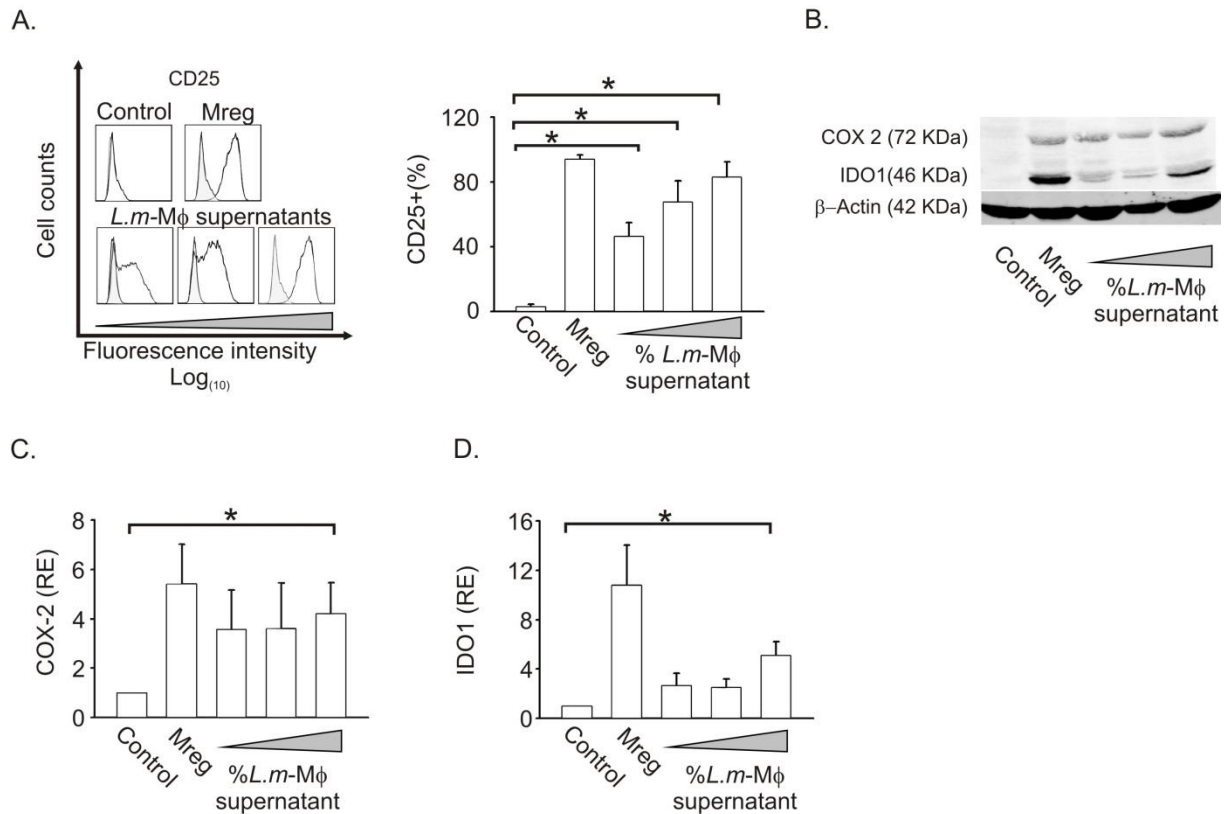


**Figure 9. Supernatants of *L.m.* infected M $\phi$  induce the expression of regulatory factors in uninfected M $\phi$**

**A.** CD25 expression was assessed by flow cytometry in Mreg and GM-CSF M $\phi$  exposed to increasing percentages of supernatants from infected M $\phi$ . As control M $\phi$  treated with 50% of control cells supernatants were used. The results were analyzed as the percentage of positive cells. **B.** The expression of IDO1 and COX-2 was assessed in the same experimental groups described in A. via western blot.  $\beta$ -Actin was used as loading control. The displayed membrane is representative of three similar experiments. **C.** RE (relative expression) for COX-2 was estimated by analyzing the intensity of each band normalized by  $\beta$ -actin. **D.** RE for IDO1 was estimated by analyzing the intensity of each band normalized by  $\beta$ -actin. The results represent the mean  $\pm$  sd of three independent experiments, \* $p < 0.05$  (student's *t* test).

Together the data presented above, suggest that soluble factors produced by infected GM-CSF M $\phi$  have a strong impact on bystander M $\phi$  and are sufficient to induce the expression of immunomodulatory molecules in these immune cells.

According to this observation, the impact of soluble factors secreted by *L.m.* infected M $\phi$  on T cell activation was investigated. CD4<sup>+</sup>T cells were cocultured with aAPCs alone or in the presence of 50% (v/v) supernatants conditioned by M1, M2, Mreg or *L.m.* infected M $\phi$ .

Strikingly, CD4<sup>+</sup> T cells treated with supernatants conditioned by infected M $\phi$  showed around 36 $\pm$ 6% less proliferation than those treated only with aAPCs or supernatants from M1 and M2 M $\phi$ . As reported previously, supernatants of Mreg exerted the highest percentage of inhibition (72 $\pm$ 7%) on CD4<sup>+</sup>T cell proliferation (Schaefer 2009). These data suggest that supernatants of *L.m.*-M $\phi$ , but not M1 or M2 are able to suppress CD4<sup>+</sup>T cell proliferation. In order to establish whether this effect is accompanied by altered cytokine secretion, naïve CD4<sup>+</sup>T cells were treated with supernatants conditioned by M1 and *L.m.*-M $\phi$  during 72h. After this incubation time, naïve T cells were stimulated with PMA in combination with ionomycin, and the production of IL-2, IL-4, IL-17 and IFN- $\gamma$  was assessed via intracellular staining followed by FACS analysis. To enhance the detection of cytokines, the protein secretion was inhibited via treatment with brefeldin A.

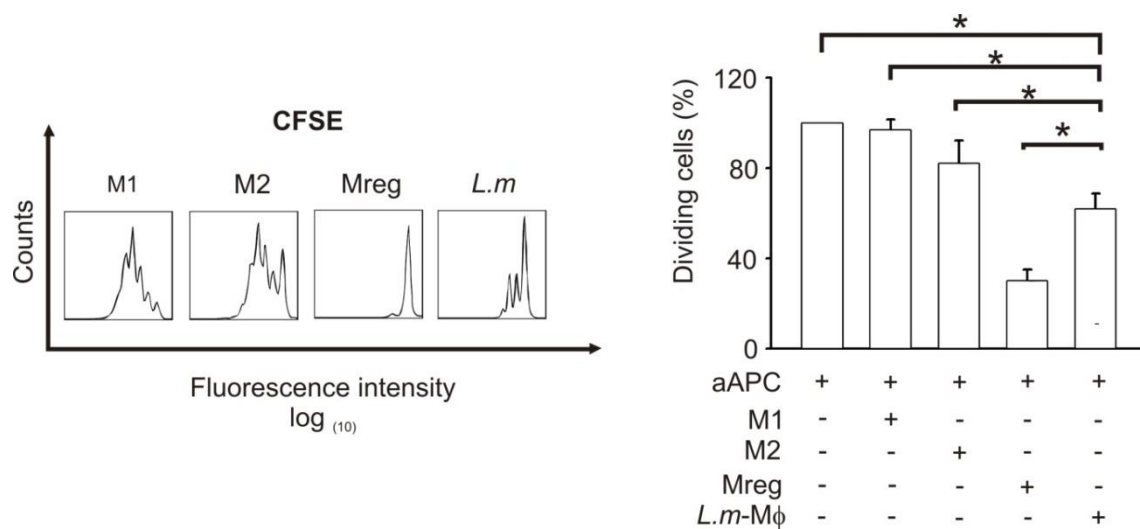


**Figure 10. Supernatants of *L.m.* infected M $\phi$ s are able to suppress T cell proliferation**

CD4<sup>+</sup> T cells were stained with CFSE and the proliferation was assessed 72 h after treatment by flow cytometry. The percentage of dividing CD4<sup>+</sup> T cells treated only with aAPCs was set as 100%. The results represent the mean  $\pm$  sd of four independent experiments \* $p$  < 0.05 (student's  $t$  test).

The percentage of IFN- $\gamma$  producing cells was significantly diminished (50 $\pm$ 11%) in CD4<sup>+</sup>T cell cultures treated with supernatants of *L.m.* infected M $\phi$  (Figure 11), whereas no significant change was observed in the production of IL-2, IL-4 or IL-17 (data not shown). Together, these observations suggest that supernatants from M $\phi$  infected with *L.m.* exert an overall suppressive effect on CD4<sup>+</sup>T cells, clearly different from the effects exerted by supernatants of M1 or M2 polarized M $\phi$ .

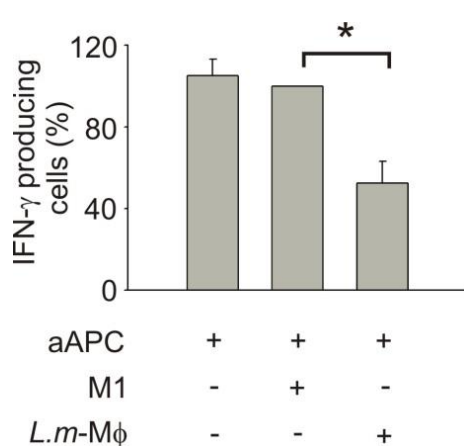


**Figure 11. Supernatants of Mφ infected with *L.m.* reduce the production of IFN-γ in activated CD4<sup>+</sup>T cells**

CD4<sup>+</sup> naïve T cells were incubated with aAPCs alone or with supernatants previously conditioned by M1 or *L.m.* infected Mφ. After 72 h, the production of IFN-γ was assessed by flow cytometry. The percentage of IFN-γ producing cells in M1 conditioned media was set as 100% and the ratio for the rest of the treatments was calculated on this basis. The results represent the mean ± sd of 3 independent experiments \* $p < 0.05$  (student's *t* test).

In summary, these data indicate that *L.m.*-Mφ acquire features classically known for proinflammatory M1 Mφ, but also gain regulatory characteristics that have been previously described for DC infected with *L.m.* as well as for regulatory myeloid cells including Mreg and DCreg. At a functional level, the evidence suggests that soluble molecules secreted by *L.m.*-Mφ are able to confer bystander Mφ with the expression of immunomodulatory molecules. In addition, factors secreted by *L.m.*-Mφ exert a suppressive effect on CD4<sup>+</sup> T cell responses.

### 5.3 The transcriptional response of macrophages to *L. monocytogenes* infection

So far the results suggests that Mφ differentiated from monocytes using GM-CSF and M-CSF show a characteristic phenotype upon *L.m.* infection and exhibit both proinflammatory and immunomodulatory features independently from the factor used in their differentiation process. However, in comparison to GM-CSF Mφ, the population of M-CSF Mφ secreted lower levels of IL-12 in response to *L.m.* infection. Similarly, previous reports suggested that upon stimuli with TLR ligands GM-CSF Mφ acquire proinflammatory functions, whereas M-CSF Mφ behave in a regulatory fashion producing high amounts of IL-10 (Fleetwood, Lawrence et al. 2007). In order to obtain a global view about the differences observed between infected GM-CSF Mφ and M-CSF Mφ the transcriptional profiles of these two cell populations was assessed via microarray analysis.

A PCA revealed that non-infected GM-CSF and M-CSF Mφ clustered in proximity, whereas their *L.m.* infected counterparts were separated in a second group (Figure 12 A).

---

In addition, hierarchical clustering analysis performed on variable genes showed again a clear separation between infected and non-infected M $\phi$  suggesting the key contribution of infection to the variability observed amongst these two groups (Figure 12 B). ANOVA analysis comparing uninfected GM-CSF and M-CSF M $\phi$  showed that 103 genes are differentially expressed (DE) ( $-2 > FC > 2$ ,  $*p < 0.05$ ) between these groups. The gene ontology enrichment (GO) analysis for these 103 DE genes showed that GM-CSF and M-CSF M $\phi$  differ in categories related to antigen processing and presentation (Table 6). In contrast to the differences observed between uninfected GM-CSF and M-CSF M $\phi$ , the direct comparison of these groups after infection with *L.m.* yielded only 3 DE genes.

To gain a better understanding of the transcriptional changes that follow *L.m.* infection, an ANOVA analysis comparing infected GM-CSF or M-CSF M $\phi$  against their respective uninfected controls was performed. GM-CSF and M-CSF M $\phi$  infected with *L.m.* shared a common transcriptional signature that comprised 921 DE genes (Figure 12 C). This transcriptional signature represented over 60% of the total transcriptional changes observed in M $\phi$  upon *L.m.* infection. Moreover, with the exception of IL-6, those genes showed comparable tendencies as this was shown by FC/FC plot (Figure 12 D).



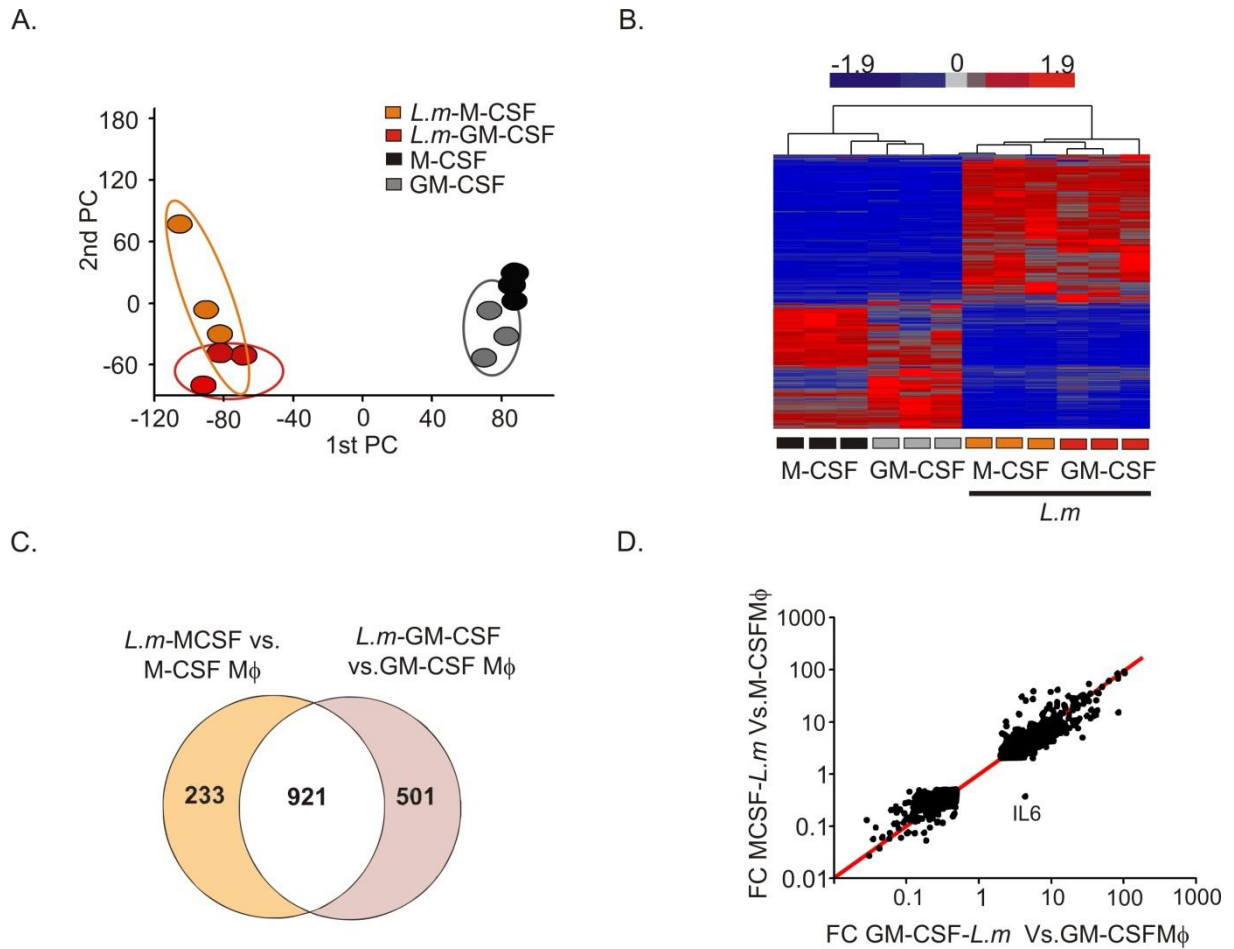


**Figure 12. GM-CSF and M-CSF derived M $\phi$  regulate a similar transcriptional profile upon *L.m.* infection**

**A.** PCA analysis of the expressed genes in GM-CSF and M-CSF M $\phi$  infected (GM-CSF-*L.m.* and M-CSF-*L.m.* respectively) and non-infected (GM-CSF and M-CSF) with *L.m.* **B.** Hierarchical clustering analysis based on 1000 variable genes observed in *L.m.* infected GM-CSF and M-CSF M $\phi$  versus control M $\phi$ . **C.** Venn diagram of DE observed between GM-CSF and M-CSF M $\phi$  infected with *L.m.* and their corresponding untreated controls. **D.** Expression of 921 genes in the intersection between GM-CSF and M-CSF M $\phi$  as FC/FC plot.

Function	Type	Enrichment Score	GM-CSF up vs. M-CSFdown
MHC class II protein complex	Cellular component	18	HLA-DRB3, HLA-DPA1, HLA-DPB1, HLA-DRA, CD74
Antigen processing and presentation of peptide or polysaccharide antigen via MHC class II	Biological process	15	HLA-DRB3, HLA-DPA1, HLA-DPB1, HLA-DRA
antigen processing and presentation	Biological process	10.4	CD1B, HLA-DPB1, HLA-DRA, CD74, CD74

**Table 6. GO enrichment analysis of DE between GM-CSF and M-CSF M $\phi$**

GO categories with the highest enrichment scores of 103 DE genes observed between control GM-CSF and M-CSF M $\phi$ .

In the next step, a GO enrichment analysis was performed on the 921 DE genes that were common between M-CSF and GM-CSF M $\phi$  upon *L.m.* infection. As expected, in the biological process category, the GO terms with higher enrichment scores were those related to immune responses. Remarkably, Type I interferon mediated signaling, pathway and the response to virus category showed the highest enrichment scores (60), followed by the IFN- $\gamma$  mediated signaling category (30). In addition, the respiratory transport electron chain and the mitochondrial ATP synthesis terms presented also high enrichment scores (25 and 23 respectively), suggesting the relevance of active energy metabolism in the inflammatory process is driven by *L.m.* infection (Figure 13).

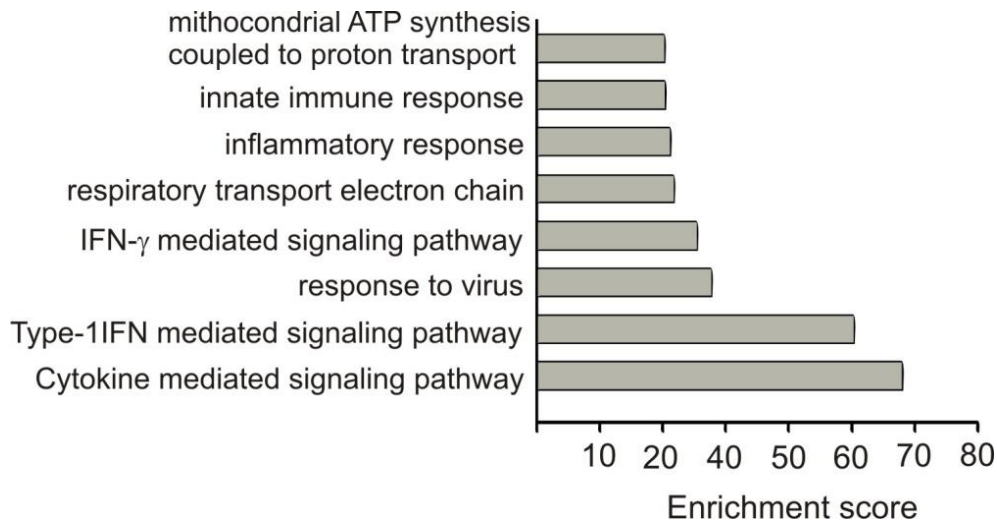


**Figure 13. GO enrichment analysis of differentially express genes in GM-CSF and M-CSF MΦs upon *L.m.* infection**

GO enrichment analysis was performed on DE genes that were common between GM-CSF and M-CSF M $\phi$  upon *L.m.* infection. The bar chart displays the GO terms with the highest enrichment scores in the biological process category.

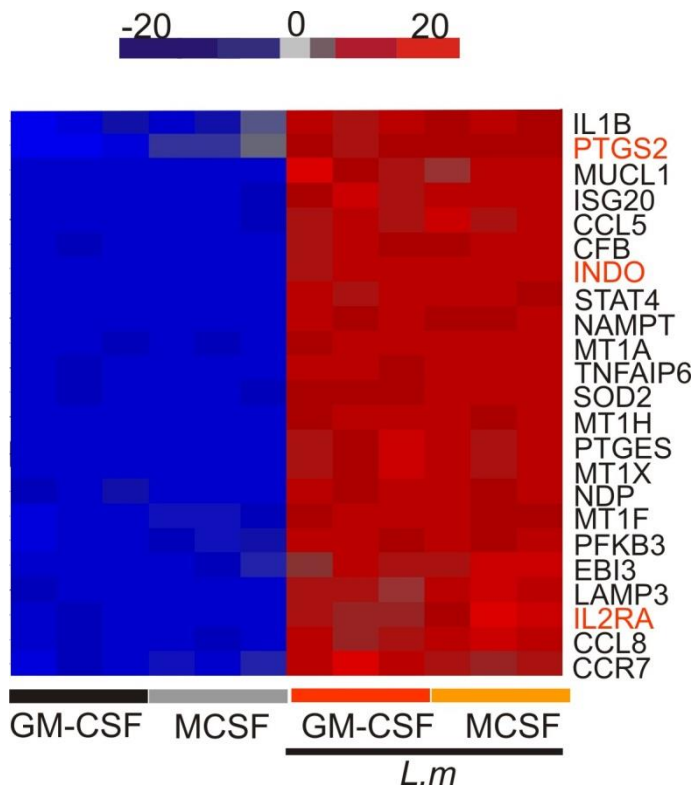


**Figure 14. Heatmap of highly regulated genes in in GM-CSF and M-CSF M $\phi$  infected with *L.m.***

Average expression signals of the most regulated genes ( $FC > 20 < FC < -20$ ,  $p < 0.05$ ) were standardized using Z score transformation. The comparative analysis included non-infected GM-CSF and M-CSF M $\phi$ , as well as *L.m.*-M $\phi$ . Expression values of up- and downregulated genes are color-coded; genes with low expression are shown in blue and genes with high expression in red, respectively. Gene symbols for transcripts previously related to immunomodulatory function of myeloid cells are highlighted in red.

Interestingly, the hallmark genes for the regulatory program (PTGS2, INDO, IL2RA) previously observed in DC infected with *L.m.* and regulatory myeloid cells appeared amongst the top DE genes (FC>20 or FC<-20, \* $p$ <0.05) in *L.m.* infected M $\phi$  together with genes coding for molecules associated with proinflammatory functions including the cytokines IL1A, IL1B, the chemokines CCL5, CCL8 and the transcription factor STAT4 (Figure 14).

In summary, the data suggest that despite the differences in growth factors that lead M $\phi$  differentiation, GM-CSF and M-CSF M $\phi$  respond to *L.m.* infection with a common transcriptional signature that includes proinflammatory and immunomodulatory genes supporting the results previously described for the in vitro assays. Taking these findings into account GM-CSF M $\phi$  were chosen for further analysis and will be referred shortly in the following sections as M $\phi$ .

## 5.4 The transcriptional response of macrophages and dendritic cells to *L. monocytogenes* infection

The transcriptome of DC and M $\phi$  were compared under resting conditions as well as upon *L.m.* infection to find a common gene signature specifically induced by *L.m.* Despite the fact that DC and M $\phi$  share GM-CSF as driving factor in their process of differentiation from monocytes, a PCA analysis performed on variable genes revealed that under steady state conditions DC and M $\phi$  cluster separately into two well defined groups, underlining the strong influence of IL-4 in the differentiation process of DC. In contrast, after infection the distance between *L.m.*-M $\phi$  and *L.m.*-DC decreased, suggesting similarities in their transcriptional responses (Figure 15 A). ANOVA analysis comparing uninfected DC and M $\phi$  revealed that 300 genes were DE between these two groups. In agreement with the functional differences between DC and M $\phi$ , the GO enrichment analysis showed that under resting conditions the DE genes between DC and M $\phi$  were related to categories like immune response and chemotaxis (Table 7). For instance, DC expressed CCL23 and CCL18, two chemokines that have been reported as strong chemoattractants for naïve T cells (Blengio, Raggi et al. 2012). In contrast, M $\phi$  expressed higher levels of molecules involved in pathogen recognition, including TLR5, 6, 8, CD14, and also NLRP3, which although does not recognize PAMPs directly, can be activated upon a plethora of microbial stimuli, including LPS, bacterial RNA and lipopeptides (Franchi, Munoz-Planillo et al. 2012). In agreement with the results observed in the PCA analysis of variable genes,

the comparison of DE genes observed in *L.m.*-DC, *L.m.*-M $\phi$  and their respective uninfected controls, showed that *L.m.* infection induces 903 genes common in DC and M $\phi$ . Furthermore, these genes were regulated in the same direction (Figure 15 B and C).

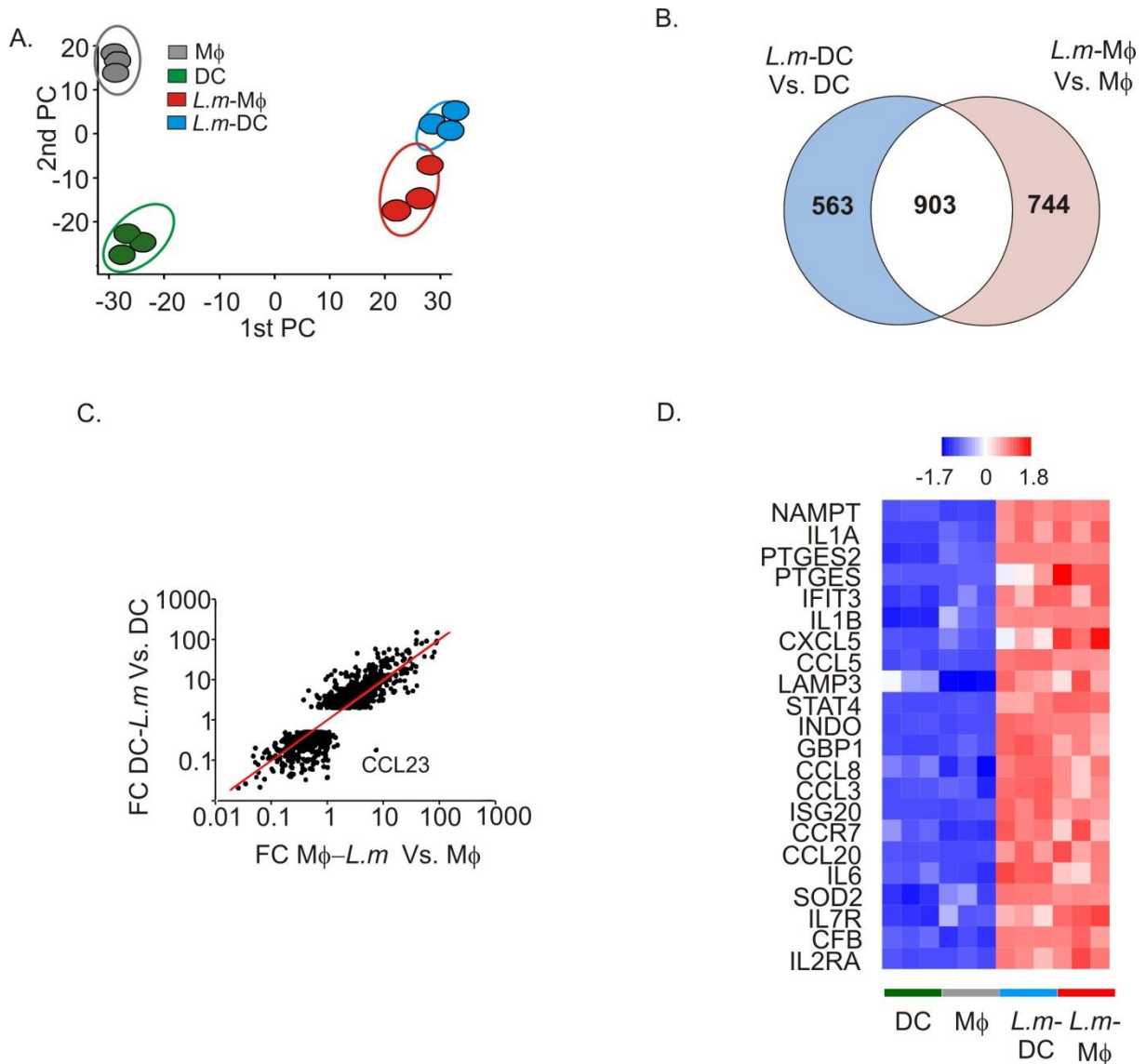


**Figure 15. DC and M $\phi$  express a common transcriptional signature upon *L.m.* infection**

**A.** PCA analysis of variable genes (1350 transcripts) expressed in uninfected and *L.m.* infected M $\phi$  and DC. **B.** Venn diagram representing the intersection between the DE genes observed in *L.m.* infected versus uninfected DC and *L.m.* infected versus uninfected M $\phi$ . **C.** FC/FC plot of the 903 genes detected as DE between non-infected vs. infected DC and non-infected vs. infected M $\phi$ . **D.** Heatmap displaying DE genes (FC < -20, FC > 20) expressed in DC and M $\phi$  after *L.m.* infection. The average expression values were obtained from microarray experiments and were standardized before visualization (z-score transformation).

Function	Type	Enrichment score	DC up vs. M $\phi$ down	M $\phi$ up vs. DC down
inflammatory response	Biological process	31	ALOX15, CCL18 CAMK1D, CRH, MMP25, CCL23, CCL26	NLRP3, RIPK2, NFKBIZ, TLR8, TLR6, TLR5, CCR2, CYBB, CD14, CD163
chemotaxis	Biological process	15	CCL23, CCL18, CCL26, CCL15, CCR6	FPR1, ENPP2, CX3CR1
defense response	Biological process	10	IL17RB	NLRP3, CD48, CSF 3R
immune response	Biological process	9	CCL23, CCL18, CCL26, CCL15, CD1 A, CCR6, NFIL3, SUSD2, CTSC	TLR6, IRF8, CCR2, GBP2, FYB, ENPP2, CEBPB

**Table 7. GO enrichment analysis of DE genes between M $\phi$  and DC**

These data indicate that DC and M $\phi$  respond to *L.m.* infection by regulating an important number of genes in a similar fashion, despite their different backgrounds. This group of common genes include IDO1, IL2RA, PTGES2, but also the cytokines IL-6, IL1A, IL1B, the chemokine ligands CCL5, CCL8, CCL3 and the transcription factor STAT4 (Figure 15 D). Nevertheless, between 40 to 46% genes are regulated only in one of the two cell types (DC and M $\phi$ ) (Figure 15 B). On the one hand, the GO enrichment analysis showed that the DE genes expressed only in DC after *L.m.* infection are related to inflammatory responses, chemotaxis and the response to LPS (Figure 16 A). On the other hand, those genes only regulated in M $\phi$  are associated to oxidoreductase and metabolic activity, but also to inflammatory and cell defense responses (Figure 16 C). Additionally, those genes with the highest FC upon DC infection with *L.m.* include molecules that amplify the

inflammation like the alarmins S100A and S100B (Ehrchen, Sunderkotter et al. 2009), the chemokine CXCL9 and the leukocyte immunoglobulin-like receptor 5 (LILRA5). Interestingly, in M $\phi$  the expression of these genes remained similar before and after *L.m.* infection. Additionally, infection of DC with *L.m.* also induced high expression of SERPINB2, a molecule that has been recently described as an immunomodulator able to control Th1 responses in vivo (Schroder, Le et al. 2010) (Figure 16 B). In contrast, the DE genes with the highest FC present in M $\phi$  upon infection with *L.m.* include the two matrix metalloproteinases MMP7 and MMP12 and several components of the chemokine system including the receptor CXCR7 and the chemokine ligand CCL23. Infected M $\phi$  also up-regulate the expression of Epstein-Barr virus induced gene 3 (EBI3) (Figure 16 D). The protein encoded by the EBI3 gene can form dimers either with IL12B leading to expression of the proinflammatory cytokine IL-27 or with IL12A producing the immunomodulatory cytokine IL-35. However, the expression of none of its dimerization partners was significantly changed upon *L.m.* infection in M $\phi$  (data not shown).

In summary, in silico data suggest that M $\phi$  and DC independently from their functional differences and their basal transcriptional background respond to *L.m.* infection with a common transcriptional signature that represents around 60% of the total transcriptional changes induced by *L.m.* in these cell populations.

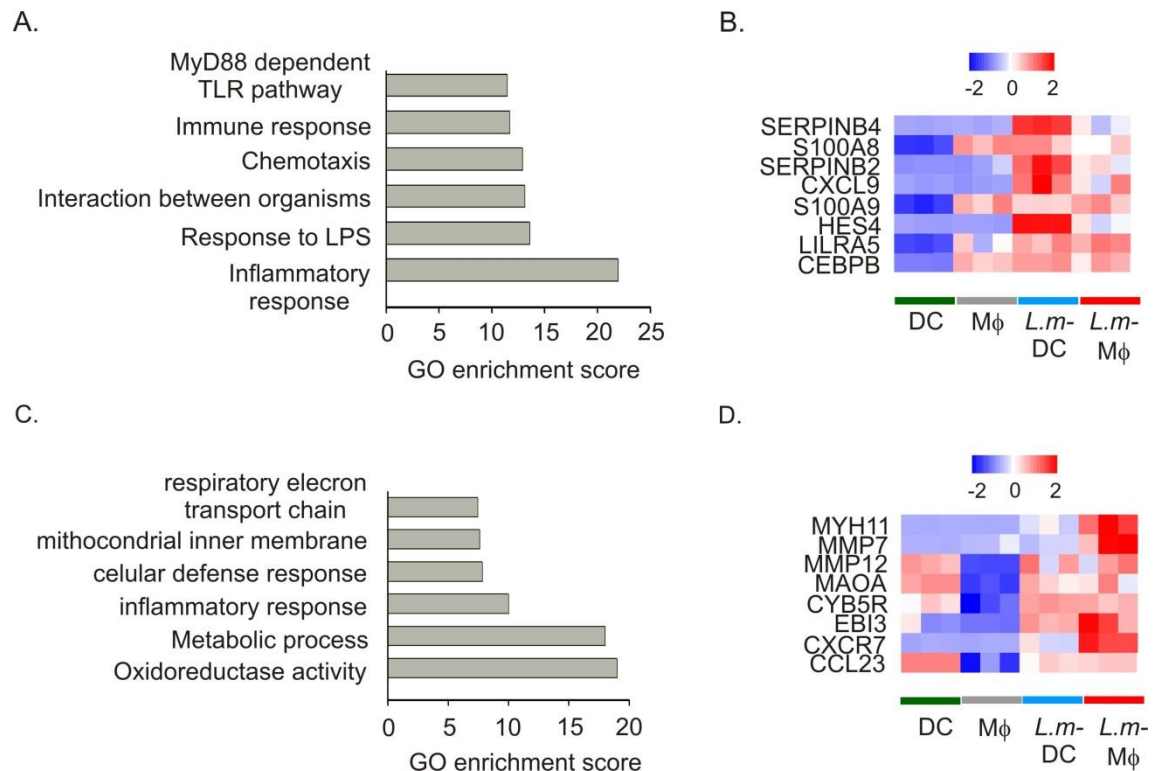


**Figure 16. DC and Mφ also express cell specific programs upon *L.m.* infection**

**A.** GO enrichment analysis of DE genes observed only in DC infected with *L.m.* **B.** Heatmap displaying DE genes (FC<-35, FC>35) expressed only in DC in response to *L.m.* infection. The average expression values were obtained from microarray experiments and were standardized before visualization (z-score transformation). **C.** GO enrichment analysis of DE genes observed only in Mφ infected with *L.m.* **D.** Heatmap displaying DE genes (FC<-30, FC>30) observed only in Mφ in response to *L.m.* infection. The average expression values were obtained from microarray experiments and were standardized before visualization (z-score transformation).

## 5.5 The transcriptional response of macrophages to infection with wild type *L. monocytogenes* or hly mutant.

Despite the identification of a common transcriptional program in Mφ and DC in response to *L.m.* infection, the events shaping this transcriptional response are still unknown. It remains also to be elucidated whether this transcriptional program can be fine adjusted depending on the intracellular fate of the bacteria. *L.m.* infection is a complex process involving two phases of recognition; the first one is carried out at the cell surface and subsequently in the phagosome, whereas the second one is executed directly in the cytoplasm once *L.m.* has reached the cytosol. To understand whether the transcriptional responses of Mφ to *L.m.* infection depend on the events triggered upon bacteria



recognition at the cell surface and inside the phagosome or at the cytosol, the transcriptomes of M $\phi$  infected either with wild type *L.m.* or the phagosome restricted hly mutant, were compared. A PCA analysis on all variable genes showed a close relationship between M $\phi$  infected with *L.m.* wt. and the hly mutant (Figure 17 A). This finding was further supported by the unsupervised hierarchical cluster analysis showing that infected cells clustered together irrespective of the infection with wt *L.m.* or the hly mutant (Figure 17 B).

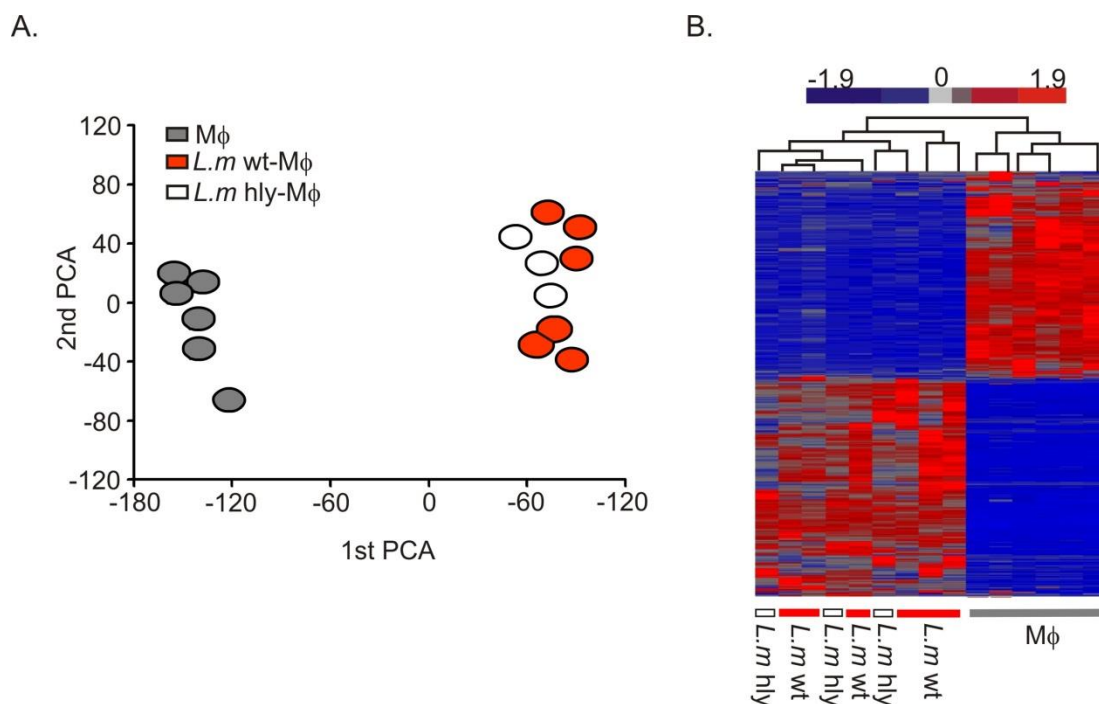


**Figure 17. *L.m.* intracellular fate does not condition the transcriptional response of M $\phi$**

**A.** PCA analysis on variable genes (2300) expressed *L.m.* wild type infected (*L.m.* wt- M $\phi$ ), *L.m.* hly mutant infected M $\phi$  (*L.m.* hly-M $\phi$ ) and control M $\phi$  **B.** Unsupervised hierarchical cluster analysis on variable genes expressed in uninfected, *L.m.* wt and *L.m.* hly infected M $\phi$ .

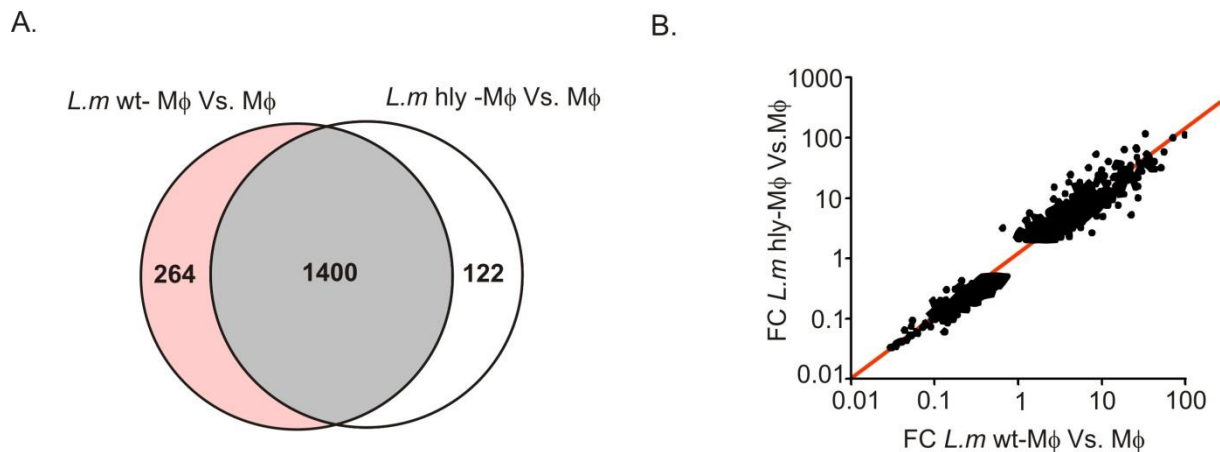


**Figure 18. M $\phi$  infected with *L.m.* and hly share 85% of DE genes**

**A.** Venn diagram comparing the DE genes observed in *L.m* wt infected and *L.m* hly versus non infected M $\phi$ . **B.** FC/FC plot for the comparison of 1400 DE genes observed in M $\phi$  infected with *L.m.* wt and with the hly mutant.

Similarly, the comparison of DE genes expressed by *L.m.* wt and hly infected M $\phi$  with uninfected cells revealed that the compared transcriptional programs shared 85% of the total DE genes observed (Figure 18 A). In addition, the comparison of the FC for the common DE genes, present in both wt and hly infected M $\phi$ , showed that they were regulated in the same direction and with a similar order of magnitude. (Figure 18 B).

Despite the fact that M $\phi$  infected with *the L.m.* wt and hly mutant have in common 85% of the total DE genes; a certain number of genes were regulated only in response to *L.m.* wt. The GO enrichment analysis on these 264 genes revealed that terms related to translational elongation; viral transcription and viral infectious cycle presented the highest enrichment scores (Figure 19A). Interestingly, the genes with the highest FC (FC<-10, FC>10) observed only upon infection with *L.m.* wt included IFNB, IRF1 and OASL1 amongst others (Figure 19 B).

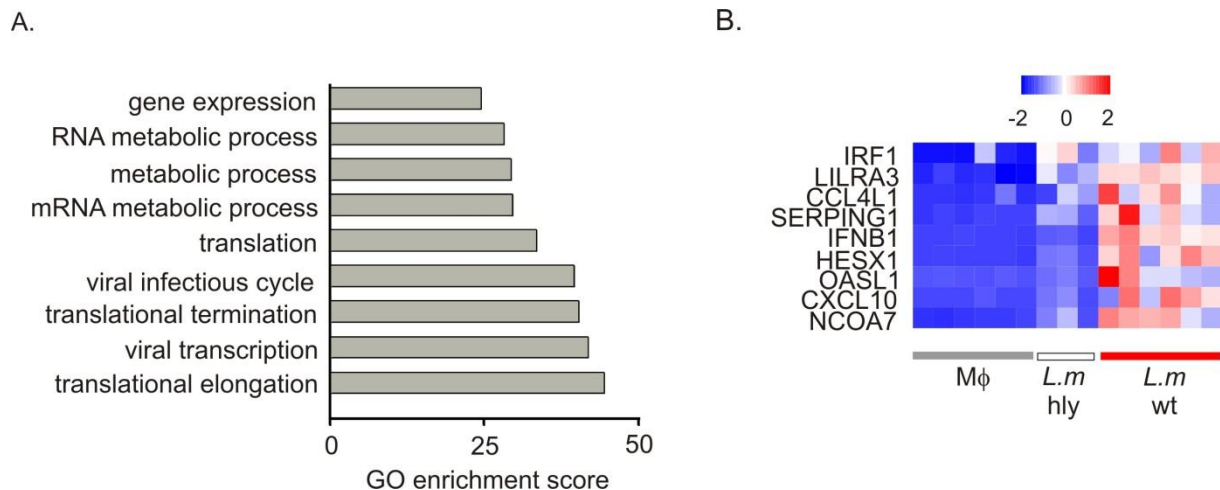


**Figure 19. GO enrichment analysis of DE present exclusively upon infection of Mφ with *L.m.* wt**

**A.** The bar chart displays 10 GO terms with the highest enrichment scores among the category of biological process. **B.** The heatmap displays the expression of DE genes ( $FC < -10$ ,  $FC > 10$ ) present only after infection of Mφ with *L.m.* wt. Average expression values were obtained from microarray experiments and were standardized before visualization.

Taken together, at transcriptional level the presented data revealed that Mφ react in a similar fashion to the threat represented by a vacuolar-restricted mutant, than to a fully competent wild type *L.m.* This observation suggests that the signals triggered in the early stages of infection like bacterial recognition at the cell surface or the phagosome are sufficient to acquire the majority of the components that integrate the transcriptional response of Mφ against *L.m.* To support these findings, the identity of the hly mutant used in this study was confirmed via PCR using primers to amplify the hlyA gene, previously reported in the literature (Conter, Vergara et al. 2010). The hlyA gene encodes the virulence factor LLO, essential for phagosome lysis and the subsequent release of *L.m.* into the cytoplasm (Figure 2). In addition, the expression of proinflammatory hallmarks (IFN- $\gamma$  and TNF- $\alpha$ ) and immunomodulatory molecules (IL-10 and CD25) were assessed via ELISA and flow cytometry at 24 hpi. The data obtained via PCR confirmed that the hly mutant used in this study lacked indeed the hlyA gene since it was amplified only in the wt strain (Figure 20 A). In addition, the hly mutant, as well as, wt bacteria were positive for the ActA gene, an essential virulence factor present in the genome of *L.m.* Finally, *L.i* one of the non-pathogenic members of the genus *Listeria* was negative for both hlyA and ActA gene (Figure 20 A). Furthermore, IFN- $\gamma$ , TNF- $\alpha$  and IL-10 were secreted in similar amounts in Mφ infected with wt *L.m.* or the hly mutant (Figure 20 B-D). Similarly, the

percentage of CD25 positive M $\phi$  was equivalent, independently whether the infection was performed with wt *L.m.* or the hly mutant (Figure 20 E).

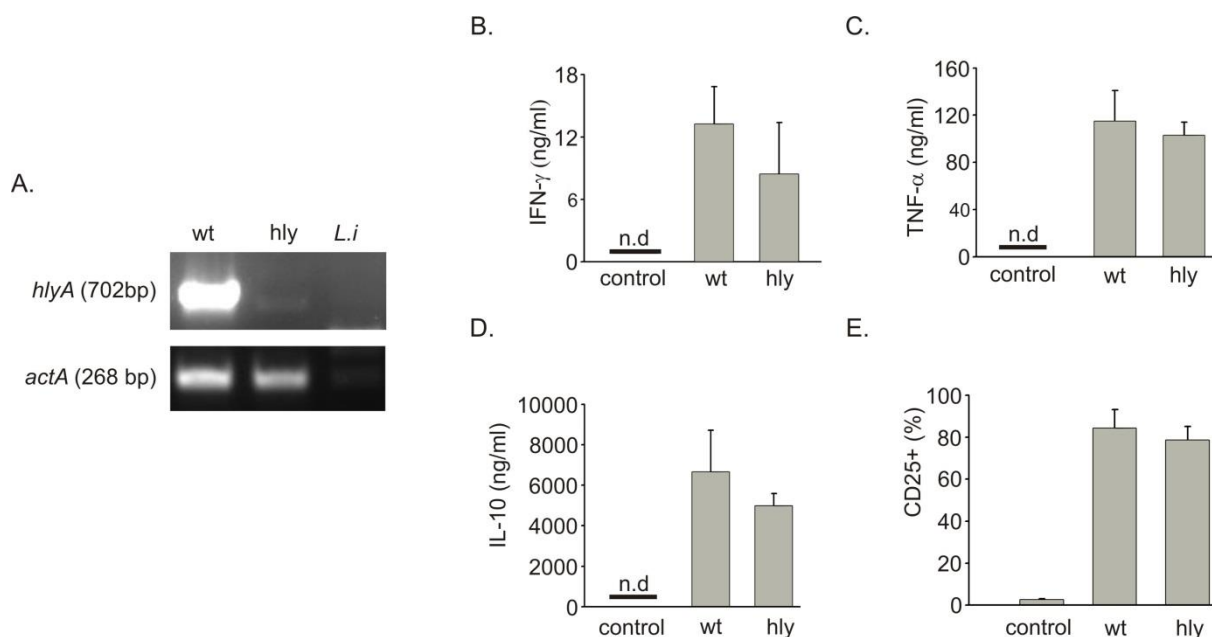


**Figure 20. M $\phi$  infected with wt *L.m.* and hly express similar amounts of proinflammatory and immunomodulatory factors**

**A.** The identity of the hly mutant was confirmed by PCR using primers directed to *hlyA* gene. The ActA gene was used as loading control. *L.i.* was included in the analysis as negative control. The secretion of **B.** IFN- $\gamma$ , **C.** TNF- $\alpha$  and **D.** IL-10 was assessed in supernatants of M $\phi$  infected with wt *L.m.* and hly mutant at 24 hpi. **E.** The percentage of CD25 expressing cells was assessed in M $\phi$  infected with *L.m.* or hly 24 hpi (n=3, mean $\pm$ sd).

In summary, the herein presented data suggest that the infection with *L.m.* drives the expression of a common transcriptional program in myeloid cells that probably depends to a significant extent on the early events of infection associated to bacterial recognition at the cell surface and inside the phagosome. These initial events might trigger a conserved defense mechanism, which is not tuned according to the level of threat represented by the invading microorganism.

## 5.6 Comparative analysis of transcriptional responses in macrophages infected with *L. monocytogenes* and classical models of macrophage polarization

The response of M $\phi$  to bacterial infection, including the infection with *L.m.*, has been identified as a classic example of M1 polarization (Benoit, Desnues et al. 2008; Mosser and Edwards 2008). However, in vitro obtained evidence suggest that M $\phi$  infected with *L.m.* acquire immunomodulatory properties previously described for alternatively activated M $\phi$  including the expression of IL-10 (Sica and Mantovani 2012), IDO1 (Lawrence and Natoli 2011) and the capacity to suppress T cell proliferation. Moreover, in silico and in vitro data herein presented, suggest that *L.m.* infection leads to the acquisition of a transcriptional signature comparable in DC and M $\phi$ . This common profile includes the expression of immunomodulatory hallmark molecules like CD25, COX-2, IL-10 and IDO1. To improve the understanding of the factors that contribute to the transcriptional response of M $\phi$  to *L.m.* infection and to elucidate how *L.m.* infected M $\phi$  fit in the current model of M $\phi$  polarization, a comparative analysis between the transcriptional profiles of M $\phi$  infected with *L.m.* and IFN- $\gamma$  derived M1 or IL-4 derived M2 M $\phi$  was performed.

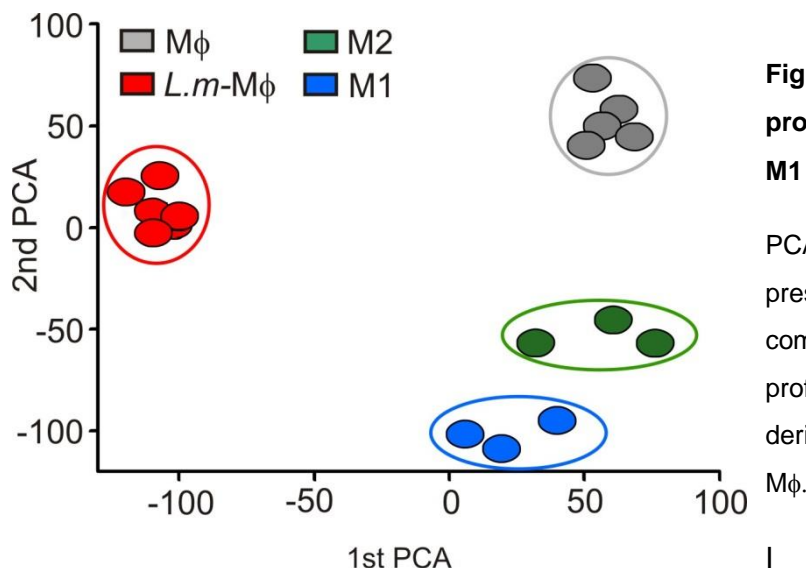


**Figure 21. The transcriptional profile of *L.m.*-M $\phi$  differs from M1 and M2 polarized M $\phi$**

PCA on variable genes (2000) present in M $\phi$  infected with *L.m.* in comparison to the transcriptional profiles of IFN- $\gamma$  generated M1, IL-4 derived M2 and untreated control M $\phi$ .

An initial analysis by two dimensional PCA revealed no direct relationship of M $\phi$  infected with *L.m.* to M1, M2 or untreated M $\phi$  since the genomic fingerprints of each cell population were separated in the two dimensional space from *L.m.*-M $\phi$  (Figure 21). Nevertheless, the analysis of the DE genes between each one of the groups and untreated control M $\phi$

---

demonstrated that the IFN- $\gamma$  signature encompasses approximately 30% of the total DE expressed genes in *L.m.*-M $\phi$  (Figure 22 A and C). Only 8 genes of the common pool regulated upon *L.m.* infection and IFN- $\gamma$  stimulation were regulated in the opposite direction. This group of genes included amino acid (SLC1A5 neutral and SLC16A10 aromatic amino acids) and fatty acids transporters (SCL27A3), the enzyme spermine synthase (SMS), but also the chromatin remodeler HMGA1 and the modulator of cell cycle cyclin-D2 (Figure 22 C). Interestingly, the increase in the expression of SLC16A10, which is significantly up-regulated upon *L.m.* infection (FC10,  $p^* < 0.05$ ), but not upon stimulation with IFN- $\gamma$  has been identified as an early event in the infection of murine M $\phi$  by *Mycobacterium tuberculosis* (Stavrum, Valvatne et al. 2012).

In contrast, the contribution of the IL-4 derived M2 M $\phi$  was minimal and represented only 9% of the transcriptional changes observed upon infection of M $\phi$  with *L.m.* Furthermore, about 13% of the common genes between *L.m.* infected and M2 M $\phi$  were regulated in the opposite direction (Figure 24 B and D). Interestingly, the expression of IL-10, the hallmark cytokine for M2 polarization (Biswas and Mantovani 2010) was not detected in IL-4 derived M2 M $\phi$  used in this study. In addition, IL-10 was not present in supernatants from this experimental group (Schaefer 2009). However, IL-4 derived M $\phi$  expressed several previously reported M2 marker genes, including FCER2 (Beyer, Mallmann et al. 2012), AIOX15 (Wuest, Crucet et al. 2012), IRF4 (Sato, Takeuchi et al. 2010), CCL17, CCL18 and CCL23 (Mantovani, Sica et al. 2004) (Figure 23 A). Moreover, M2 and *L.m.* infected M $\phi$  expressed MMP7 and MMP12 and the chemokines CCL22 and CCL23 at similar levels (Figure 23 A).

In agreement with previous reports, the intersection of similarly expressed genes in *L.m.* infected and IFN- $\gamma$  treated M $\phi$  comprised hallmark genes for M1 polarization, including transcription factors like STAT1 and IRF1, the chemokine ligands CCL5, CXCL10 and CCL8, the proinflammatory cytokine IL-6 (Sica and Mantovani 2012), but also a set of genes that are well-known targets of IFN- $\gamma$ , like IDO1 (Mellor and Munn 2004), members of the guanylate binding protein (GBP) family (GBP1, GBP4 GBP5) and the protein myxovirus resistance 1 (MX1) (Martens and Howard 2006) (Figure 25). Although, M1 M $\phi$  expressed IDO1, neither M1 nor M2 M $\phi$  expressed the complete set of immunomodulatory molecules expressed by *L.m.* infected M $\phi$ .

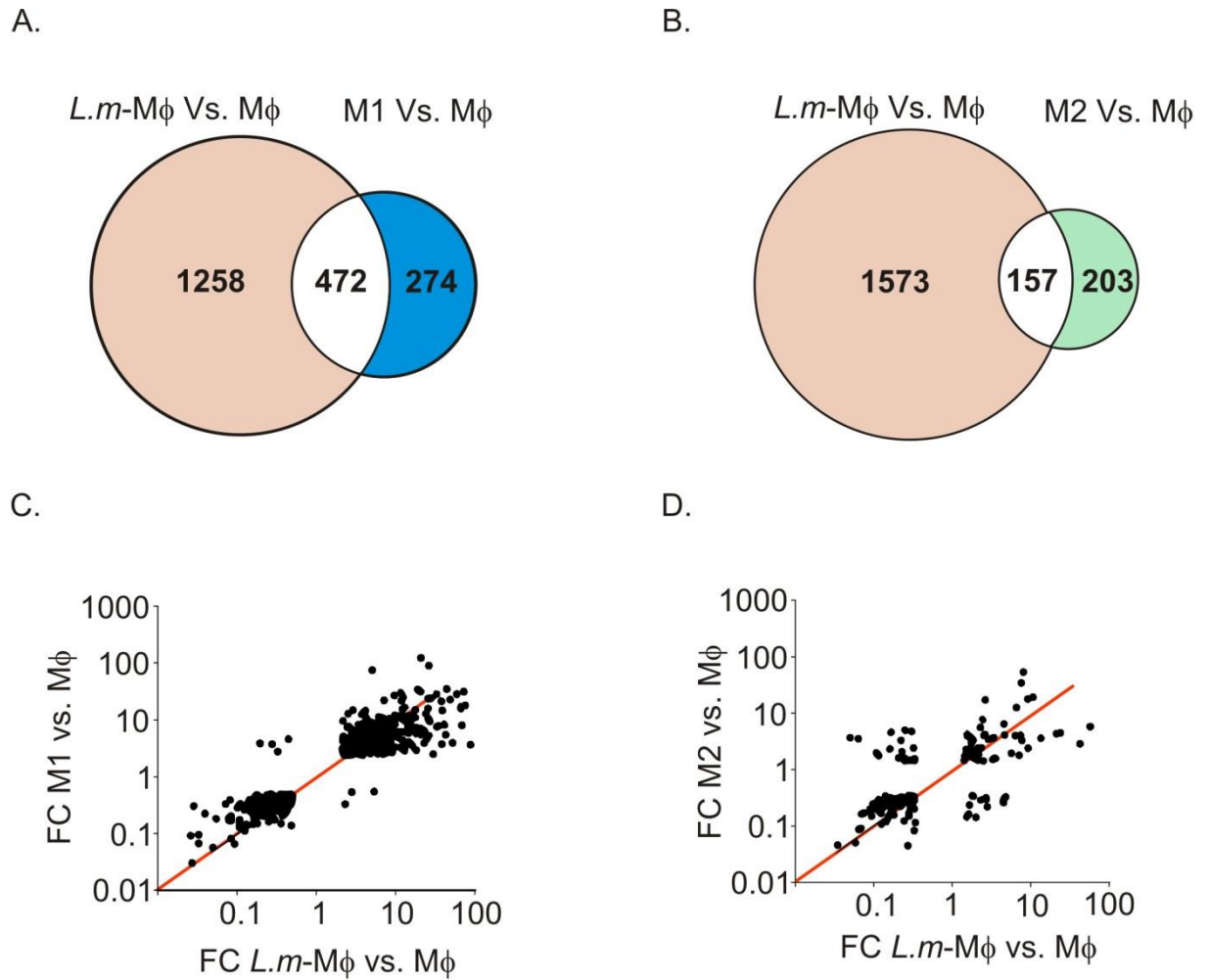


**Figure 22. The observed IFN- $\gamma$  signature in *L.m.* infected M $\phi$  represents 30% of DE genes**

**A.** Venn-diagram visualizing the intersection between DE genes expressed in M1 and *L.m.* infected M $\phi$  in comparison to control M $\phi$ . **B.** The Venn diagram displays the intersection between the set of DE genes expressed in M2 and *L.m.* infected M $\phi$ . **C.** FC/FC plot of the DE genes being common between M1 and *L.m.* infected M $\phi$ . **D.** FC/FC plot of the DE genes common between M2 and *L.m.* infected M $\phi$ .

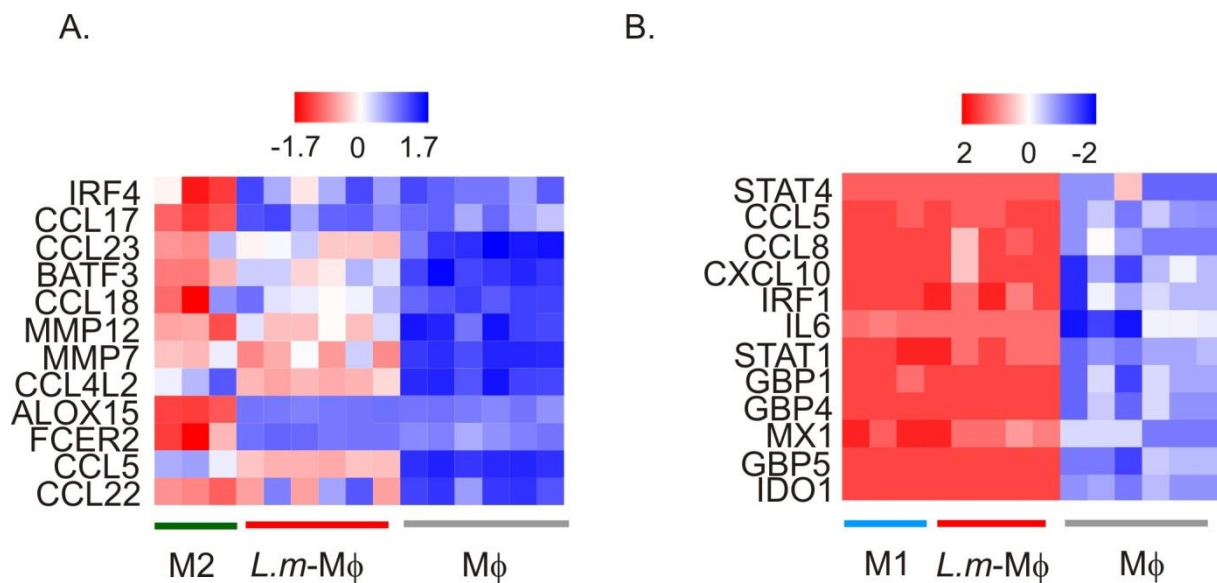


**Figure 23. Hallmark genes of M1 and M2 polarization and their expression in *L.m.*- M $\phi$**

**A.** The heatmap displays the expression of hallmark genes for M2 polarized M $\phi$  in comparison to untreated and *L.m.* infected M $\phi$ . **B.** The heatmap displays the expression for DE genes found in IFN- $\gamma$  and *L.m.*-M $\phi$ . The average expression values were obtained from microarray experiments and were standardized before visualization (z-score transformation).

In summary, these findings suggest that while it is true that the transcriptome of *L.m.* infected M $\phi$  has an IFN- $\gamma$  signature common to M1 polarized M $\phi$ , this explains only one third of the total transcriptional variability induced by *L.m.* infection. However, in the original characterization of classical activated M $\phi$  the combination of two signals coming from IFN- $\gamma$  and TNF- $\alpha$  was described as a necessary event to promote the acquisition of the M1 phenotype with the capacity to secrete high levels of proinflammatory cytokines (O'Shea and Murray 2008). Posterior findings indicate that some TLR agonists are able to induce TNF- $\alpha$  transcription via MyD88 and can - at the very same time - activate TRIF which in turn promotes the production of endogenous IFN- $\beta$ . In this manner, synergistic action of TNF- $\alpha$  and IFN- $\beta$  overcomes the signaling provided by IFN- $\gamma$  to obtain a proinflammatory phenotype in M $\phi$  (Mosser and Edwards 2008). Along the same lines TNF- $\alpha$  (Collart, Belin et al. 1986; Vila-del Sol, Punzon et al. 2008) and IFN- $\beta$  (Schroder, Hertzog et al. 2004) have been identified as downstream targets of IFN- $\gamma$  signaling. In principle the endogenous signal from TNF- $\alpha$  might provide the second signal necessary for the acquisition of a proinflammatory phenotype. Interestingly, TNF- $\alpha$  and IFN- $\beta$  were



not found amongst the DE genes observed after stimulation of M $\phi$  with IFN- $\gamma$  (TNF FC 1,  $p^* < 0.05$ ; IFN- $\beta$  FC-1.1,  $p^* < 0.05$ ). Despite this initial finding, the secretion of endogenous TNF- $\alpha$  ( $1.5 \pm 0.7$  ng/ml) and IFN- $\beta$  ( $26 \pm 6$  pg/ml) was validated by ELISA in supernatants of IFN- $\gamma$  treated M $\phi$ , although in lower amounts than those detected in supernatants of *L.m.* infected M $\phi$  (Figure 24). Together these findings suggest that the stimulation of M $\phi$  with IFN- $\gamma$  leads to the production of endogenous IFN- $\beta$  and TNF- $\alpha$ . Therefore, a single signal from the IFN- $\gamma$  receptor might provide the necessary activation for the acquisition of a M1 proinflammatory program in M $\phi$ . However, it does only reflect a smaller part of the transcriptional program of infected *L.m.* infected M $\phi$ .

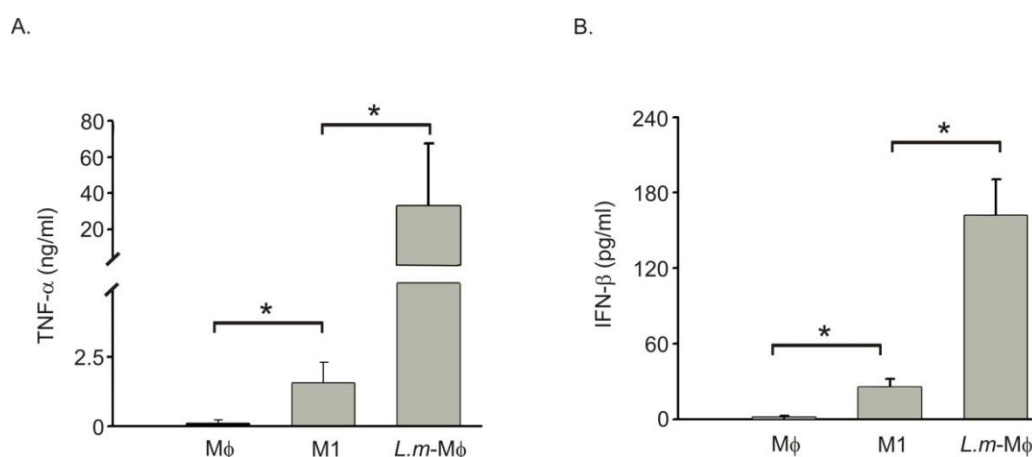


**Figure 24. M1 M $\phi$  stimulate the production of endogenous TNF- $\alpha$  and IFN- $\beta$**

**A.** TNF- $\alpha$  was measured via ELISA in the supernatants of untreated, M1 and *L.m.*-M $\phi$ . **B.** IFN- $\beta$  was measured in the supernatants of untreated, M1 and *L.m.*-M $\phi$  ( $n=4$ , mean $\pm$ std,  $p^* < 0.05$ , student's *t* test).

## 5.7 Comparative analysis of transcriptional responses in macrophages infected with *L. monocytogenes* and regulatory macrophages

Despite the overlap of the genomic profile between *L.m.* infected M $\phi$  and M1, soluble factors secreted by *L.m.*-M $\phi$  did not engage T cell proliferation as it is supported by M1 M $\phi$  (Figure 10). This finding suggests that also at a functional level *L.m.* infected M $\phi$  differ from the classic models of polarization. Moreover, *L.m.*-M $\phi$  share functional and phenotypic characteristics with Mreg, including the capacity to suppress T cell proliferation and the expression of immunomodulatory molecules like, IDO1, CD25, COX-2 and IL-10. Therefore, it was questioned whether the transcriptional responses of *L.m.* infected M $\phi$

are better explained by the responses generated by the factors that determine Mreg polarization, namely TNF- $\alpha$  in combination with PGE<sub>2</sub> and Pam<sub>3</sub>. To answer this question, biological samples of Mreg were investigated on whole transcriptome level by microarray analysis.

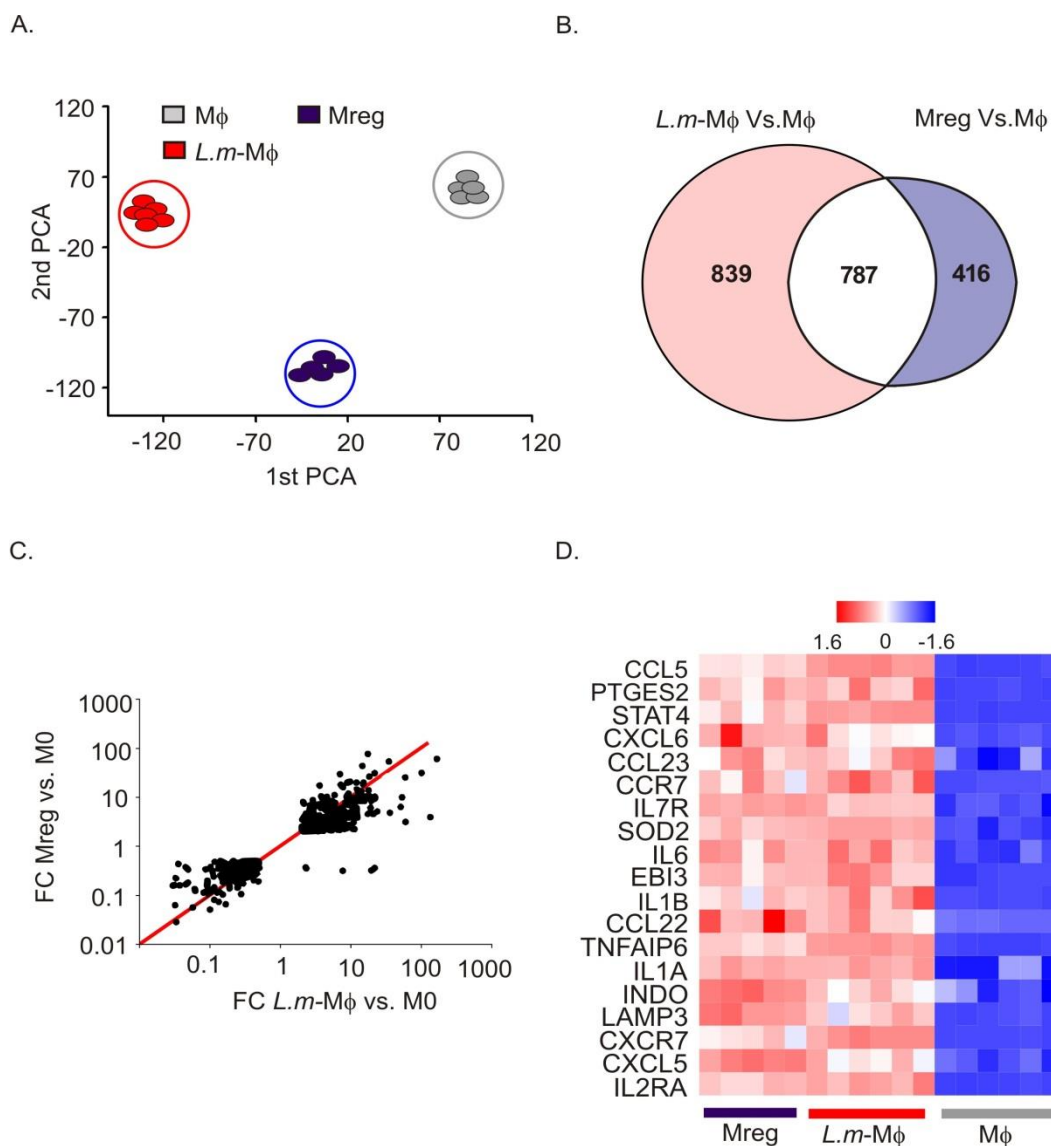


**Figure 25. *L.m.*-M $\phi$  and Mreg share a transcriptional signature that represents 50% of the transcriptional response observed upon *L.m.* infection**

**A.** PCA analysis on 2380 variable genes of *L.m.*-M $\phi$ , Mreg and untreated M $\phi$ . **B.** Venn diagram of DE genes in *L.m.*-M $\phi$  or Mreg calculated against the untreated control **C.** FC/FC plot of the genes DE in Mreg but also in *L.m.*-M $\phi$ . **D.** Heatmap of the top 20 DE genes similarly regulated in Mreg and *L.m.*-M $\phi$ . The average expression values were obtained from microarray experiments and were standardized before visualization (z-score transformation).

Using the expression values of variable genes present in the data set, a PCA revealed that the transcriptional responses of *L.m.*-M $\phi$  differed substantially from those observed in Mreg (Figure 25 A). However, the comparison between the DE genes in *L.m.*-M $\phi$  and Mreg against resting M $\phi$  showed that infection with *L.m.* as well as a combinatorial signal provided by TNF- $\alpha$ , PGE<sub>2</sub> and Pam<sub>3</sub> lead to the expression of a common transcriptional program integrated by 787 genes (Figure 25 B). This common transcriptional program of *L.m.*-M $\phi$  and Mreg represents 48% of the total transcriptional variation triggered by *L.m.* infection. In addition, over 98% of these genes were regulated in the same direction (Figure 25 C). In total, only four transcripts were regulated in the opposite direction. Those genes were upregulated in *L.m.*-M $\phi$  but downregulated in Mreg cells. This group of genes encompasses MX1, OAS2, IFI44 and TNFSF10. Interestingly, those genes have been identified as part of the response to type I interferon in humans (Kemp, Elzey et al. 2003; Barr, Smiley et al. 2008; Onomoto, Morimoto et al. 2011) underlining once more the relevance of the type I interferon pathway in the fight against *L.m.* infection. In agreement with the in vitro data, Mreg and *L.m.*-M $\phi$  express simultaneously genes like IL6, IL1A, IL1B, CCR7, CCL5, STAT4, which are all involved in proinflammatory processes, but express also genes linked to immunomodulatory functions including INDO, PTGES2 and IL2RA (Figure 25 D). Taken together, these findings lead to the conclusion that the transcriptional program of Mreg is closer to the program observed in *L.m.*-M $\phi$ , than to the transcriptional programs induced in M1 and M2 M $\phi$ .

Since the transcriptional changes in Mreg are a consequence of signaling processes triggered by the combination of TNF- $\alpha$ , PGE<sub>2</sub> and Pam<sub>3</sub>, the contribution of each one of these factors to the common transcriptional profile of *L.m.*-M $\phi$  and Mreg was explored. For this purpose M $\phi$  were treated independently with TNF- $\alpha$ , PGE<sub>2</sub> or Pam<sub>3</sub> and harvested 24 h after the stimulation and used for microarray analysis.

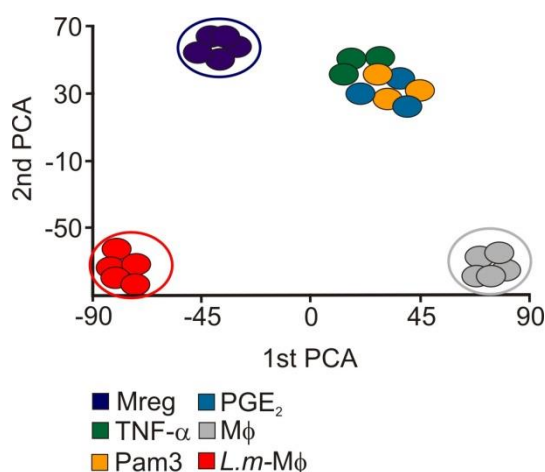


**Figure 26. The transcriptional responses of M $\phi$  treated with TNF- $\alpha$ , PGE<sub>2</sub> or Pam<sub>3</sub> do not explain in detail the transcriptome of *L.m.*-M $\phi$**

PCA analysis on variable genes (1925 transcripts) of Mreg, *L.m.*-M $\phi$  and M $\phi$  treated with TNF- $\alpha$ , PGE<sub>2</sub> or Pam<sub>3</sub>.

The PCA analysis for all M $\phi$  treated with the immune activators described above, revealed that each single stimulus does not induce transcriptional changes comparable to those observed in Mreg or *L.m.*-M $\phi$  24 post-stimuli or infection (Figure 26).

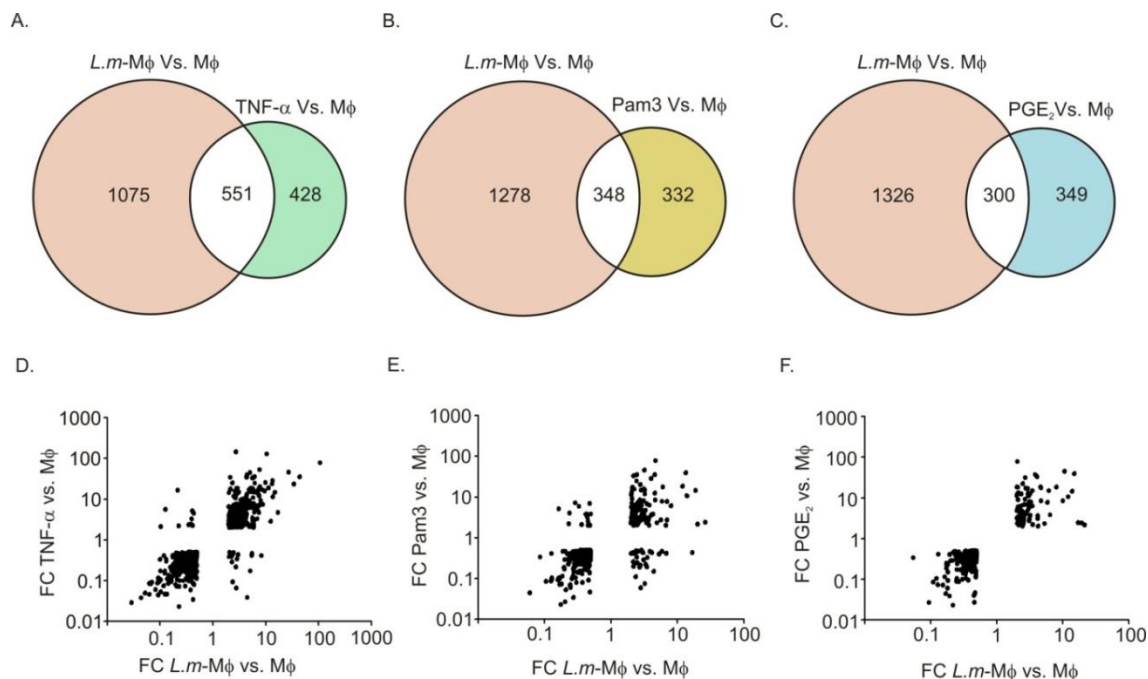


**Figure 27. The single stimuli provided by TNF- $\alpha$ , PGE<sub>2</sub> and Pam3 do not reproduce transcriptional signature common between Mreg and *L.m.*-M $\phi$**

**A.** Venn-diagram of DE genes between *L.m.*-M $\phi$  and TNF- $\alpha$  treated M $\phi$  and the untreated control. **B.** Venn-diagram of DE genes between *L.m.*-M $\phi$  and PGE<sub>2</sub> treated M $\phi$  and the untreated control. **C.** Venn-diagram of DE genes between *L.m.*-M $\phi$  and Pam<sub>3</sub> treated M $\phi$  and the untreated control. **D.** FC/FC plot of the DE common between TNF- $\alpha$  treated and *L.m.*-M $\phi$ . **E.** FC/FC plot of the DE common Pam<sub>3</sub> treated and *L.m.*-M $\phi$ . **F.** FC/FC plot of the DE common PGE<sub>2</sub> treated and *L.m.*-M $\phi$ .

In detail, TNF- $\alpha$  treated M $\phi$  shared 551 DE genes with *L.m.*-M $\phi$  (Figure 27 A). This group of genes represented 34% of those genes being regulated upon *L.m.* infection. In addition, a TNF- $\alpha$  signature was present in infected M $\phi$  and encompassed 50% of the genes common between IFN- $\gamma$  induced M1 and *L.m.*-M $\phi$ . The majority of the DE genes (96%) common between *L.m.*-M $\phi$  and TNF- $\alpha$  stimulated M $\phi$  were regulated in the same direction (Figure 27 D). However, 4% of the genes presented an opposite behavior. These genes included CCL8, LILRA3, DUSP19 and NAMPT which were up-regulated in response to *L.m.* infection, but not after TNF- $\alpha$  treatment. Unexpectedly, although Pam<sub>3</sub> and

lipoteichoic acid from *L.m.* are both ligands for the TLR2 receptor, M $\phi$  treated with this synthetic agonist shared only 348 DE genes with *L.m.*-M $\phi$  (Figure 27 B). A certain amount of these transcripts (12%) were regulated with an opposite trend (Figure 27 E) suggesting that a mere activation of TLR2 signaling does not play a crucial role in the transcriptional changes occurring 24 h after *L.m.* infection. Along the same lines, M $\phi$  treated only with PGE<sub>2</sub> shared only 300 DE genes with *L.m.*-M $\phi$  (Figure 27 C), all of them regulated in the same direction (Figure 27 F). The data demonstrate that amongst the factors driving Mreg polarization, TNF- $\alpha$  exerts the strongest similarity to *L.m.*-M $\phi$ . Nevertheless, it is important to note that the genes regulated by TNF- $\alpha$  treated M $\phi$  represent only 50% of the total common genes observed between Mreg and *L.m.*-M $\phi$ . Furthermore, the union of the genes common to *L.m.*-M $\phi$  and each one of the single stimuli represents only 40% of the total genes common between Mreg and *L.m.*-M $\phi$ . These findings suggest that beyond the transcriptional responses provided by each separated factor (TNF- $\alpha$ , PGE<sub>2</sub> and Pam<sub>3</sub>) the interactions between them are relevant to explain the transcriptional changes that follow *L.m.* infection.

In summary, the data suggest that early events following *L.m.* infection lead to a strong transcriptional response in M $\phi$  and DC. In addition, the results indicate that the transcriptional modifications driven by *L.m.* infection in M $\phi$  are better mirrored by Mreg than by the model of M1 polarized M $\phi$ .

## **5.8 Integration of host factor derived signals and its comparison with the transcriptome of *L. monocytogenes* infected macrophages**

The evidence suggested that, stimulation with TNF- $\alpha$  in concert with PGE<sub>2</sub> and Pam<sub>3</sub> reproduces important aspects of *L.m.* infection in M $\phi$ . However, IFN- $\gamma$  stimulation alone represented approximately a third part of the transcriptional program observed in infected cells (Figure 22). Furthermore, GO enrichment analysis has revealed a key role of a type I interferon signature in the transcriptional changes of M $\phi$  to *L.m.* infection (Figure 13). Interestingly, previous work suggested that IFN- $\beta$  expression is regulated only in response to infection with wild type *L.m.* but not in response to the phagosome restricted hly mutant (Figure 19 B) (Leber, Crimmins et al. 2008; Abdullah, Schlee et al. 2012). Furthermore, IFN- $\beta$  has been described as a key factor in the orchestration of transcriptional responses once *L.m.* has reached the cytosol (Leber, Crimmins et al. 2008). To evaluate whether the addition of IFN- $\gamma$  and IFN- $\beta$ , to the signals provided by TNF- $\alpha$ , PGE<sub>2</sub> and Pam<sub>3</sub>, results in

a better reproduction of the transcriptional features of M $\phi$  infected with *L.m.*, M $\phi$  were stimulated with IFN- $\gamma$  and IFN $\beta$  separately or in concert with TNF- $\alpha$ , PGE $_2$  and Pam $_3$ . The transcriptome of the different experimental groups was compared to the one derived from M $\phi$  infected with *L.m.*

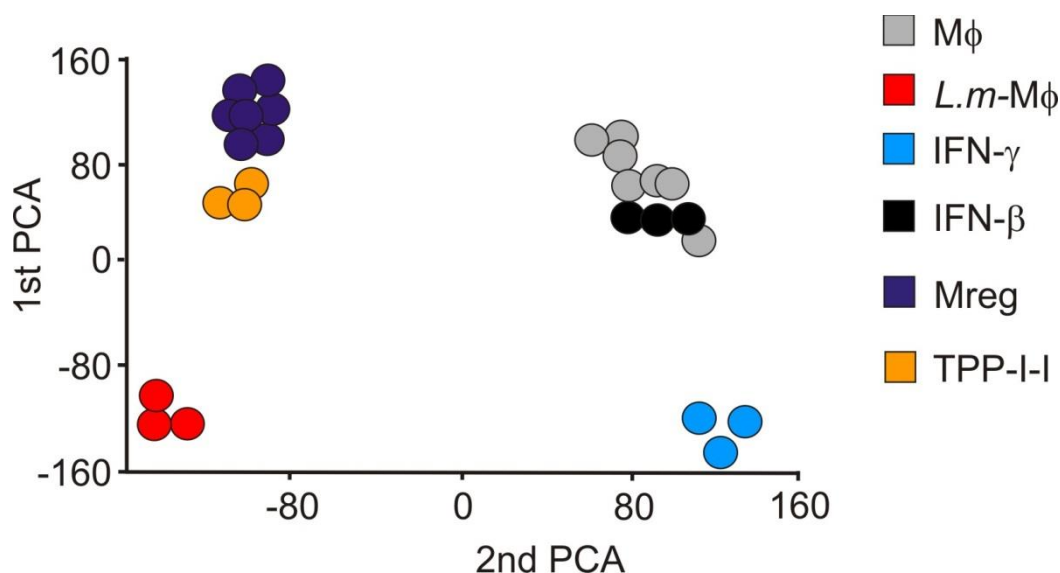


**Figure 28. Addition of IFN- $\beta$  and IFN- $\gamma$  to TNF- $\alpha$ , PGE $_2$  and Pam $_3$  does not lead to major changes in the transcriptome of M $\phi$ .**

PCA analysis on variable genes (1124 transcripts) expressed by M $\phi$  treated with IFN- $\gamma$ , IFN- $\beta$ , TNF- $\alpha$  in combination with PGE $_2$  and Pam $_3$ , infected with *L.m.* and treated with TNF- $\alpha$ , PGE $_2$ , Pam $_3$  in combination with IFN- $\alpha$  and IFN- $\gamma$  (TPP-I-I).

The two dimensional PCA analysis revealed that M $\phi$  treated with IFN- $\gamma$  and IFN- $\beta$  in concert with TNF- $\alpha$ , PGE $_2$  and Pam $_3$  (abbreviated as TPP-I-I) maintained a close relationship with Mreg, suggesting that the addition of IFN- $\gamma$  and IFN- $\beta$  to the triple stimuli constituted by TNF- $\alpha$ , PGE $_2$  and Pam $_3$ , did not lead to a major modification of the transcriptome observed in Mreg M $\phi$ . Interestingly, the stimulation of M $\phi$  with IFN- $\beta$  alone did not involve drastic changes in their transcriptome since IFN- $\beta$  treated M $\phi$  clustered in proximity to non-polarized M $\phi$  (Figure 28). Furthermore, the comparison between non-polarized and IFN- $\beta$  treated M $\phi$  revealed only 20 genes to be differentially expressed between these groups. As expected this group of genes included several well-known targets of type I IFN, including: MX1, OAS2, CCL8 (Waddell, Popper et al. 2010), and several members of the IFN-induced protein with tetratricopeptide repeats (IFIT) family

amongst others (Diamond and Farzan 2013) (Table 8). Additionally, 5 of the DE genes were also expressed in response to the infection with wt *L.m.* including, OASL, OAS2, IFI44L, IFIT1 and IFIT3.

Gene symbol	FC	Description
IFI27	8.0	IFN- $\beta$ up vs. M $\phi$
MX1	5.0	IFN- $\beta$ up vs. M $\phi$
OASL	4.2	IFN- $\beta$ up vs. M $\phi$
<b>IFI44L</b>	3.0	IFN- $\beta$ up vs. M $\phi$
<b>OAS2</b>	3.0	IFN- $\beta$ up vs. M $\phi$
<b>IFIT1</b>	3.0	IFN- $\beta$ up vs. M $\phi$
<b>IFIT3</b>	3.0	IFN- $\beta$ up vs. M $\phi$
CCL8	2.5	IFN- $\beta$ up vs. M $\phi$

**Table 8. Transcripts regulated upon stimulation with IFN- $\beta$  in M $\phi$**

Table shows 8 genes with the highest FC regulated upon treatment of M $\phi$  with IFN- $\beta$  the genes highlighted in bold were regulated also in response to infection with wt *L.m.*

Although the addition of IFN- $\beta$  and IFN- $\gamma$  to the stimuli provided by TNF- $\alpha$ , PGE<sub>2</sub> and Pam<sub>3</sub>, did not result in major changes of location in the PCA analysis, the addition of interferons led to the regulation of 244 transcripts in common with *L.m.* infected M $\phi$ , that were not observed between those and Mreg (Figure 29). Moreover, 190 of these transcripts were not regulated in M $\phi$  treated with IFN- $\beta$  or IFN- $\gamma$  separately (Data not shown).

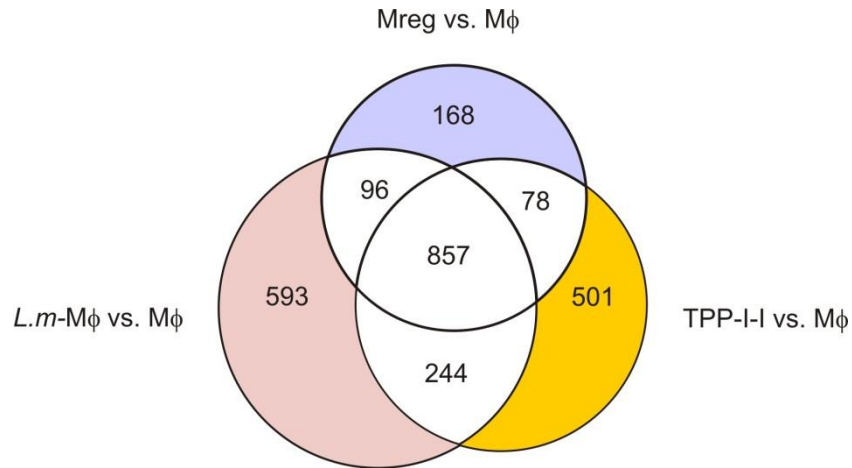


**Figure 29. IFN- $\gamma$  and IFN- $\beta$  addition to TNF- $\alpha$ , PGE $_2$  and Pam $_3$  resulted in the regulation of 200 new genes in common with *L.m*-M $\phi$**

The Venn diagram depicts DE genes observed in Mreg, *L.m.* infected and TPP-I-I in comparison to untreated M $\phi$

The GO enrichment analysis of the 200 genes common to TPP-I-I stimulated and *L.m.* infected M $\phi$  revealed that genes belonging to the type I interferon mediated signaling pathway are highly represented in this group since this category showed one of highest enrichment scores (27). Similarly, the GO category 'response to virus' presented an enrichment score of 16, suggesting once more the predominant presence of genes related to the type I IFN pathway (Figure 30 A). In addition, IRF7 a key regulator of the type I IFN production (Genin, Vaccaro et al. 2009), is amongst the genes that exhibited the highest FC common in TPP-I-I and *L.m.* infected M $\phi$ . Along the same lines, the transcription factor STAT1 which is activated in response to type I and II IFN signaling, was also highly upregulated in TPP-I-I treated and *L.m.* infected M $\phi$ . Finally, several members of the family of guanylate binding proteins are regulated similarly in TPP-I-I and *L.m.* infected M $\phi$ , indicating the strong response to IFN- $\gamma$  observed in both groups (Martens and Howard 2006) (Figure 30 B).



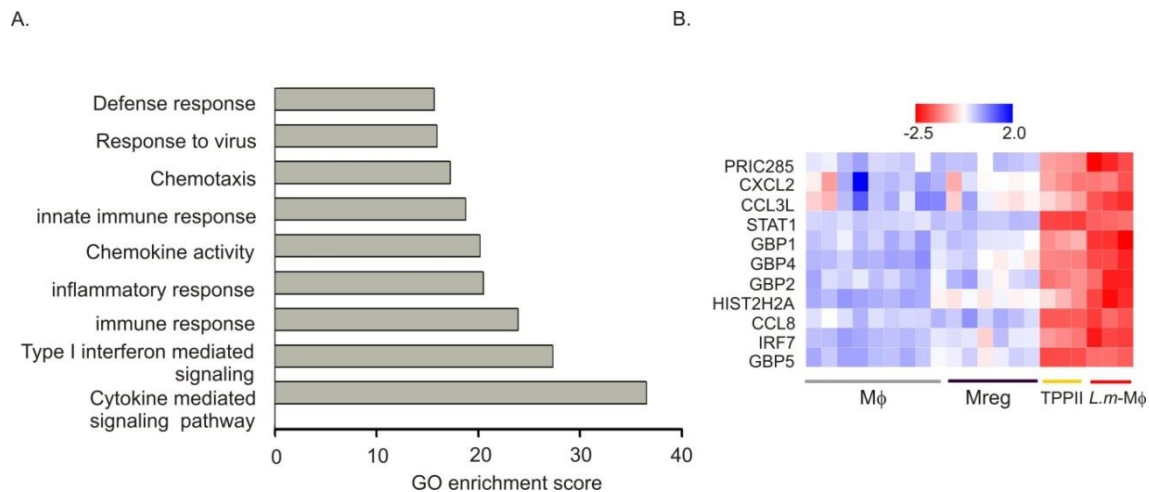


**Figure 30. The genes in TPP-I-I and *L.m.* infected M $\phi$  are related mainly to Type I interferon mediated signaling.**

**A.** GO enrichment analysis of 200 genes common between TPP-I-I treated and *L.m.* infected M $\phi$  **B.** Heatmap of the top 12 DE genes similarly regulated in TPP-I-I and *L.m.*-M $\phi$ . The average expression values were obtained from microarray experiments and were standardized before visualization (z-score transformation).

The presented findings indicated that signaling cascades activated by TNF- $\alpha$ , Pam<sub>3</sub> and PGE<sub>2</sub> together with IFN- $\beta$  and IFN- $\gamma$  induced a genomic profile that explains 64% of the total transcriptional changes of M $\phi$  upon *L.m.* infection. These data further support the notion that the transcriptional reprogramming of non-infected macrophages e.g. at the outside of the ringwall within granuloma can be explained to a large extent by a cascade of host factors induced by infection and then resembling the transcriptional program induced by infection itself.

## 5.9. IDO1 is expressed in human myeloid cells upon *L. monocytogenes* infection

The enzyme IDO1 catalyzes the degradation of the essential amino acid Trp generating metabolites such as Kyn. In recent years, the pivotal role of IDO1 in immunomodulation has been documented (Munn and Mellor 2004). In vitro assays showed that an increased turnover of Trp leads to Trp depletion inducing T cell proliferation arrest and induction of apoptosis (Fallarino, Grohmann et al. 2002; Terness, Bauer et al. 2002; von Bergwelt-Baildon, Popov et al. 2006). More recently, the immunomodulatory effects of IDO1 have

been associated to the expansion (Chung, Rossi et al. 2009) and induction of T<sub>reg</sub> cells (Mezrich, Fechner et al. 2010). However, IDO1 was first described as an important effector in the clearance of a broad range of pathogens via a mechanism that involved Trp depletion (Pfefferkorn 1984; MacKenzie, Hadding et al. 1998; Oberdorfer, Adams et al. 2003). In addition, more recently it has been described that Trp catabolites might also exert a toxic effect on different microorganisms, including bacteria and protozoa (Narui, Noguchi et al. 2009; Knubel, Martinez et al. 2010; Knubel, Martinez et al. 2011). The data presented in previous chapters showed that IDO1 expression is a distinctive feature in the response of myeloid cells to *L.m.* infection. Moreover, previous studies have demonstrated that DCreg which share several common hallmarks with DC infected with *L.m.*, including the expression of IDO1, CD25 and COX-2 can control the intracellular growth of *L.m.* more efficiently than immDC and matDC (Popov, Driesen et al. 2008). To assess the potential role of IDO1 as microbicidal effector in DC but also other myeloid cells, time kinetics of IDO1 expression was explored via western blot analysis.

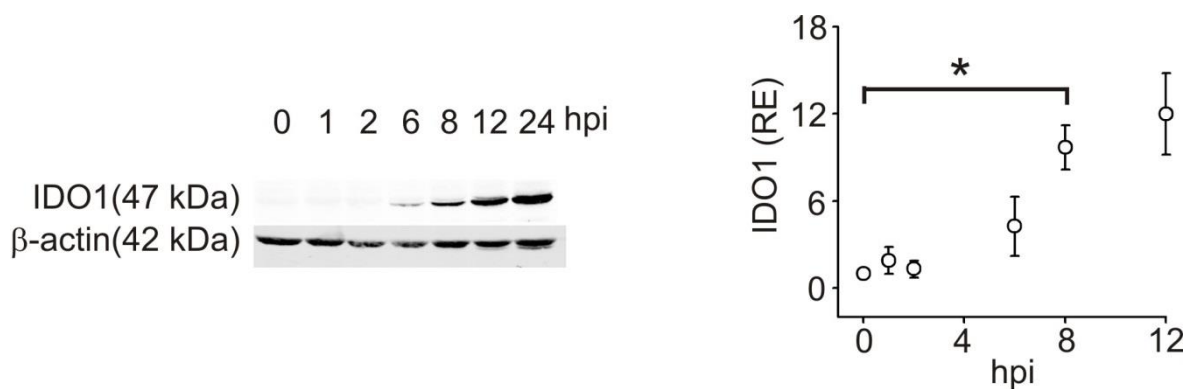


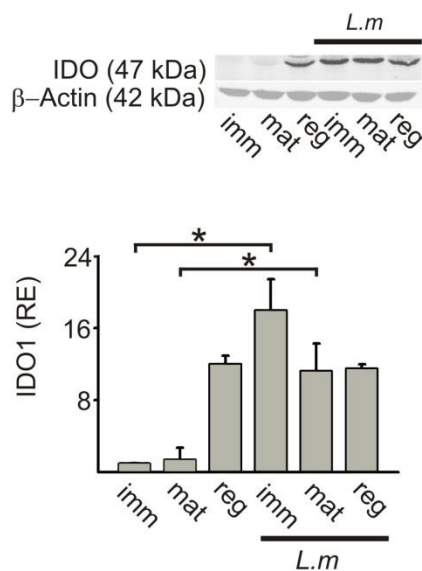
**Figure 31. IDO1 expression is an early event after *L.m.* infection**

IDO1 protein expression was assessed by western blot technique in human infected immDC at indicated time points after infection. In all cases  $\beta$ -actin was used as loading control. IDO1 RE was estimated by analyzing the intensity of each band normalized to the intensities of  $\beta$ -actin. The displayed membrane is representative of 3 experiments. The results for the FC are presented as mean  $\pm$ sd. \*p-value <0.05 (student's *t*-test)

IDO1 was detectable already at 6 hpi, and its expression reached a significant level at 8 hpi (Figure 31). These findings differed from previous results that reported a significant induction of IDO1 only at 12 hpi (Popov, Abdullah et al. 2006). This discrepancy might be due to the lower sensitivity provided by the ECL (enhanced chemiluminescence) method used previously to detect the signal from the secondary antibody when compared to the

infrared detection method used currently. IDO1 is early induced after *L.m.* infection in immDC (Figure 31) and untreated M $\phi$  (Figure 8). The question whether IDO1 expression could also become induced in already matured matDC as well as in different polarized M $\phi$  infected with *L.m.* was addressed via western blot 24 hpi. The results revealed that *L.m.* infection induces the expression of IDO1 in matDC (Figure 32 A), but also in M1 and M2 polarized M $\phi$  (Figure 32 B). For instance, IDO1 was two times higher expressed in M1 M $\phi$  after *L.m.* infection. In contrast, DCreg and Mreg did not further increased IDO1 expression after *L.m.* infection (Figure 32).

A.



B.

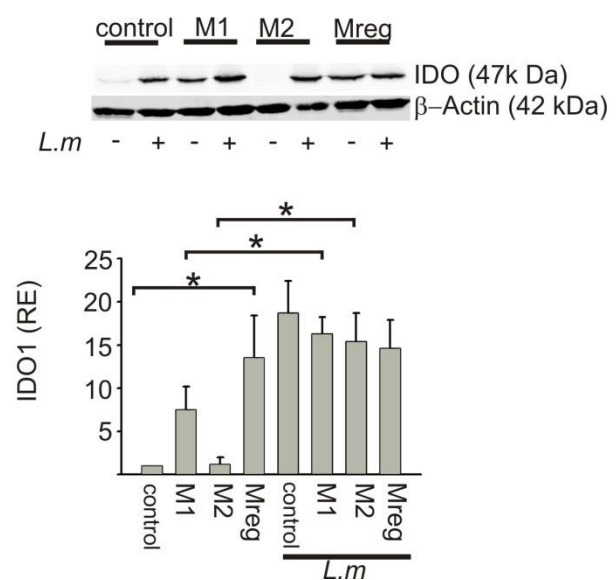


**Figure 32. IDO1 is induced upon *L.m.* infection in mat DC and polarized M $\phi$**

**A.** IDO1 expression was assessed by western blot analysis at 24hpi in human immDC, matDC and DCreg.  $\beta$ -actin was used as loading control. IDO1 FC was calculated by the same procedure described before (n=4, mean $\pm$ sd). **B.** IDO1 expression was evaluated in control, M1, M2 and Mreg M $\phi$  24 hpi via western blot.  $\beta$ -Actin was used as loading control and IDO1 RE was calculated as described before. (n=3, mean $\pm$ sd, \*p-value <0.05, student's *t*-test)

## 5.10 IDO1 competent myeloid cells efficiently control the intracellular growth of *L. monocytogenes*

The data described in section 5.9 suggested that IDO1 expression is an early event in the response of myeloid cells to *L.m.* infection occurring even after maturation or polarization of these cells. To gain more insight into the potential microbicidal role of IDO1 in myeloid

cells, the capacity to restrain the intracellular growth of *L.m.* was assessed in IDO1 competent and non-competent DC and M $\phi$  during 6 h after *L.m.* infection via CFU assay. During the first 2 hpi no significant difference between the microbicidal activity could be observed in IDO1 competent and non-competent myeloid cells. However, at 6 hpi DCreg, Mreg and M1 M $\phi$  showed significantly less (between 60 and 90%) bacterial burden than their IDO1- counterparts and as a consequence controlled *L.m.* growth for longer periods of time (Figure 33). Although, the data suggest that IDO1 is key for the control of *L.m.* growth in myeloid cells, other mechanisms like the production of reactive oxygen and nitrogen species (ROS and RNS respectively) are well-known defense mechanisms that enable the control of intracellular microorganisms in mammalian cells. To evaluate the role of these microbicidal mediators in infected DC and M $\phi$ , ROS and nitrite production were determined via the peroxidase luminol-enhanced chemiluminescence method (LEC) and Griess colorimetric reaction respectively.

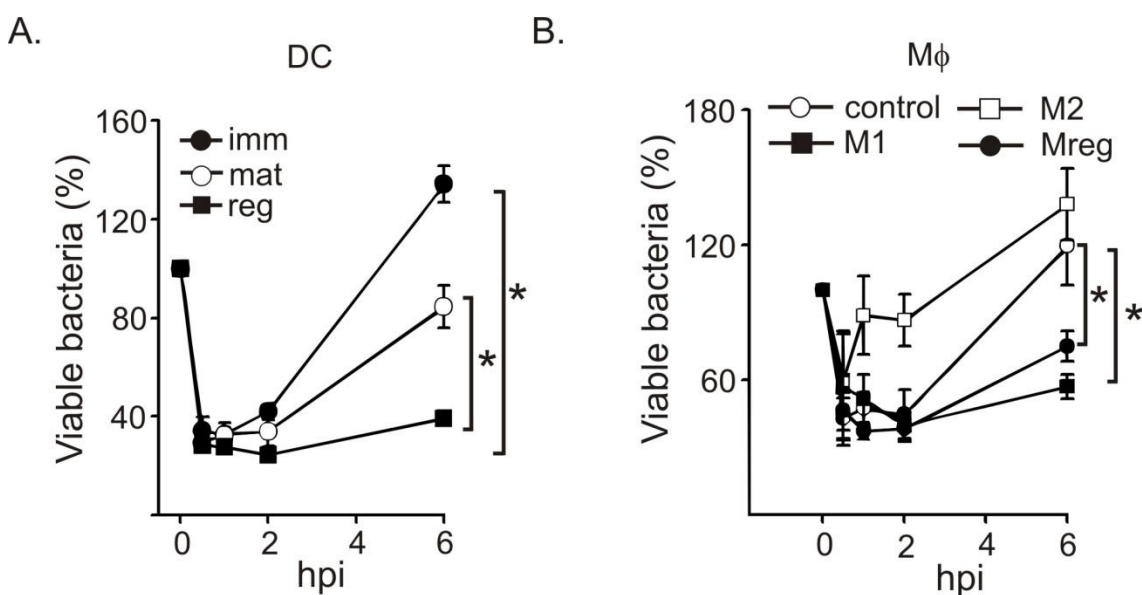


**Figure 33. The microbicidal activity of IDO1 competent and non-competent myeloid cells**

**A.** The intracellular growth of *L.m.* was assessed via CFU analysis in immDC, matDC and DCreg during 6hpi. **B.** The intracellular growth of *L.m.* was assessed via CFU analysis in non-polarized, M1, M2 and Mreg M $\phi$  during 6hpi. In both cases the bacterial load at 0 time point was set to 100%. The bacterial burden for the indicated time points was calculated on this basis. (n=4 mean $\pm$ sd, \*p-value <0.05, student's *t*-test).

Human DC and M $\phi$  produced ROS already between 0.5 and 4hpi (Figure 34 A and B). After this time point the detected luminescence intensities were similar to the background

levels observed in non-infected cells. M $\phi$  were more efficient in ROS production and started the process only half an hour after infection, whereas DC showed delayed ROS production distinguishable from the background at 1 hpi. Along the same lines, the ROS production in infected M $\phi$  was approximately three fold higher than in infected DC (maximal luminescence intensities of  $120\pm7$  for DC and  $324\pm3$  for M $\phi$ ). In contrast, neither increased accumulation of nitrite nor iNOS expression were detected in infected cells at 24 hpi (Figure 34 C). Together the results suggest that ROS production, possibly in concert with bacterial degradation in the phagosome, but not nitrite production play a role in the control of *L.m.* infection at early time points of infection. Meanwhile, IDO1 might play a decisive role in the control of *L.m.* once ROS production and phagosome containment have been overcome.

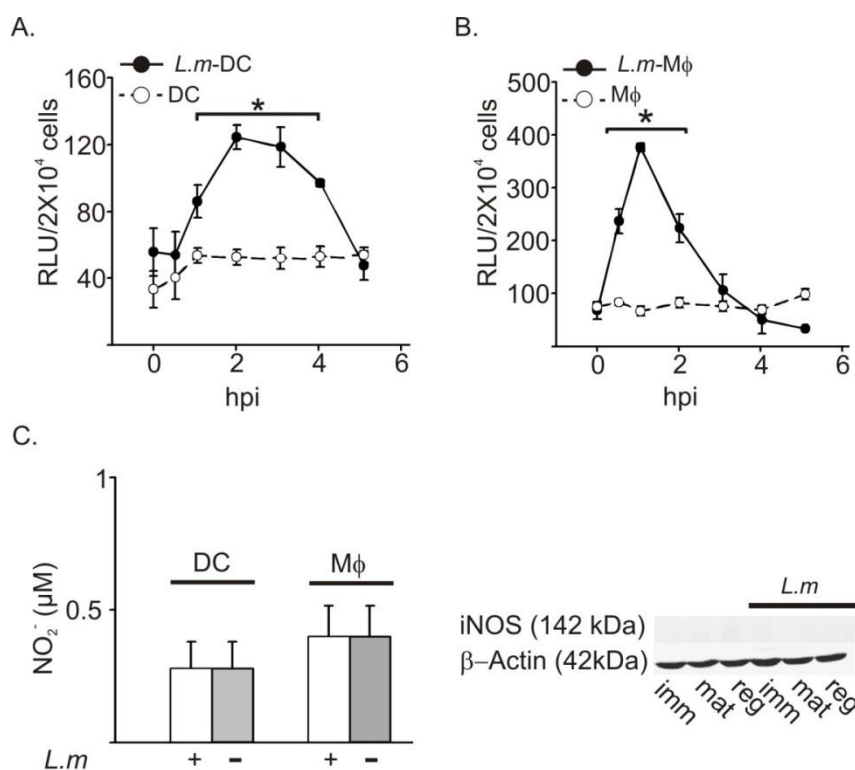


**Figure 31. ROS and nitrite production in *L.m.* infected DC and M $\phi$**

**A.** Screening of ROS production via LEC method in human DC infected with *L.m.* versus non-infected DC during 5hpi. The results are presented as relative light units (RLU)/2x10<sup>4</sup> cells. **B.** Production of ROS in human M $\phi$  infected with *L.m.* (*L.m.*-M $\phi$ ) and non-infected M $\phi$ . The results are presented as RLU/2x10<sup>4</sup> cells. **C.** NO<sub>3</sub> production was measured via Griess colorimetric reaction in DC and M $\phi$  infected with *L.m.* In addition iNOS expression was assessed in DC at different maturation phases via western blot (n=4, mean $\pm$ sd, \*p-value <0.05, student's *t*-test).

## 5.11 Loss of IDO1 function leads to unrestrained bacterial growth

To test if a loss of IDO1 function impacts the growth of *L.m.*, IDO1 was knocked down in DC, and the microbicidal performance of DCreg and IDO1- DCreg was monitored over 6hpi.

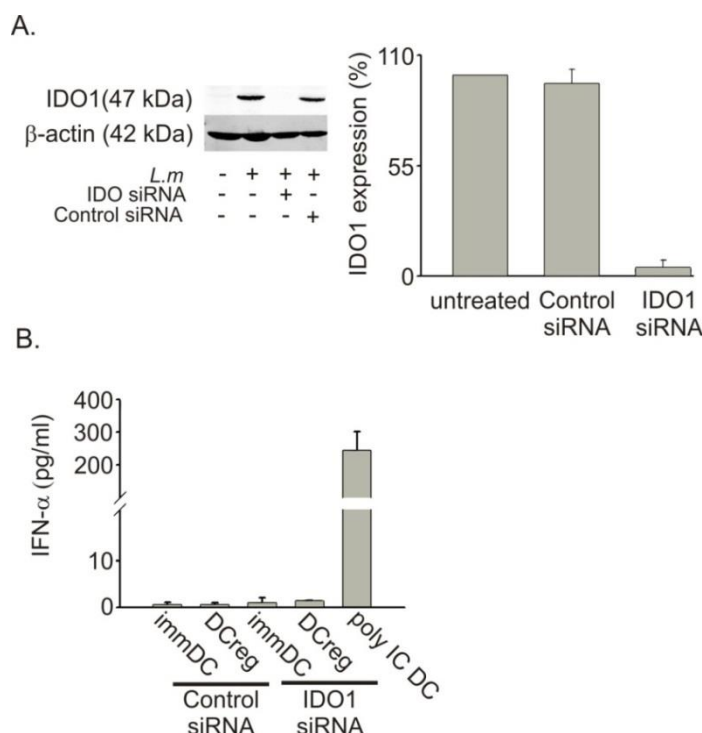


**Figure 32. Knock-down of IDO1 in DC**

**A.** IDO1 silencing experiments were performed via electroporation in DC. The efficiency of silencing was controlled by western blot analysis 24h after *L.m.* infection. The percentage of IDO expression was estimated by analyzing the intensity of each band normalized by the β-actin intensity. Expression of IDO in DCreg treated with control siRNA was set to 100%. **B.** The production of IFN-α was assessed in DC treated with control and IDO1 specific siRNA via ELISA. Poly IC (1μg/ml) treated DC were used as a positive control for this assay. .

DC transfected with IDO1 targeting siRNA showed a reduction of  $94\pm 3\%$  in protein expression in comparison to untreated or control transfected cells (Figure 35 A). In addition, DC transfected with IDO1 or unspecific siRNA did not produce IFN-α, whereas DC treated with poly IC were able to produce significant amounts of this cytokine (Figure 35 B). To extend the experimental settings to Mφ, these cells were transfected with siRNA targeting IDO1. However, the electroporation of Mφ caused massive cell death since  $70\pm 20\%$  of the population was not viable after the procedure. In contrast, lipofection treatment led to insufficient rates of silencing (less than 20%) (data not shown). Due to these reasons, all further silencing experiments were only performed in DC.

After IDO1 knockdown, immDC were treated during 48h with TNF-α in combination with PGE<sub>2</sub> and Pam<sub>3</sub> to obtain DCreg. Untreated, control siRNA and IDO1 siRNA transfected

DCreg were infected with *L.m.* and the intracellular viability of bacteria was evaluated via CFU analysis. The silencing of IDO1 in DCreg caused a dramatic increase of  $80\pm 12\%$  in the bacterial load at 6 hpi in comparison to untreated or control siRNA transfected DCreg. No significant change in the anti-bacterial performance of these cells was observed at earlier time points (Figure 36).

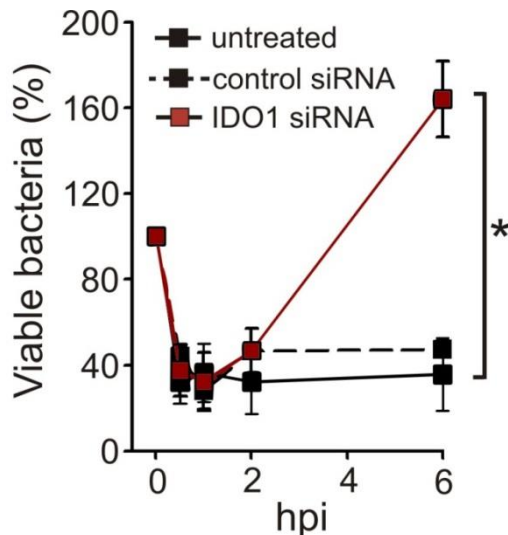


**Figure 33. IDO1 mediates the control of *L.m.* infection in DCreg**

The bacterial load of DCreg untreated or treated with control or IDO1 specific siRNA was assessed via CFU analysis during 6hpi. The bacterial load at 0h time point was set to 100% and the bacterial burden for the following time points was calculated on this basis. (\*p-value <0.05, student's *t*-test)

Indoleamine 2,3-dioxygenase 2 (IDO2) has emerged as a Trp catabolizing enzyme, possibly redundant to IDO1 (Ball, Yuasa et al. 2009). To evaluate the role of IDO2 in myeloid cells upon *L.m.* infection, the expression of this enzyme was evaluated in control and infected myeloid cells via qRT-PCR. Additionally Trp catabolism was assessed indirectly by measuring Kyn accumulation in supernatants of infected DC after IDO1 silencing or treatment with control siRNA. The results showed that IDO2 expression is induced after *L.m.* infection in DC and M $\phi$  (Figure 37 A). However, Kyn accumulation decreased in 92% after silencing of IDO1, but not after treatment with control siRNA (Figure 37 B). These results indicate that in human DC IDO1 is the key enzyme that catalyzes Trp degradation, whereas IDO2 does not seem to play a role.



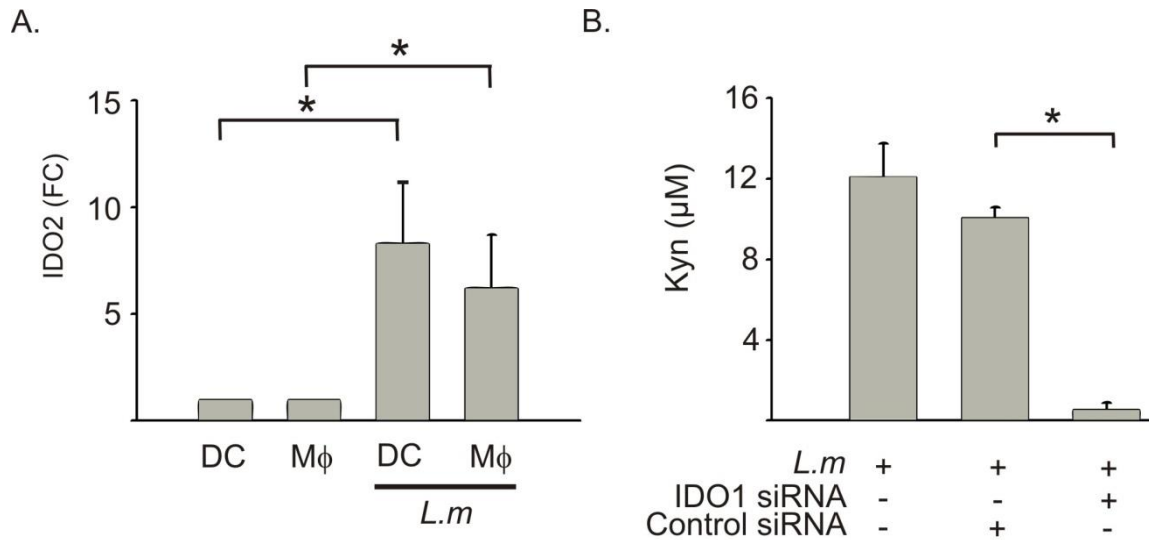


**Figure 34. IDO1 but not IDO2 is essential for Trp catabolism in human DC**

**A.** IDO2 expression in DC and Mφ upon *L.m.* infection. In all the test conditions, the expression of the target mRNA was normalized by GAPDH expression and the FC was calculated in respect to the non-infected control cells. **B.** Kyn accumulation in supernatants of DCreg infected by *L.m.* treated with control or IDO1 specific siRNA was evaluated by Ehrlich colorimetric method. (\*p-value <0.05, student's *t*-test)

So far the results suggest that IDO1 plays a key role for the control of the intracellular growth of *L.m.* in DC. However, it is not yet clear whether this effect depends on the enzymatic activity of IDO1 or its recently discovered function as signaling molecule (Pallotta, Orabona et al. 2011). Along the same lines, due to technical difficulties, the role of IDO1 in the microbicidal performance of Mφ has not been assessed yet. To evaluate the role of IDO1 enzymatic activity in the control of *L.m.* intracellular growth in DC and Mφ, the catalytic function of IDO1 was inhibited via treatment with 1-MT in DCreg and M1 Mφ. Kyn accumulation was measured subsequently via Ehrlich reaction, as a surrogate indicator of IDO1 activity.

Treatment with 1-MT (150μM) reduced the accumulation of Kyn in the medium down to 50% in cultures of DCreg and M1 Mφ. The percentage of viable cells was similar in 1-MT treated and non-treated cells, suggesting that this important reduction in the enzymatic activity of IDO1 is not due to an unspecific decrement in cell viability, caused by the inhibitor or the solvent used for its reconstitution (Figure 38 A and B). In DCreg, loss of the enzymatic activity of IDO1 led to an increment in bacterial burden of 80±15% (Figure 38 C). Similarly, 1-MT treated M1 Mφ also showed 60±11% increment in bacterial burden



relative to untreated controls (Figure 38 D). Altogether the presented data suggest that in vitro the enzymatic activity of IDO1 is crucial to control *L.m.* growth in human DC and M $\phi$ .

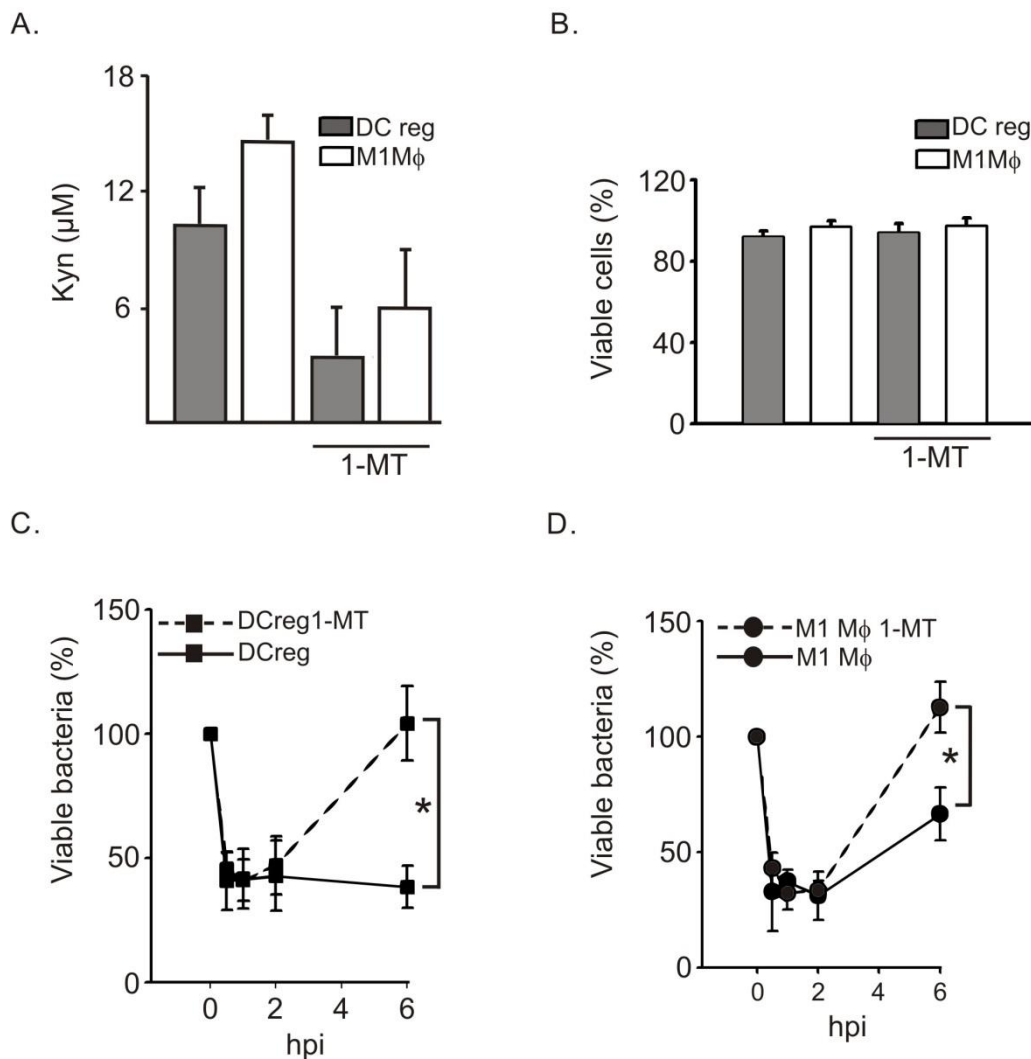


**Figure 35. IDO1 enzymatic activity is important for the control of *L.m.* infection in IDO competent cells**

**A.** The efficiency of 1-MT inhibition was evaluated by measuring Kyn accumulation in the medium of treated and untreated cells via Ehrlich reaction. **B.** Cell viability was determined after treatment with 1-MT via PI staining and flow cytometry. **C.** *L.m.* intracellular viability was tested in DCreg treated and untreated with 1-MT. The bacterial load at the 0h time point was set to 100% and the bacterial burden for the following time points was calculated on this basis. **D.** *L.m.* intracellular viability was evaluated in M1 M $\phi$  treated and untreated with 1-MT. The bacterial load at 0h was set to 100% and the bacterial burden for the following time points was calculated on this basis. (n=4, mean $\pm$ sd, \*p-value <0.05, student's *t*-test)

## 5.12 IDO1 microbicidal activity is mediated by tryptophan catabolites

The microbicidal activity of IDO1 has been attributed to Trp starvation (Pfefferkorn 1984; Byrne, Lehmann et al. 1986; MacKenzie, Hadding et al. 1998). However, more recently the accumulation of Trp catabolites has shown to be toxic for different bacteria including *Staphylococcus aureus*, *Enterococcus faecalis*, and *Escherichia coli* (Narui, Noguchi et al. 2009) and for the protozoan parasite *T. cruzi* (Knubel, Martinez et al. 2010; Knubel, Martinez et al. 2011). To evaluate the impact of Trp starvation on the control of *L.m.* growth, DCreg were cultured under Trp enriched (50  $\mu$ M), and Trp depleted conditions (no Trp was added to the medium). The anti-bacterial activity of DCreg was followed during 6 h by CFU analysis.

High concentrations of Trp (50 $\mu$ M) enabled DCreg to increase their bactericidal activity against *L.m.* Strikingly, conditions of Trp excess led to a 3-fold reduction of the bacterial burden of DCreg compared to cells cultured in the absence of this amino acid (Figure 39 A). In contrast, the bactericidal performance of immDC was not affected by Trp starvation or enrichment since around 120% bacterial burden was observed in both cases. In addition, the enhanced microbicidal performance of DCreg cultured in the presence of Trp was associated to Kyn accumulation in the supernatants. Already 6 hpi DCreg cultured under excess of Trp produced 3-times more Kyn ( $12 \pm 3.5 \mu$ M, p-value 0.02) than their counterparts cultured under Trp depleted conditions (Figure 39 B).

In summary, Trp depletion does not play a key role in microbicidal activity of IDO1+ DCreg whereas Kyn accumulation was associated with an enhanced control of *L.m.* growth. To test the impact of Kyn on bactericidal activity of DC, immDC were cultured up to 6 hpi in presence of 50 and 100  $\mu$ M of Kyn. The bacterial burden was followed during this time frame. Treatment with 50 $\mu$ M Kyn led to a 3-fold reduction of the bacterial burden of immDC whereas the incubation with higher concentrations (100 $\mu$ M) did not represent a further improvement of the anti-bacterial performance of these cells (Figure 40).

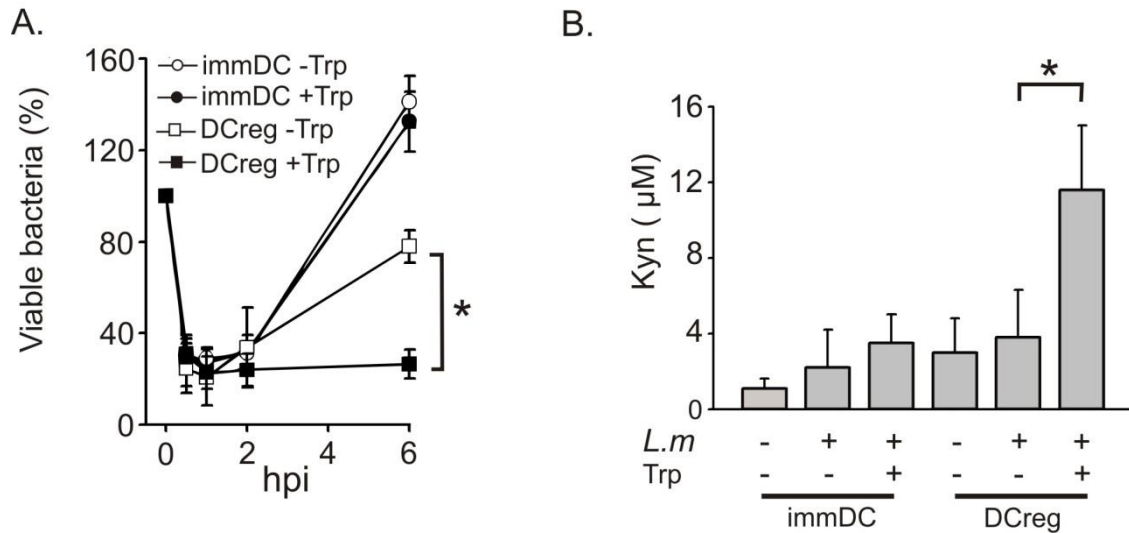


**Figure 36. Tryptophan starvation does not mediate the anti-bacterial activity of DCreg**

**A.** Bacterial burden of infected immDC and IDO+ DC cultured under Trp excess (98 µM) or depletion was evaluated in CFU assays during 6h after *L.m.* infection (n=4, mean±sd). **B.** Kyn production was assessed by Ehrlich colorimetric reaction in supernatants of infected immDC and IDO+ DC at 6 hpi under Trp excess or Trp depleted conditions (n=4 mean±sd). (\*p-value <0.05, student's *t*-test)

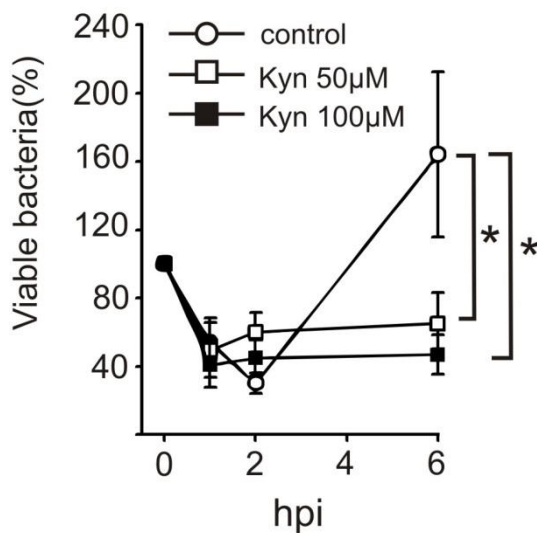


**Figure 40. Kyn addition enhances the anti-bacterial activity of immDC**

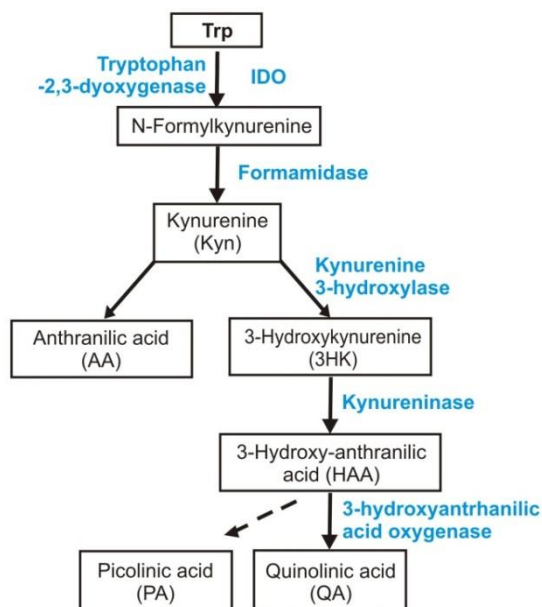
Anti-bacterial activity of immDC was assessed by CFU under normal culture conditions or in the presence of Kyn 50µM and 100µM (n=4, mean±sd). (\*p-value <0.05, student's *t*-test)

The evidence presented above suggests that Kyn might have an intrinsic toxic effect on *L.m.* Trp degradation encompasses several enzymatic steps leading to the production of several catabolites including formylkynurenine, Kyn, anthranilic acid (AA), 3-hydroxykynurenine (3HK), 3-hydroxy-anthranilic acid (HAA), picolinic acid (PA), and quinolinic acid (QA) (Figure 41 A). It has been described that Trp catabolites in a concentration range of 10 to 200µM can induce apoptosis of T cells, thymocytes and Mφ

from murine origin (Fallarino, Grohmann et al. 2002). To assess the potential cytotoxic effect of Trp catabolites on human myeloid cells, DCreg and immDC were incubated with 48h up to 100 $\mu$ M of several stable catabolites of the Kynurenine pathway (Figure 41 A). Subsequently, the cell viability was assessed via PI staining followed by FACS analysis.

The data showed that DC cultures exposed to different kinds of Trp catabolites showed similar percentages of viability to those maintained under control cell culture conditions (Figure 41 B). This finding indicates that Trp catabolites do not have a deleterious impact on human DC viability. Suggesting that Kyn has an intrinsic anti-bacterial activity on *L.m.*, whereas DC are refractory to its effects. Furthermore, the toxicity of Kyn, but not Trp depletion, might be the principal mechanism of DCreg to control the intracellular growth of *L.m.* after the bacteria has invaded the cytoplasm.

A.



B.

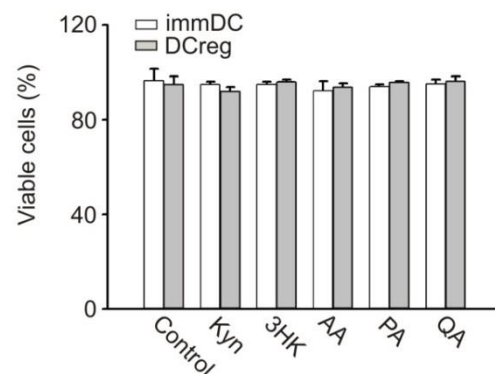


**Figure 41. Trp catabolites did not affect human DC viability**

**A.** Schematic representation of the kynurenine pathway including important intermediates. **B.** Viability of immDC and DCreg left untreated or exposed to 100 $\mu$ M of different Trp catabolites for 24h was assessed by PI staining (n=3, mean $\pm$ sd). The following acronyms were used: control, C; Hydroxykynurenine, 3HK; Anthranilic acid, AA; Picolinic acid, PA; Quinolinic acid, QA.

Since all enzymes of the kynurenine pathway are expressed in M $\phi$  (Guillemin, Smith et al. 2003), the possibility that other Trp catabolites might also contribute to the observed bactericidal activity of DCreg and M1 M $\phi$  was investigated. In order to address this point,

*L.m.* was cultured in the presence of several stable catabolites of the kynurenine pathway for 24 h and the bacterial viability was evaluated by CFU analysis.

At a concentration of 100  $\mu$ M *L.m.* was sensitive to all the tested catabolites, and virtually no colonies were detected. However, at lower concentrations (25 to 50 $\mu$ M) the impact of Trp catabolites on *L.m.* viability varied. For instance, QA did not exert any significant effect at the lowest concentration tested, whereas Kyn and 3HK reduced bacterial viability between 70-80% (Figure 42). In conclusion, *L.m.* viability is strongly decreased by the intermediaries of the kynurenine pathway. Furthermore, this evidence supports the hypothesis of the toxic effect of Trp catabolites and their key function in restraining *L.m.* in the cytoplasm of human myeloid cells.

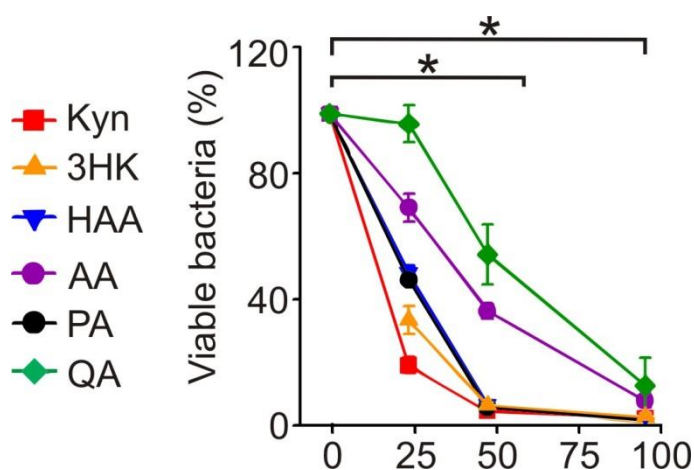


**Figure 42. Trp catabolites have intrinsic anti-bacterial properties on *L.m.***

*L.m.* viability was assessed by CFU 24h after exposure to Trp catabolites in a concentration range from 25 to 100 $\mu$ M (n=3, mean $\pm$ sd). The following acronyms were used: Kynurenine, Kyn  $\blacksquare$ ; 3 Hydroxykynurenine, 3HK  $\blacktriangle$ ; Anthranilic acid, AA  $\bullet$ ; Picolinic acid, PA  $\bullet$ ; Quinolinic acid, QA  $\blacklozenge$ ; Hydroxyanthranilic acid, HAA  $\blacktriangledown$ . (\*p-value <0.05, student's *t*-test)

In the next step, the question was addressed whether Trp catabolites might also have an impact on other bacteria such as *S.p.* and *L.i.*. These bacteria were cultured with several intermediates of the kynurenine pathway and their viability was evaluated after 24h via CFU analysis.

Similar to *L.m.* most Trp catabolites had bactericidal activity on *S.p.*, albeit the pattern was different (Figure 43 A). After treatment with high concentrations of QA, AA, PA or Kyn a reduction of 70% in *S.p.* was observed. While 3HK was very effective against *L.m.*, it did not show a significant effect on *S.p.* even at the highest concentration tested. In contrast, *L.i.* was practically insensitive to low and intermediate concentrations of the catabolites

and only at high concentrations a significant reduction of viability was observed for Kyn, 3HK, AA, and QA (Figure 43 B).

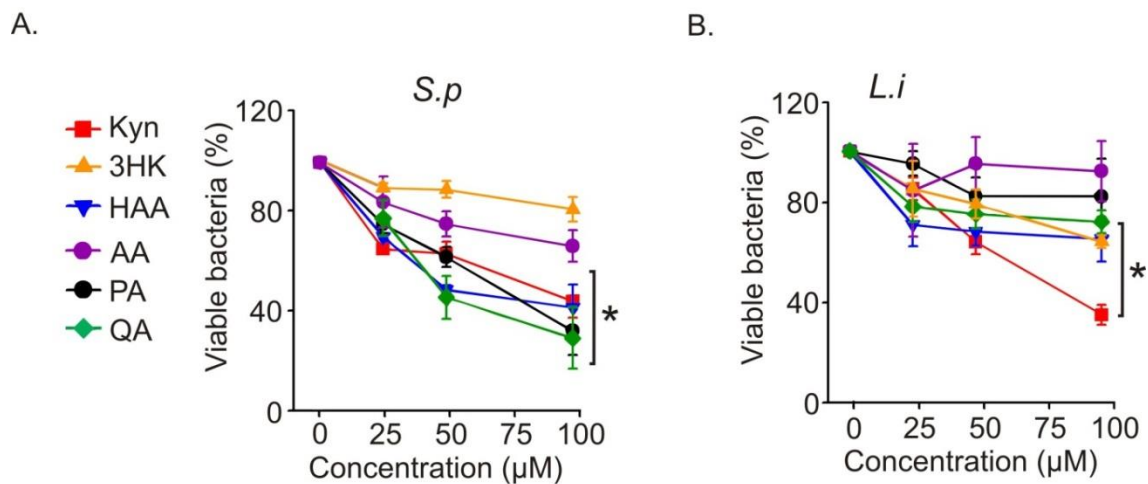


**Figure 37. The sensitivity of bacteria against Trp catabolites varies between species**

**A.** *L.i.* viability was evaluated by CFU 24h after exposure to Trp catabolites in a concentration range from 25 to 100µM (n=3, mean±sd). **B.** *S.p.* viability was evaluated by CFU 24h after exposure to increasing kynurenine concentrations indicated in the diagram (n=3, mean±sd). The following abbreviations were used for A and B: Kynurenine, Kyn ■; 3 Hydroxykynurenine, 3HK ▲; Anthranilic acid, AA ●; Picolinic acid, PA ●; Quinolinic acid, QA ◆; Hydroxyanthranilic acid, HAA ▼. (\*p-value <0.05, student's *t*-test)

In summary, the data suggest that the anti-bacterial effects of kynurenines differ across bacterial species. Therefore, their contribution as microbicidal mechanism cannot be extrapolated a priori to different host cell-bacteria interactions.

### 5.13 Exposure to kynurenine does not impair *L. monocytogenes* invasive capabilities

So far, the data demonstrated that DCreg and M1 Mφ can restrain the intracellular growth of *L.m.* efficiently through an IDO1 and Trp-catabolite dependent mechanism. However, a substantial number of bacteria (30% of the infecting bacteria) still evaded the surveillance exerted by IDO1 expressing myeloid cells and therefore could potentially infect neighboring cells. To test whether pre-exposure of *L.m.* with Kyn would alter infection kinetics of *L.m.* in DCreg and immDC, *L.m.* were precultured under conditions of high Kyn concentrations (25 µM) for 3h prior to infection. No difference in bacterial recovery during the infection cycle of *L.m.* pre-treated with high levels of Kyn in both DC subtypes was observed (Figure 44 A).

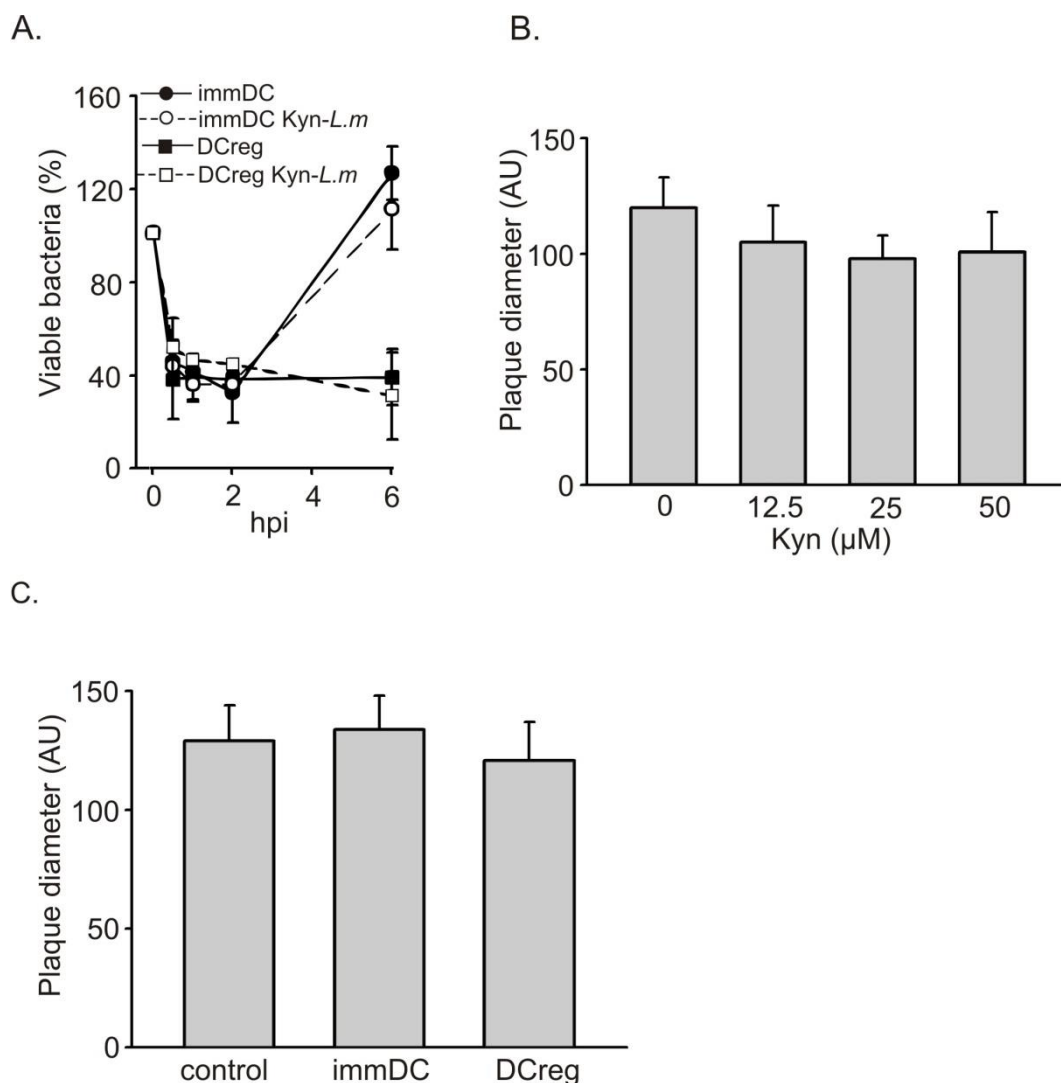


**Figure 38. Kynurenine exposure to *L.m.* does not affect infective capabilities**

**A.** immDC and DCreg were infected with *L.m.* and cultivated in BHI broth alone (solid lines) or BHI supplemented with 25 $\mu\text{M}$  of Kyn (dashed lines) **B.** Plaque diameter were evaluated on confluent 3T3 fibroblasts infected with *L.m.* cultivated in BHI broth alone or in broth supplemented with Kyn concentrations of 12.5, 25 and 50 $\mu\text{M}$ . **C.** Plaque diameter was evaluated on confluent 3T3 fibroblasts infected with *L.m.* recovered after lysis of immDC and DCreg at 6 hpi or BHI cultured *L.m.*. (n=3, mean $\pm$ sd).

To test whether elevated levels of Trp catabolites can impair the ability of *L.m.* to infect non-phagocytic cells, *L.m.* were exposed to increasing concentrations of Kyn for 3h and their capability to invade 3T3 fibroblasts in a standard plaque assay was tested. In contrast to professional phagocytes, *L.m.* is known to actively trigger its entry to fibroblasts (Cossart, Pizarro-Cerda et al. 2003). No difference in plaque size could be

identified between *L.m.* exposed to increasing concentrations of Kyn and untreated control bacteria (Figure 44 B) suggesting that the exposure of *L.m.* to Trp catabolites alone is not sufficient to impair invasiveness of *L.m.* for non-phagocytic cells.

The infectious potential of *L.m.* might be altered post exposure to the bactericidal milieu of DCreg. To address this question immDC and DCreg were infected with *L.m.*, recovered 6 hpi from cell lysates of infected DC and their capacity to infect 3T3 fibroblasts was compared by plaque assay with *L.m.* cultured under standard culture conditions in BHI. The plaque diameter of these three *L.m.* preparations did not differ significantly (Figure 44 C) suggesting that the antimicrobial activity of DCreg does not change the capacity of *L.m.* to invade non-phagocytic cells such as fibroblasts. In summary, these findings suggest that IDO1 expression in human myeloid cells confers a bactericidal intracellular environment. However, *L.m.* evading this milieu are still fully capable of infecting non-infected phagocytic as well as non-phagocytic cells.

#### **5.14 IDO1 is not expressed in murine myeloid cells upon *L. monocytogenes* infection**

The herein presented data have shown that, IDO1 plays a key role in the defense of human myeloid cells against *L.m.* infection. However, is not yet clear whether IDO1 also plays a crucial role in murine cells. To answer this question murine bone marrow derived M $\phi$  (mM $\phi$ ) and DC (mDC) were infected with *L.m.* After an incubation period of 24 h cell pellets and supernatants were collected to evaluate IDO1 and iNOS expression and activity. IDO1 was neither expressed in mDC nor in mM $\phi$  24 hpi (Figure 45 A). In contrast, murine myeloid cells expressed high levels of iNOS (RE 12 compared to non-infected cells) upon *L.m.* infection. These results were further supported by the indirect measure of enzymatic activity in supernatants of murine myeloid cells at 24 hpi. Whereas high amounts of nitrite (NO $_2^-$ ) accumulated in the supernatants of murine infected cells, Kyn levels remained below detection limit (Figure 45 B).



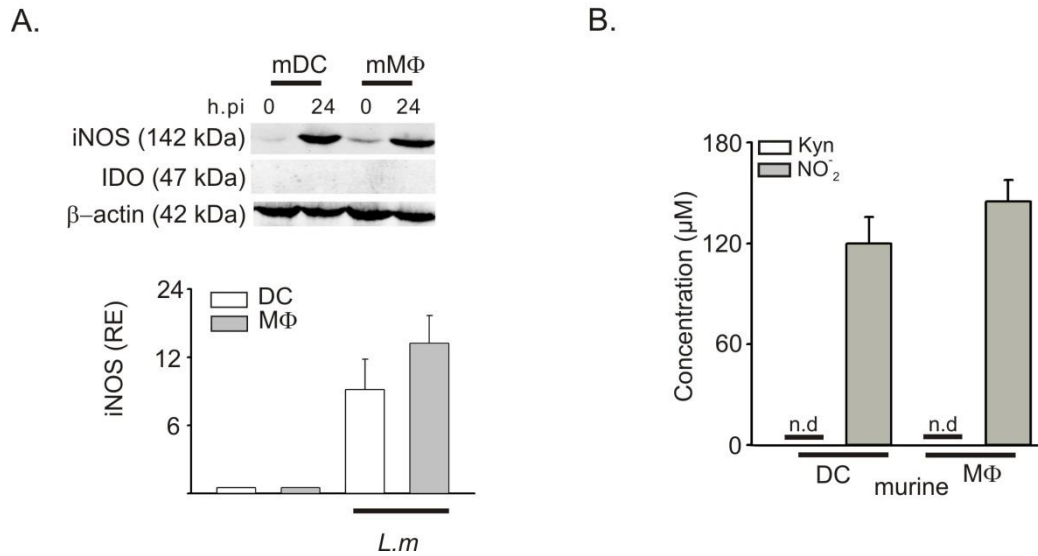


**Figure 39. IDO1 expression is not induced in murine myeloid cells upon *L.m.* infection**

**A.** IDO1 and iNOS protein expression in murine infected Mφ and DC 24 hpi was evaluated by western blot. The RE of iNOS was calculated by analyzing the intensity of each band of iNOS normalized to the signal intensity of β-actin (n=3, mean±sd). **B.** The enzymatic activity of IDO1 and iNOS were evaluated in supernatants of infected murine Mφ and DC 24 hpi by Ehrlich and Griess reaction (n=3, mean±sd).

Taken together the data indicate that the regulation pattern of IDO1 expression in mouse myeloid cells infected with *L.m.* differs from the one observed in their human counterparts. This might indicate that in murine myeloid cells iNOS, but not IDO1, plays a role in the control of *L.m.* intracellular growth.

---

## 6. Discussion

### 6.1 The phenotype of macrophages infected with *L. monocytogenes* and their regulatory properties

The infection of M $\phi$  with different kinds of bacteria including *L.m.* has been associated with the acquisition of an M1 proinflammatory phenotype (Shaughnessy and Swanson 2007; Benoit, Desnues et al. 2008; Sica and Mantovani 2012). However, the herein presented data show that M $\phi$  infected with *L.m.* express proinflammatory, but also immunomodulatory molecules. This set of immunomodulators includes the two enzymes IDO1 and COX-2, the receptor CD25 in its transmembrane and soluble form, as well as the secretion of high amounts of IL-10 (Figure 5-8). Moreover, this regulatory program is not restricted to M $\phi$ , but is also present in DC infected with *L.m.* in vitro as well as in situ in granulomas of patients who have been chronically infected with this bacterium (Popov, Abdullah et al. 2006; Popov, Driesen et al. 2008). In addition, the data presented in this study suggest that at a functional level, the regulatory program of M $\phi$  prevails over the inflammatory program since soluble factors in the supernatants of infected M $\phi$  were able to induce the expression of regulatory mediators in non-infected cells, and are also able to suppress the proliferation of activated T cells (Figure 9-11). These contradictory findings might be explained by the high plasticity of M $\phi$  which is a crucial factor beyond the classical model of M1 and M2 polarization.

M $\phi$  are key components in the clearance of pathogens, but also play a role in the phase of resolution to guarantee the return of the immune system to homeostasis. Furthermore, the failure of M $\phi$  to switch from a proinflammatory to a resolution phenotype has been associated with a number of pathological conditions, including sepsis (O'Reilly, Newcomb et al. 1999), atherosclerosis (Khallou-Laschet, Varthaman et al. 2010) and chronic venous ulcers (Sindrilaru, Peters et al. 2011). Therefore, it is possible that the same cells participating in proinflammatory responses can also later play a role in the resolution phase. Alternatively, they might prepare the microenvironment at the site of infection for the functional switch of new infiltrating M $\phi$ . Infection of M $\phi$  with *L.m.* at 24 hpi led to the secretion of high levels of IL-10 (Figure 8). This interleukin has been recognized as a key factor in the control of inflammation upon infection and injury. For instance, it is known that upon stimulation with TLR agonists including microbial products, M $\phi$  (Fiorentino, Zlotnik et al. 1991; Boonstra, Rajsbaum et al. 2006; Chang, Guo et al. 2007) and DC (McGuirk,

McCann et al. 2002; Popov, Driesen et al. 2008) increase their IL-10 secretion in vitro and in vivo (Siewe, Bollati-Fogolin et al. 2006). In addition, the loss of IL-10 function is associated with the development of a hyperinflammatory pathological immune response upon a variety of infections including *L.m.* (Gazzinelli, Wysocka et al. 1996; Deckert, Soltek et al. 2001; Roffe, Rothfuchs et al. 2012). Cerebral listeriosis in IL-10 knockout mice led to severe brain edema and hemorrhage, associated with lethal ubiquitous encephalitis. Interestingly in these mice the bacterial load was not reduced in comparison with their wild type littermates (Deckert, Soltek et al. 2001). Similarly, in mice infected with *Borrelia burgdorferi* M $\phi$  and CD4<sup>+</sup> T cells are the leading producers of IL-10 in the joints. In this model of infection, abrogation of IL-10 signaling led to arthritis associated with the recruitment of high numbers of IFN- $\gamma$  producing NK and T cells (Sonderregger, Ma et al. 2012).

IDO1 is well-known for its antimicrobial and immunomodulatory properties (Mellor and Munn 2004). Upon infection with *L.m.* IDO1 is highly expressed in both M $\phi$  (Figure 8 and 12) and DC (Figure 15). Systemic expression of IDO1 has been linked to an impairment of the immune response against pathogens (Makala, Baban et al. 2011; Plain, de Silva et al. 2011; Loughman and Hunstad 2012). However, IDO1 modulation can have beneficial effects on the host by limiting the damage caused by unrestricted inflammation. Along these lines, mice deficient for IL-4 $\alpha$  receptor cannot generate M2 polarized M $\phi$ . However, upon infection with *Schistosoma mansoni*, IDO1 expressed by M1 M $\phi$  controls tissue damage associated with inflammation, and protects the host against otherwise lethal disease (Rani, Jordan et al. 2012). COX-2 and PTGES are highly upregulated in *L.m.* infected M $\phi$  (Figure 8) and DC. These enzymes are crucial for the synthesis of PGE<sub>2</sub>. This molecule is commonly classified as proinflammatory mediator due to its high expression at sites of inflammation and tissue injury (Chan and Moore 2010; Kalinski 2012). Moreover, COX-2 and PTGES expression have been associated with the M1 phenotype (Martinez, Gordon et al. 2006). Nevertheless, it is known that PGE<sub>2</sub> exerts important modulatory functions on the phenotype and function of M $\phi$ . For instance, it efficiently suppresses the production of proinflammatory cytokines like TNF- $\alpha$ , IL-1 $\beta$ , the chemotactic factor MCP-1 and IL-8 (Takayama, Garcia-Cardena et al. 2002). Similarly, PGE<sub>2</sub> has been detected in the wound-fluid of patients. M $\phi$  treated with PGE<sub>2</sub> or wound-fluid express the cytokine oncostatin M which in turn suppresses the secretion of TNF- $\alpha$  and IL-1, suggesting that PGE<sub>2</sub> plays a key role in wound healing by limiting inflammation (Ganesh, Das et al. 2012). In synovial fibroblasts PGE<sub>2</sub> enhanced the expression of I $\kappa$ B $\alpha$  avoiding the activation of NF $\kappa$ B and thereby attenuated their inflammatory responses (Gomez,

Pillinger et al. 2005). Primary murine epithelial cells infected with *Helicobacter pylori* expressed COX-2 in response to infection. Moreover, the treatment of mice with PGE<sub>2</sub> inhibited chronic inflammation and the development of precancerous lesions (Toller, Hitzler et al. 2010).

The role of regulatory myeloid cells in chronic infections remains controversial. A number of studies support the idea that myeloid cells with regulatory properties dampen the development of an efficient immune response, fostering the persistence of pathogens. Two examples for this model are infections with hepatitis C virus (Higashitani, Kanto et al. 2012) and *L. major* (Makala, Baban et al. 2011). However, in case of chronic infections that lead to granuloma formation the presence of myeloid cells with regulatory and proinflammatory functions might contribute to control the growth of pathogens while avoiding its dissemination. In patients suffering from chronic listeriosis, DC with similar characteristics to those observed in M $\phi$  infected with *L.m.* constitute the ringwall of granuloma. It has been proposed that these cells might avoid T cell proliferation in this structure via an IDO1 dependent mechanism. This function might be important to prevent the destruction of granuloma and the dissemination of bacteria (Popov, Driesen et al. 2008). Granuloma disruption has been associated with reactivation of chronic diseases. For instance, patients treated with anti-TNF- $\alpha$  antibodies suffer from a reactivation of chronic granulomatous diseases including *L.m.* (Ehlers 2005) and *M. tuberculosis* (Keane, Gershon et al. 2001).

In summary, it is possible that M $\phi$  and DC acquire proinflammatory as well as immunomodulatory programs depending on the inflammatory milieu, to defend the host against the pathogens and at the same time limit the damage to healthy tissues. Moreover, in case of chronic infections associated with granuloma formation, the presence of myeloid cells with these mixed characteristics might be beneficial for the host since at the same time these cells control the bacterial burden and ensure the confinement of the bacteria when mechanisms of the adaptive immune system have failed to eradicate them.

## **6.2 Genomic profiling of macrophages infected with *L. monocytogenes***

M-CSF and GM-CSF are factors promoting monocyte differentiation into M $\phi$  (Lacey, Achuthan et al. 2012). However, it has been suggested that GM-CSF and M-CSF derived M $\phi$  might exert different functions upon stimulation with proinflammatory factors like LPS (Verreck, de Boer et al. 2004; Fleetwood, Lawrence et al. 2007; Lacey, Achuthan et al.

2012). Comparisons of the transcriptomes of GM-CSF and M-CSF derived M $\phi$  under basal conditions revealed that these cells have closely related transcription profiles independently of the factor used for their differentiation. Additionally, only 103 genes were found to be DE expressed between GM-CSF and M-CSF M $\phi$ . Most of them are involved in antigen presentation (Table 7). This evidence is in line with previous reports, suggesting that GM-CSF might enhance antigen presenting properties of DC and M $\phi$  in vivo and in vitro. For instance, it has been reported that mice deficient for CFS2 gene (the murine homologue of GM-CSF) show a similar recruitment of M $\phi$  and DC to the uterus during the estrous cycle. However, these cells showed an impaired antigen presentation via MHC class II molecules (Moldenhauer, Keenihan et al. 2010). It has also been reported, that a recombinant respiratory syncytial virus expressing GM-CSF promotes the recruitment of DC and M $\phi$  to the lung and increases MHC class II expression in both cell types (Bukreyev, Belyakov et al. 2001). Recently, Lacey and coworkers compared the transcriptome of human GM-CSF and M-CSF M $\phi$  (Lacey, Achuthan et al. 2012), despite they find remarkable similarity between the transcriptomes of these two groups (87%), they reported over 3000 genes as DE expressed between them. This discrepancy might be attributed to the different experimental approaches used in both cases. For instance, Lacey and coworkers differentiated M $\phi$  during 7 days, whereas in this study 3 days were established as sufficient to achieve a complete differentiation of M $\phi$ . In addition, differentiation of M-CSF was obtained using 2500 U/ml of rhM-CSF an amount 100 times superior to the one used in the present work. These findings further support the similarities between GM-CSF and M-CSF M $\phi$  at the transcriptional level. However, the observed discrepancies indicate that the findings obtained in vitro must be carefully considered before extrapolations to in vivo situations are made.

After infection with *L.m.*, it was shown that M-CSF derived M $\phi$  secreted significantly reduced amounts of IL-12 when compared with their GM-CSF counterparts (Figure 6). However, the levels of IL-10 were similar for both cell types. Also these cells expressed similar levels of IDO1, COX-2, CD25 and IFN- $\gamma$  whereas the differences in IL-6 and TNF- $\alpha$  secretion were not statistically significant. In addition, it was shown that 65% of the transcriptional changes due to *L.m.* infection were comparable in GM-CSF and M-CSF M $\phi$ . This common program was associated with both proinflammatory as well as immunomodulatory functions. For instance, both cell types increased their expression of IL-1B, STAT4, CCL5 CCR7, but also IDO1, PTGS2 and EBI3 (Figure 14). In summary, there is no clear tendency suggesting that only M-CSF derived M $\phi$  acquired anti-inflammatory features. In contrast to these findings, it has been shown that GM-CSF and

---

M-CSF skew M $\phi$  polarization towards M1 and M2 phenotypes respectively (Verreck, de Boer et al. 2004). Furthermore, it has been suggested that upon stimulation with LPS, M-CSF derived M $\phi$  secrete lower levels of proinflammatory cytokines including TNF- $\alpha$ , IL-12 and higher levels of IL-10 than GM-CSF derived M $\phi$  (Fleetwood, Lawrence et al. 2007). Although in vitro, the differential behavior of GM-CSF and M-CSF M $\phi$  seems clear; the experiments considered the stimulation with one single TLR ligand, a process simpler than the infection with a microorganism. Along these lines, it has been shown that infection with several species of the genus *Mycobacterium* led to GM-CSF secretion by M $\phi$  (Beltan, Horgen et al. 2000). Interestingly, under in vivo situations the interplay between GM-CSF, M-CSF and the M $\phi$  population is complex. It has been described that M-CSF is secreted under resting conditions by a number of cells including fibroblast, epithelial, stromal cells, but also M $\phi$  (Hamilton 2008). Furthermore, M $\phi$  differentiation in the tissues depends in some extent on M-CSF since mice deficient for CSF-1 receptor show a decrement in the number of tissue resident M $\phi$  and present severe deficiency in osteoclast generation (Pixley and Stanley 2004). In addition, the blockage of CSF-1R reduces the number of monocytes and peritoneal M $\phi$  under homeostatic conditions in mice (Lenzo, Turner et al. 2012). Therefore, it has been proposed that under resting conditions M-CSF promotes proliferation and differentiation of M $\phi$  populations (Pixley and Stanley 2004; Hamilton 2008). In contrast, GM-CSF is not detectable under resting conditions. However, upon infection or inflammation, GM-CSF is secreted by similar cell types that secrete M-CSF (Hamilton 2008). Moreover in models of peritonitis and lung inflammation, it has been shown that both growth factors are necessary for the recruitment and maintenance of the M $\phi$  population (Lenzo, Turner et al. 2012). Following this observation it has been proposed that the balance between M-CSF and GM-CSF influences the development of *M. tuberculosis* infection in the lung. Whereas M-CSF levels are decreased over the course of infection, GM-CSF is elevated during this process enhancing the phagocytic activity and proliferation of M $\phi$  (Higgins, Sanchez-Campillo et al. 2008). In summary, it is likely that M-CSF M $\phi$  behave more like a steady state population that would constitute the first responder to an invading pathogen, whereas GM-CSF derived M $\phi$  or the resulting population shaped by the action of both growth factors in concert with cytokines at the infection site, might play a role in sustaining the inflammatory process. This model would explain better or at least in part differences but also similarities observed between GM-CSF and M-CSF M $\phi$  upon *L.m.* infection. It might be interesting to assess the transcriptional profile of M $\phi$  exposed simultaneously to GM-CSF and M-CSF in

response to the infection with *L.m.* to characterize M $\phi$  responses under conditions similar to those observed in vivo.

### **6.3 Comparative analysis of the transcriptional responses of macrophages and dendritic cells to *L. monocytogenes* infection**

GM-CSF in concert with IL-4 have been described as essential factors, which promote DC differentiation from human monocytes (Sallusto and Lanzavecchia 1994). However, in murine models it has been established that GM-CSF alone is sufficient to drive DC differentiation from bone marrow cells (Inaba, Inaba et al. 1992). The data obtained in the present study have shown via PCA analysis that the transcriptomes of GM-CSF M $\phi$  and DC have important differences (Figure 13). In contrast, under resting conditions the transcriptomes of GM-CSF and M-CSF derived M $\phi$  are closely related (Figure 15). In addition, GO enrichment analysis showed that monocyte derived DC and GM-CSF M $\phi$  differed in key aspects, including chemotaxis and inflammatory responses. In agreement with these observations are the higher expression levels of CCR6, CCL23, and CCL18 amongst other chemokines in DC. These factors attract naïve T cells to sites of infections and reflect the central function of DC as a bridge between the innate and adaptive immune system. In contrast, M $\phi$  expressed higher levels of TLRs including TLR5, 6, 7, 8 and 9, but also NLRP3. These findings underline the role of M $\phi$  in pathogen recognition. It has been recently reported that TLR3 and 5 activation promotes the phagocytosis of bacteria in M $\phi$  (Deng, Feng et al. 2012), suggesting that higher expression of TLRs might contribute to the high phagocytic capacity of these cells. Also a recent report showed that human monocyte derived GM-CSF-M $\phi$  and murine DC generated via single stimulation with GM-CSF treatment from bone marrow regulated only 17% of the genes in common (Lacey, Achuthan et al. 2012). This observation suggests that the features of murine bone marrow DC cannot be directly extrapolated to human monocyte GM-CSF derived M $\phi$ . Despite their background differences, M $\phi$  and DC acquire a common transcriptional program upon *L.m.* infection (Figure 15). These findings are in agreement with in vitro data showing that M $\phi$  and DC express a similar program that includes IDO1, CD25 and COX-2. Moreover, supernatants of both DC and M $\phi$  infected with *L.m.* were able to suppress T cell responses (Figure 7, 8, 10) (Popov, Abdullah et al. 2006). This evidence supported the hypothesis that DC and M $\phi$  as major constituent elements of granuloma in patients with chronic listeriosis (Popov, Abdullah et al. 2006) might act in concert to

guarantee the containment of bacteria and the suppression of potentially damaging T cell responses. Besides their common transcriptional response against *L.m.* infection, DC and M $\phi$  also expressed cell type specific programs. GO enrichment analysis for each cell type showed that the genes regulated exclusively on DC upon *L.m.* infection are related to the inflammatory response and the response to LPS amongst others. Along these lines, DC expressed SERPINB2 (Figure 16 B), a molecule which expression is up-regulated upon treatment with LPS and other TLR ligands. Interestingly, SERPINB2 expression by APC seems to be important in the regulation of T<sub>H</sub>1 responses in mice since APC from mice lacking this gene promote elevated T<sub>H</sub>1 cytokine secretion in vivo and in vitro (Schroder, Le et al. 2010). Furthermore, elevated SERPINB2 expression has been observed in inflammatory diseases like asthma (Woodruff, Boushey et al. 2007) and certain forms of scleroderma (Kessler-Becker, Smola et al. 2004). Genes only regulated in M $\phi$  upon *L.m.* infection were related to oxidoreductase and metabolic activity (Figure 16 C). These evidence is in line with previous reports and herein presented data (Figure 31) showing that M $\phi$  are more efficient than DC in the production of ROS (Werling, Hope et al. 2004). Additionally, M $\phi$  infected with *L.m.* up-regulated the expression of MAOA which encodes the enzyme monoamine oxidase A (Figure 16 D). This enzyme has been associated with enhanced ROS production in epithelial cells upon stimulation with LPS (Ekuni, Firth et al. 2009). In addition, M $\phi$  infected with *L.m.* increased the transcription of matrix metalloproteinase (MMP) -7 and 12. Interestingly, several members of the matrix metalloproteinase family have been implicated in granuloma formation upon infection with *M. tuberculosis*. For instance, mice treated with a broad spectrum inhibitor of MMPs showed smaller granulomas or at least a delayed granuloma formation upon infection with this pathogen (Hernandez-Pando, Orozco et al. 2000; Izzo, Izzo et al. 2004). In addition, MMP-9 seems to be a key factor in granuloma formation since mice lacking this gene showed poor granuloma formation in response to *M. tuberculosis* infection (Taylor, Hattle et al. 2006). However, it has been shown that MMP-1 is implicated in collagen degradation in granuloma with the concomitant release of the bacteria to the airways (Elkington, Shiomi et al. 2011).

Taken together the presented evidence suggest that M $\phi$  and DC acquire a similar program in response to the infection with *L.m.* that might allow these cells to act in concert to suppress the growth of this bacterium and modulate the responses of the adaptive immune system. Nevertheless, these cells expressed cell type specific programs that should be further validated in pertinent in vivo and in vitro models.



## 6.4 Transcriptional responses of macrophages to phagosome restricted and cytosolic *L. monocytogenes*

M $\phi$  infected with *L.m.* wt and hly, a mutant of this bacterium which fails to enter the cytosol, activated a common transcriptional response that comprised 85% of the genes regulated upon infection (Figure 18). The unsupervised hierarchical clustering and PCA analysis showed important similarities between the transcriptomes of M $\phi$  infected with hly and wt *L.m.* (Figure 17 and 18). Furthermore, it has been shown that the concentration of TNF- $\alpha$ , IFN- $\gamma$  and IL-10 were similar in the supernatants of M $\phi$  infected with hly and wt *L.m.* (Figure 20). In line with these findings, the comparison between the transcriptional responses of innate immune cells in response to a wide variety of pathogens including bacteria, virus, and fungi performed in previous studies, showed that around 340 genes were regulated similarly in immune cells regardless of the infecting pathogen (Jenner and Young 2005). Interestingly, 60% of these common response genes was regulated also in M $\phi$  infected with both wt and hly *L.m.* Additionally, it has been reported that human M $\phi$  respond to a variety of pathogenic bacteria inducing a core transcriptional response that covers around 200 genes (Nau, Richmond et al. 2002). This core response includes proinflammatory cytokines including IL-6, TNF- $\alpha$ , the chemokines CCL5 and IL-8 amongst others. Moreover, stimulation with TLR2 and 4 agonists was sufficient to acquire the key elements of this response (Nau, Richmond et al. 2002). It has been proposed that this common transcriptional response constitutes the first alarm signal against invading pathogens (Jenner and Young 2005). The herein presented data suggest that an important part of the transcriptome of M $\phi$  infected with *L.m.* might represent, at least partially this first alarm response and therefore is not tuned according to the level of threat represented by a phagosome restricted or fully invasive bacterium. However, in mice the infection of wt and hly *Listeria* differed in a crucial point: whereas the infection with wt *L.m.* leads to protective CD8+ T cell mediated immunity, the hly mutant does not induce proper T cell responses. Since cells from the innate immune system drive the process of inflammation, it has been proposed that they are in charge of integrating signals provided by the different PPRs and contribute to the escalation of the immune response (Blander and Sander 2012). The herein described data showed that 15% of the total transcriptional changes induced by *L.m.* were exclusive for the wt bacteria. These findings suggest, that the fine tuning of the M $\phi$  response to a phagosome restricted or fully competent bacteria might relay in this group of genes. GO enrichment analysis of the genes regulated exclusively upon infection with wt *L.m.* revealed that some of them are related to viral transcription and viral infectious cycle (Figure 19 A). The enrichment in these categories

---

might be explained by recent evidence demonstrating that cytosolic *L.m.* secretes RNA molecules that can be sensed by RIG-I and MDA 5 leading to IFN- $\beta$  production (Abdullah, Schlee et al. 2012). In addition, IFN- $\beta$  expression has been identified as a primary response gene, induced once *L.m.* has reached the cytoplasm. Moreover, it has been proposed that IFN- $\beta$  activates the transcriptional response to cytosolic *L.m.* to a significant extent (Leber, Crimmins et al. 2008). Strikingly, the stimulation of M $\phi$  only with IFN- $\beta$  resulted in the differential expression of only 21 genes of which only 5 were found as exclusively regulated in M $\phi$  infected with wt *L.m.* (Table 8). In contrast to these findings, previous studies suggested that IFN- $\beta$  has profound effects on the transcriptome of diverse cell types, regulating the expression of a number of genes that varies between 100 and 500 (Geiss, Carter et al. 2003; Fernald, Knott et al. 2007; Zou, Kim et al. 2007; Farnsworth, Flaman et al. 2010). However, it is important to note that these reports are not entirely comparable to the present work. For instance, some of these studies measured the global response of peripheral blood cells to IFN- $\beta$  stimulus (Fernald, Knott et al. 2007). Moreover, some of them have been performed in cells non-related to the immune system (Farnsworth, Flaman et al. 2010) or in cell lines (Geiss, Carter et al. 2003); hence the tissue specific regulation might explain at least in part these differences. Similarly, it is important to consider the time point after stimulation used to detect DE genes. Along these lines, Zhou and coworkers have reported that IFN- $\beta$  led to differential expression of 110 genes as early as 6 h post stimulation in bone marrow M $\phi$ . However, the expression of these DE genes decreased to basal levels 24 h after treatment (Zou, Kim et al. 2007). Taking into account this evidence, it is possible that human M $\phi$  presented a similar time kinetic of gene expression upon stimulation with IFN- $\beta$  leading to the detection of a reduced number of DE genes at 24 hpi. The stimulation of M $\phi$  with IFN- $\beta$  resulted in the regulation of only 5 genes in common with M $\phi$  infected with wt *L.m.* This can be explained because during *L.m.* infection IFN- $\beta$  does not act alone, but in concert with signals triggered by the vacuolar phase of infection including IFN- $\gamma$  and TNF- $\alpha$  (Leber, Crimmins et al. 2008). For instance, it has been shown that IFN- $\gamma$  primed M $\phi$  showed an enhanced response to type I IFN. This enhanced response was enabled by an increased expression of STAT1 triggered by IFN- $\gamma$  signaling (Tassiulas, Hu et al. 2004). Moreover the herein presented data suggested that M $\phi$  stimulated simultaneously with TNF- $\alpha$ , PGE<sub>2</sub>, IFN- $\gamma$  and IFN- $\beta$  expressed 180 genes in common with *L.m.* that are not regulated by these factors acting separately. These findings suggest the crucial role of signal integration in the transcriptional response of M $\phi$  to *L.m.* infection.

In addition to IFN- $\beta$  and its targets, the pool of genes upregulated in response to wild type *L.m.* include the transcription factor HESX1, essential for development of the forebrain in mice and humans via repression of targets of the Wnt- $\beta$  catenin pathway (Andoniadou, Signore et al. 2011). Although HESX1 has not been yet associated to infection or inflammation, alterations of the Wnt- $\beta$  catenin pathway have been found in a number of infections (Ahmed, Chandrakesan et al. 2012; Kessler, Zielecki et al. 2012). Similarly, the expression of LILRA3 is elevated in M $\phi$  infected with wt *L.m.* Despite LILRA3 has not been linked yet to the infection response, it has been reported as putative natural anti-inflammatory protein in patients with rheumatoid arthritis. Moreover, in monocytes its expression is strongly induced upon stimulation with IL-10 while it is downregulated by TNF- $\alpha$  (An, Chandra et al. 2010). Additionally, the chemokine CXCL10 is regulated only in M $\phi$  infected with wt *L.m.* It has been reported that, CXCL10 promotes the recruitment of M $\phi$  in the process of arterial remodeling (Zhou, Tang et al. 2010). More recently, it has been found that M $\phi$  infected with *Mycobacterium avium* produce CXCL10, probably as a strategy to recruit new M $\phi$  at the sites of infection (Vazquez, Rekka et al. 2012).

Together, it can be postulated that an important part of the transcriptional response of M $\phi$  against *L.m.* is driven by events of recognition at the cell surface and in the phagosome. This primary transcriptional response is not tuned according to the intracellular fate of this bacterium. However, 15% of the genes that are regulated exclusively in response to wt *Listeria* might contribute to a modulation of M $\phi$  responses according to the level of threat, as it has been proposed for IFN- $\beta$ . Interestingly, the genes regulated only with wt *L.m.* encompass genes that have not been linked yet to the response of M $\phi$  to infection and might constitute interesting targets for further studies.

## **6.5 Macrophage polarization upon infection with *L. monocytogenes***

The infection of M $\phi$  with bacteria including *L.m.* has been associated to M1 polarization (Shaughnessy and Swanson 2007) and is characterized in vitro by IFN- $\gamma$  stimulation. However, the herein presented data showed that although IFN- $\gamma$  stimulated and *L.m.* infected M $\phi$  expressed the hallmark markers of M1 polarization, the signal provided by IFN- $\gamma$  explains only 30% of the total transcriptional response of infected M $\phi$ . Furthermore, the comparison between the transcriptome of regulatory and *L.m.* infected M $\phi$  revealed that TNF- $\alpha$ , PGE<sub>2</sub> and Pam<sub>3</sub>, the three signals required for Mreg polarization, explained

50% of the total transcriptional changes that follow after *L.m.* infection including the regulatory program integrated by IDO1, COX-2 and CD25. These findings, led to the conclusion that the transcriptional profile of Mreg is the so far closest to the one observed in M $\phi$  infected with *L.m.* Surprisingly, the data has shown that the stimuli with IFN- $\gamma$  (Figure 21) or TNF- $\alpha$  are sufficient to induce up to 40% of the transcriptional responses observed in M $\phi$  upon *L.m.* infection (Figure 26). These data are further supported by evidence generated in vitro showing that soluble factors secreted by infected cells are able to induce an infected-like phenotype in non-infected M $\phi$  (Figure 9). In fact, there is an important body of evidence showing the essential role of host factors in the pathogenesis of infections like *M. tuberculosis* and *Schistosoma mansoni*. In granuloma developed upon *M. tuberculosis* infection, M $\phi$  are the most abundant cell type (Dannenberg 1993). However, not all M $\phi$  present in this structure are infected, yet the uninfected cells help to contain the infection (Silva Miranda, Breiman et al. 2012). Additionally, in an in vitro model of granuloma formation, a relative low inoculum of *M. tuberculosis* or supernatants of infected M $\phi$  were able to promote the formation of granuloma-like cell aggregates (Birkness, Guarner et al. 2007). Furthermore, it has been shown that TNF- $\alpha$  signaling is crucial to keep a persistent granuloma structure since usage of blocking antibodies against TNF- $\alpha$  led to granuloma disruption (Keane, Gershon et al. 2001). More recently, it has been suggested that IFN- $\gamma$  secreted by T cells in concert with the interaction between CD40L on this cells and CD40 expressed in M $\phi$  leads to the development of Langhans giant cells, a key signature of granulomatous disorders including tuberculosis and sarcoidosis (Sakai, Okafuji et al. 2012). In addition, CCL3 seems to play an important role in granuloma formation upon infection with *S. mansoni* since knockout mice for this factor showed reduced granuloma generation in response to the infection with this parasite (Souza, Roffe et al. 2005). Moreover it has been shown that, mice deficient for macrophage inhibitory factor (MIF) developed smaller granulomas upon infection with *S. mansoni*, suggesting the important role of this factor in granuloma formation (Magalhaes, Paiva et al. 2009). In summary, the herein presented data indicate that beyond a model of M $\phi$  polarization there are key host derived factors that remodel the transcriptional landscape of M $\phi$  upon *L.m.* These factors include TNF- $\alpha$ , IFN- $\gamma$ , IFN- $\beta$  and PGE<sub>2</sub>. Strikingly, the experiments comparing the transcriptome of M $\phi$  treated simultaneously with these factors reproduces over 60% of the transcriptional responses observed upon infection of M $\phi$  (Figure 29). The 40% of genes regulated upon *L.m.* infection that cannot be explained by host derived factors might be regulated by the interaction between the host cell and specific features associated to *L.m.* biology and cycle of infection. It is well-

---

known that microorganisms have multiple PAMPs that can be recognized by several PPRs placed in different cell compartments, and in some cases the same PAMP can be recognized by more than one sensor (Takeda, Kaisho et al. 2003; Kawai and Akira 2006; Witte, Archer et al. 2012). It has been proposed that this, in appearance of redundant recognition, can provide in concert important information that shapes the response of cells of the innate immune system (Vance, Isberg et al. 2009). For instance, TLR2 recognizes PAMPs present on the surface of *L.m.*, including lipoteichoic acid, lipoprotein, and peptidoglycan. The stimulation of TLR2 leads to activation of MyD88, a common adaptor for the members of the TLR family, yet TLR2 stimulation via Pam<sub>3</sub> only changed the expression of 348 genes in common with M $\phi$  infected with *L.m.* Furthermore, only 12% of the genes were regulated in the same direction between those two cell populations. Similarly, it has been reported that M $\phi$  deficient for TLR2 were able to control efficiently *L.m.* growth. In contrast M $\phi$  obtained from MyD88 knockout mice were susceptible to *L.m.* infection (Edelson and Unanue 2002). These findings suggest that mere TLR2 activation is not sufficient to reproduce important aspects of M $\phi$  response against *L.m.* infection. Another example that illustrates the non-redundancy of the information provided by different PPRs is the recognition of bacterial nucleic acids in the phagosome and the cytosol. *L.m.* DNA can be recognized by TLR9 (Kawai and Akira 2006) inside the phagosome and probably by LRRFIP1 in the cytoplasm (Yang, An et al. 2010). Whereas, recognition of *L.m.* DNA in the phagosome does not trigger IFN- $\beta$  production, the transfection of DNA directly into the cytoplasm leads to secretion of this cytokine (Stetson and Medzhitov 2006). More recently, it has been proposed that the recognition of so called vita-PAMPs by the innate immune system might provide information about the viability of the invader helping the immune cells to tune their responses according to the level of threat (Sander, Davis et al. 2011). In this sense *L.m.* produce cyclic adenosine monophosphate (*c*-di-AMP), a second messenger that is secreted by live bacteria into the cytoplasm of infected cells (Woodward, Iavarone et al. 2010). The entry of this molecule into the cytoplasm triggers IFN- $\beta$  production mediated by the adaptor molecule STING (stimulator of interferon genes protein) (Sauer, Sotelo-Troha et al. 2011). Taken together, this evidence highlights the importance to consider the interaction between the signals provided by different PPRs as a crucial factor in the tuning of responses of innate immune cells to infection.

In summary, approximately half of the transcriptional changes observed upon *L.m.* are dependent on host derived factors and can be characterized by in vitro models of

polarization. Nevertheless, the remaining transcriptional modifications might result from specific interactions between the host cell and viable invading bacteria.

## 6.6 IDO1 plays a role as microbicidal mechanism in human myeloid cells

Trp depletion mediated by IDO1 has been recognized previously as an important microbicidal mechanism (Pfefferkorn 1984; Byrne, Lehmann et al. 1986; MacKenzie, Hadding et al. 1998). The herein presented data suggests that in vitro human DCreg use IDO1 as an important molecule for the clearance of *L.m.* infection (Figure 33). Moreover, the evidence indicates that the microbicidal activity of IDO1 is mediated by the toxicity of Trp catabolites and not by Trp depletion itself (Figures 39, 40 and 41). In contrast to the observations in human myeloid cells, murine DC and M $\phi$  did not expressed IDO1 in response to *L.m.* infection; instead these cells responded to the infection expressing iNOS. The role of IDO1 and iNOS as microbicidal mediators in human and rodents respectively remains controversial. Previously it has been reported that NO or peroxyntirite donors inhibited IDO1 activity (Thomas, Terentis et al. 2007) via nitration of the Tyrosine residues Tyr<sup>15</sup>, Tyr<sup>345</sup> and Tyr<sup>353</sup> (Fujigaki, Saito et al. 2006). Furthermore, Hucke *et al.* demonstrated NO as a regulator of IDO1 expression at post-translational level promoting its degradation in the proteasome (Hucke, MacKenzie et al. 2004). However, based on murine in vivo experiments, there is evidence that IDO1 plays an important role in the murine antiparasitic response against protozoa like *Toxoplasma gondii* (Divanovic, Sawtell et al. 2012). Additionally, during pregnancy IDO1 is basally expressed in mouse placenta, after *L.m.* infection its expression is further enhanced (Mackler, Barber et al. 2003). This evidence suggests that IDO1 expression can be differentially regulated among cell types and tissues in mice. Interestingly, the relevance of IDO1 as microbicidal mechanism might also depend on particular aspects of the host-pathogen interaction. Whereas IDO1 seems to dampen the immune response of mice infected with *L. major*, promoting parasite persistence (Makala, Baban et al. 2011), this enzyme plays a key role in the control of *T. cruzi* (Knubel, Martinez et al. 2010; Knubel, Martinez et al. 2011). In contrast, although IDO1 is induced strongly in murine and human cells upon infection with *M. tuberculosis*, the experiments performed in IDO1 knockout mice demonstrated that this enzyme is not essential to control the growth of this pathogen (Blumenthal, Nagalingam et al. 2012).

IDO1 microbicidal activity against a wide range of pathogens has been attributed mainly to Trp starvation (MacKenzie, Worku et al. 2003; Heseler, Spekker et al. 2008). However, it

---

was shown herein that the IDO1-mediated accumulation of Trp catabolites has a striking impact on *L.m.* viability once this pathogen has reached the cytoplasm, whereas Trp depletion does not favor bacterial clearance in immDC and is deleterious for DCreg cells (Figure 40 and 41). These findings are in agreement with the fact that *L.m.* virulent strains can synthesize aromatic amino acids amongst them Trp (Marquis, Bouwer et al. 1993). Therefore they do not depend on their host to obtain these resources. Interestingly, it has been reported that once *L.m.* has reached the cytoplasm, it up-regulates the expression of genes related with Trp biosynthesis (Joseph, Przybilla et al. 2006), probably as an adaptation to survive in mammalian cells that are unable to synthesize this amino acid and depend on external sources to obtain it. Furthermore, mutants that lack the common branch of aromatic amino acid synthesis showed reduced replication in the cytoplasm of epithelial cells (Stritzker, Janda et al. 2004), reinforcing the hypothesis that intrinsically the supply of aromatic amino acids provided by the host cell is not enough to guarantee *L.m.* cytoplasmic growth. More recently, the comparison between the transcriptome of intracellular *L.m.* in unstimulated and IFN- $\gamma$  stimulated M $\phi$  has revealed that genes involved in Trp biosynthesis are upregulated specifically in *L.m.* confined in IFN- $\gamma$  activated M $\phi$ . Moreover, the up-regulation of genes participating in Trp synthesis is associated with an increment in IDO1 mRNA (Mraheil, Billion et al. 2011).

The presented data demonstrated that Trp catabolites externally added to *L.m.* culture media, have an impact in the viability of this pathogen (Figure 41). Furthermore, the sensibility to Trp catabolites varied amongst different bacteria species: *L.m.* was found to be highly susceptible to Kyn and 3HK whereas *S.p.* was preferentially susceptible to Q and HA (Figure 43). Similarly Narui *et al.* reported that Trp catabolites can affect bacterial viability. In addition, they have shown that the anti-bacterial capacity varies among the compounds of the kynurenine pathway and depends on the sensitivity of the tested bacteria (Narui, Noguchi et al. 2009). Until now the mechanism that mediates the anti-bacterial effect of Trp catabolites is unknown. Interestingly, *L.i.*, a non-pathogenic bacterium, phylogenetically related to *L.m.*, showed only a moderate susceptibility to Trp catabolites. This finding might suggest, that the target of kynurenines action might be related to the approximately 20% of the genes that are not shared between this two species including virulence factors (Glaser, Frangeul et al. 2001). Nevertheless it is important to consider that the regulation of gene expression in *L.m.* is highly complex and differs substantially from *L.i.* (Wurtzel, Sesto et al. 2012). Therefore, a detailed comparison between the transcriptome of this species in presence of Trp catabolites might be necessary to identify the potential targets of Trp catabolites.

In humans, it has been demonstrated that IDO1 is expressed in granulomatous diseases including listeriosis (Popov, Abdullah et al. 2006; Popov, Driesen et al. 2008). Furthermore, IDO1 expression in granuloma associated myeloid cells, has been proposed as an important mechanism to prevent T cell mediated disruption of the granuloma, avoiding therefore bacterial dissemination (Popov, Driesen et al. 2008). However, recent observations in the zebra fish strongly argue for the granuloma to function as a reservoir for bacteria allowing spreading of the disease (Davis and Ramakrishnan 2009; Ramakrishnan 2012). These observations might suggest that granuloma formation is rather harmful for the host. Nevertheless, is important to notice that in non-mammalian vertebrates like zebra fish (*Danio rerio*) or *Xenopus laevis* only proto-IDO proteins with low efficiency for Trp degradation have been described (Yuasa, Takubo et al. 2007). Therefore, the granuloma function in such models might not be entirely comparable to the one observed in humans.

To finally conclude, the herein presented data suggest that in human myeloid cells the production of Trp catabolites, mediated by IDO1, is an important mechanism to control cytoplasmic *L.m.* However, these findings are not easy to extrapolate between species or different models of host-microorganism interaction, pointing out the necessity to carefully consider these aspects when addressing the role of IDO1 in human disease.



---

## Bibliography

- Abdullah, Z., M. Schlee, et al. (2012). "RIG-I detects infection with live *Listeria* by sensing secreted bacterial nucleic acids." *EMBO J* **31**(21): 4153-4164.
- Abramson, S. L. and J. I. Gallin (1990). "IL-4 inhibits superoxide production by human mononuclear phagocytes." *J Immunol* **144**(2): 625-630.
- Adams, D. O. and T. A. Hamilton (1984). "The cell biology of macrophage activation." *Annu Rev Immunol* **2**: 283-318.
- Ahmed, I., P. Chandrakesan, et al. (2012). "Critical roles of Notch and Wnt/beta-catenin pathways in the regulation of hyperplasia and/or colitis in response to bacterial infection." *Infect Immun* **80**(9): 3107-3121.
- Ajami, B., J. L. Bennett, et al. (2007). "Local self-renewal can sustain CNS microglia maintenance and function throughout adult life." *Nat Neurosci* **10**(12): 1538-1543.
- Akbari, O., R. H. DeKruyff, et al. (2001). "Pulmonary dendritic cells producing IL-10 mediate tolerance induced by respiratory exposure to antigen." *Nat Immunol* **2**(8): 725-731.
- Allerberger, F. and M. Wagner (2010). "Listeriosis: a resurgent foodborne infection." *Clin Microbiol Infect* **16**(1): 16-23.
- An, H., V. Chandra, et al. (2010). "Soluble LILRA3, a potential natural antiinflammatory protein, is increased in patients with rheumatoid arthritis and is tightly regulated by interleukin 10, tumor necrosis factor-alpha, and interferon-gamma." *J Rheumatol* **37**(8): 1596-1606.
- Andoniadou, C. L., M. Signore, et al. (2011). "HESX1- and TCF3-mediated repression of Wnt/beta-catenin targets is required for normal development of the anterior forebrain." *Development* **138**(22): 4931-4942.
- Baban, B., A. M. Hansen, et al. (2005). "A minor population of splenic dendritic cells expressing CD19 mediates IDO-dependent T cell suppression via type I IFN signaling following B7 ligation." *Int Immunol* **17**(7): 909-919.
- Ball, H. J., H. J. Yuasa, et al. (2009). "Indoleamine 2,3-dioxygenase-2; a new enzyme in the kynurenine pathway." *Int J Biochem Cell Biol* **41**(3): 467-471.
- Ballinger, M. N., D. M. Aronoff, et al. (2006). "Critical role of prostaglandin E2 overproduction in impaired pulmonary host response following bone marrow transplantation." *J Immunol* **177**(8): 5499-5508.
- Banchereau, J., F. Briere, et al. (2000). "Immunobiology of dendritic cells." *Annu Rev Immunol* **18**: 767-811.
- Bancroft, G. J., R. D. Schreiber, et al. (1991). "Natural immunity: a T-cell-independent pathway of macrophage activation, defined in the scid mouse." *Immunol Rev* **124**: 5-24.
- Barr, S. D., J. R. Smiley, et al. (2008). "The interferon response inhibits HIV particle production by induction of TRIM22." *PLoS Pathog* **4**(2): e1000007.
- Beltan, E., L. Horgen, et al. (2000). "Secretion of cytokines by human macrophages upon infection by pathogenic and non-pathogenic mycobacteria." *Microb Pathog* **28**(5): 313-318.
- Benoit, M., B. Desnues, et al. (2008). "Macrophage polarization in bacterial infections." *J Immunol* **181**(6): 3733-3739.
- Beyer, M., M. R. Mallmann, et al. (2012). "High-resolution transcriptome of human macrophages." *PLoS One* **7**(9): e45466.
- Birkness, K. A., J. Guarner, et al. (2007). "An in vitro model of the leukocyte interactions associated with granuloma formation in *Mycobacterium tuberculosis* infection." *Immunol Cell Biol* **85**(2): 160-168.

- Biswas, S. K. and A. Mantovani (2010). "Macrophage plasticity and interaction with lymphocyte subsets: cancer as a paradigm." *Nat Immunol* **11**(10): 889-896.
- Blander, J. M. and L. E. Sander (2012). "Beyond pattern recognition: five immune checkpoints for scaling the microbial threat." *Nat Rev Immunol* **12**(3): 215-225.
- Blengio, F., F. Raggi, et al. (2012). "The hypoxic environment reprograms the cytokine/chemokine expression profile of human mature dendritic cells." *Immunobiology*.
- Bloom, B. R. and B. Bennett (1970). "Macrophages and delayed-type hypersensitivity." *Semin Hematol* **7**(2): 215-224.
- Blumenthal, A., G. Nagalingam, et al. (2012). "M. tuberculosis induces potent activation of IDO-1, but this is not essential for the immunological control of infection." *PLoS One* **7**(5): e37314.
- Bode, J. G., C. Ehltling, et al. (2012). "The macrophage response towards LPS and its control through the p38(MAPK)-STAT3 axis." *Cell Signal* **24**(6): 1185-1194.
- Bonizzi, G. and M. Karin (2004). "The two NF-kappaB activation pathways and their role in innate and adaptive immunity." *Trends Immunol* **25**(6): 280-288.
- Boonstra, A., R. Rajsbaum, et al. (2006). "Macrophages and myeloid dendritic cells, but not plasmacytoid dendritic cells, produce IL-10 in response to MyD88- and TRIF-dependent TLR signals, and TLR-independent signals." *J Immunol* **177**(11): 7551-7558.
- Bozza, F. A., J. I. Salluh, et al. (2007). "Cytokine profiles as markers of disease severity in sepsis: a multiplex analysis." *Crit Care* **11**(2): R49.
- Bukreyev, A., I. M. Belyakov, et al. (2001). "Granulocyte-macrophage colony-stimulating factor expressed by recombinant respiratory syncytial virus attenuates viral replication and increases the level of pulmonary antigen-presenting cells." *J Virol* **75**(24): 12128-12140.
- Byrne, G. I., L. K. Lehmann, et al. (1986). "Induction of tryptophan catabolism is the mechanism for gamma-interferon-mediated inhibition of intracellular Chlamydia psittaci replication in T24 cells." *Infect Immun* **53**(2): 347-351.
- Campbell, P. A., B. P. Canono, et al. (2001). "Measurement of bacterial ingestion and killing by macrophages." *Curr Protoc Immunol* **Chapter 14**: Unit 14 16.
- Carr, K. D., A. N. Sieve, et al. (2011). "Specific depletion reveals a novel role for neutrophil-mediated protection in the liver during Listeria monocytogenes infection." *Eur J Immunol* **41**(9): 2666-2676.
- Cavaillon, J. M. (2011). "The historical milestones in the understanding of leukocyte biology initiated by Elie Metchnikoff." *J Leukoc Biol* **90**(3): 413-424.
- Cella, M., A. Engering, et al. (1997). "Inflammatory stimuli induce accumulation of MHC class II complexes on dendritic cells." *Nature* **388**(6644): 782-787.
- Chakravorty, D. and M. Hensel (2003). "Inducible nitric oxide synthase and control of intracellular bacterial pathogens." *Microbes Infect* **5**(7): 621-627.
- Chan, M. M. and A. R. Moore (2010). "Resolution of inflammation in murine autoimmune arthritis is disrupted by cyclooxygenase-2 inhibition and restored by prostaglandin E2-mediated lipoxin A4 production." *J Immunol* **184**(11): 6418-6426.
- Chang, E. Y., B. Guo, et al. (2007). "Cutting edge: involvement of the type I IFN production and signaling pathway in lipopolysaccharide-induced IL-10 production." *J Immunol* **178**(11): 6705-6709.
- Chen, G., M. H. Shaw, et al. (2009). "NOD-like receptors: role in innate immunity and inflammatory disease." *Annu Rev Pathol* **4**: 365-398.
- Chung, D. J., M. Rossi, et al. (2009). "Indoleamine 2,3-dioxygenase-expressing mature human monocyte-derived dendritic cells expand potent autologous regulatory T cells." *Blood* **114**(3): 555-563.
- Collart, M. A., D. Belin, et al. (1986). "Gamma interferon enhances macrophage transcription of the tumor necrosis factor/cachectin, interleukin 1, and urokinase genes, which are controlled by short-lived repressors." *J Exp Med* **164**(6): 2113-2118.

- Conter, M., A. Vergara, et al. (2010). "Polymorphism of actA gene is not related to in vitro virulence of *Listeria monocytogenes*." *Int J Food Microbiol* **137**(1): 100-105.
- Cossart, P., J. Pizarro-Cerda, et al. (2003). "Invasion of mammalian cells by *Listeria monocytogenes*: functional mimicry to subvert cellular functions." *Trends Cell Biol* **13**(1): 23-31.
- Dannenbergh, A. M., Jr. (1993). "Immunopathogenesis of pulmonary tuberculosis." *Hosp Pract (Off Ed)* **28**(1): 51-58.
- Davis, J. M. and L. Ramakrishnan (2009). "The role of the granuloma in expansion and dissemination of early tuberculous infection." *Cell* **136**(1): 37-49.
- De Smedt, T., M. Van Mechelen, et al. (1997). "Effect of interleukin-10 on dendritic cell maturation and function." *Eur J Immunol* **27**(5): 1229-1235.
- Deckert, M., S. Soltek, et al. (2001). "Endogenous interleukin-10 is required for prevention of a hyperinflammatory intracerebral immune response in *Listeria monocytogenes* meningoencephalitis." *Infect Immun* **69**(7): 4561-4571.
- Deng, T., X. Feng, et al. (2012). "Toll-like receptor 3 activation differentially regulates phagocytosis of bacteria and apoptotic neutrophils by mouse peritoneal macrophages." *Immunol Cell Biol*.
- Diamond, M. S. and M. Farzan (2013). "The broad-spectrum antiviral functions of IFIT and IFITM proteins." *Nat Rev Immunol* **13**(1): 46-57.
- Divanovic, S., N. M. Sawtell, et al. (2012). "Opposing biological functions of tryptophan catabolizing enzymes during intracellular infection." *J Infect Dis* **205**(1): 152-161.
- Domann, E., J. Wehland, et al. (1992). "A novel bacterial virulence gene in *Listeria monocytogenes* required for host cell microfilament interaction with homology to the proline-rich region of vinculin." *EMBO J* **11**(5): 1981-1990.
- Doyen, V., M. Rubio, et al. (2003). "Thrombospondin 1 is an autocrine negative regulator of human dendritic cell activation." *J Exp Med* **198**(8): 1277-1283.
- Driesen, J., A. Popov, et al. (2008). "CD25 as an immune regulatory molecule expressed on myeloid dendritic cells." *Immunobiology* **213**(9-10): 849-858.
- Duffy, M. M., J. Pindjakova, et al. (2011). "Mesenchymal stem cell inhibition of T-helper 17 cell-differentiation is triggered by cell-cell contact and mediated by prostaglandin E2 via the EP4 receptor." *Eur J Immunol* **41**(10): 2840-2851.
- Edelson, B. T., T. R. Bradstreet, et al. (2011). "CD8alpha(+) dendritic cells are an obligate cellular entry point for productive infection by *Listeria monocytogenes*." *Immunity* **35**(2): 236-248.
- Edelson, B. T. and E. R. Unanue (2002). "MyD88-dependent but Toll-like receptor 2-independent innate immunity to *Listeria*: no role for either in macrophage listericidal activity." *J Immunol* **169**(7): 3869-3875.
- Ehlers, S. (2005). "Tumor necrosis factor and its blockade in granulomatous infections: differential modes of action of infliximab and etanercept?" *Clin Infect Dis* **41 Suppl 3**: S199-203.
- Ehrchen, J. M., C. Sunderkotter, et al. (2009). "The endogenous Toll-like receptor 4 agonist S100A8/S100A9 (calprotectin) as innate amplifier of infection, autoimmunity, and cancer." *J Leukoc Biol* **86**(3): 557-566.
- Ekuni, D., J. D. Firth, et al. (2009). "Lipopolysaccharide-induced epithelial monoamine oxidase mediates alveolar bone loss in a rat chronic wound model." *Am J Pathol* **175**(4): 1398-1409.
- Elkington, P., T. Shiomi, et al. (2011). "MMP-1 drives immunopathology in human tuberculosis and transgenic mice." *J Clin Invest* **121**(5): 1827-1833.
- Fallarino, F., U. Grohmann, et al. (2002). "T cell apoptosis by tryptophan catabolism." *Cell Death Differ* **9**(10): 1069-1077.
- Farnsworth, A., A. S. Flaman, et al. (2010). "Acetaminophen modulates the transcriptional response to recombinant interferon-beta." *PLoS One* **5**(6): e11031.

- Fernald, G. H., S. Knott, et al. (2007). "Genome-wide network analysis reveals the global properties of IFN-beta immediate transcriptional effects in humans." *J Immunol* **178**(8): 5076-5085.
- Fiorentino, D. F., A. Zlotnik, et al. (1991). "IL-10 inhibits cytokine production by activated macrophages." *J Immunol* **147**(11): 3815-3822.
- Fleetwood, A. J., T. Lawrence, et al. (2007). "Granulocyte-macrophage colony-stimulating factor (CSF) and macrophage CSF-dependent macrophage phenotypes display differences in cytokine profiles and transcription factor activities: implications for CSF blockade in inflammation." *J Immunol* **178**(8): 5245-5252.
- Fleming, B. D. and D. M. Mosser (2011). "Regulatory macrophages: setting the threshold for therapy." *Eur J Immunol* **41**(9): 2498-2502.
- Franchi, L., R. Munoz-Planillo, et al. (2012). "Sensing and reacting to microbes through the inflammasomes." *Nat Immunol* **13**(4): 325-332.
- Freitag, N. E., G. C. Port, et al. (2009). "Listeria monocytogenes - from saprophyte to intracellular pathogen." *Nat Rev Microbiol* **7**(9): 623-628.
- Freitag, N. E., L. Rong, et al. (1993). "Regulation of the prfA transcriptional activator of Listeria monocytogenes: multiple promoter elements contribute to intracellular growth and cell-to-cell spread." *Infect Immun* **61**(6): 2537-2544.
- Fujigaki, H., K. Saito, et al. (2006). "Nitration and inactivation of IDO by peroxynitrite." *J Immunol* **176**(1): 372-379.
- Gallucci, S. and P. Matzinger (2001). "Danger signals: SOS to the immune system." *Curr Opin Immunol* **13**(1): 114-119.
- Ganesh, K., A. Das, et al. (2012). "Prostaglandin E(2) induces oncostatin M expression in human chronic wound macrophages through Axl receptor tyrosine kinase pathway." *J Immunol* **189**(5): 2563-2573.
- Gazzinelli, R. T., M. Wysocka, et al. (1996). "In the absence of endogenous IL-10, mice acutely infected with Toxoplasma gondii succumb to a lethal immune response dependent on CD4+ T cells and accompanied by overproduction of IL-12, IFN-gamma and TNF-alpha." *J Immunol* **157**(2): 798-805.
- Geiss, G. K., V. S. Carter, et al. (2003). "Gene expression profiling of the cellular transcriptional network regulated by alpha/beta interferon and its partial attenuation by the hepatitis C virus nonstructural 5A protein." *J Virol* **77**(11): 6367-6375.
- Genin, P., A. Vaccaro, et al. (2009). "The role of differential expression of human interferon--a genes in antiviral immunity." *Cytokine Growth Factor Rev* **20**(4): 283-295.
- Gerber, J. S. and D. M. Mosser (2001). "Stimulatory and inhibitory signals originating from the macrophage Fcgamma receptors." *Microbes Infect* **3**(2): 131-139.
- Glaser, P., L. Frangeul, et al. (2001). "Comparative genomics of Listeria species." *Science* **294**(5543): 849-852.
- Gomez, P. F., M. H. Pillinger, et al. (2005). "Resolution of inflammation: prostaglandin E2 dissociates nuclear trafficking of individual NF-kappaB subunits (p65, p50) in stimulated rheumatoid synovial fibroblasts." *J Immunol* **175**(10): 6924-6930.
- Gordon, S. and P. R. Taylor (2005). "Monocyte and macrophage heterogeneity." *Nat Rev Immunol* **5**(12): 953-964.
- Gray, M. L. and A. H. Killinger (1966). "Listeria monocytogenes and listeric infections." *Bacteriol Rev* **30**(2): 309-382.
- Gregory, S. H., L. P. Cousens, et al. (2002). "Complementary adhesion molecules promote neutrophil-Kupffer cell interaction and the elimination of bacteria taken up by the liver." *J Immunol* **168**(1): 308-315.
- Guillemin, G. J., D. G. Smith, et al. (2003). "Expression of the kynurenine pathway enzymes in human microglia and macrophages." *Adv Exp Med Biol* **527**: 105-112.

- Hamilton, J. A. (2008). "Colony-stimulating factors in inflammation and autoimmunity." Nat Rev Immunol **8**(7): 533-544.
- Harris, S. G. and R. P. Phipps (2002). "Prostaglandin D(2), its metabolite 15-d-PGJ(2), and peroxisome proliferator activated receptor-gamma agonists induce apoptosis in transformed, but not normal, human T lineage cells." Immunology **105**(1): 23-34.
- Hartmann, E., B. Wollenberg, et al. (2003). "Identification and functional analysis of tumor-infiltrating plasmacytoid dendritic cells in head and neck cancer." Cancer Res **63**(19): 6478-6487.
- Harty, J. T. and M. J. Bevan (1995). "Specific immunity to *Listeria monocytogenes* in the absence of IFN gamma." Immunity **3**(1): 109-117.
- Herbert, D. R., C. Holscher, et al. (2004). "Alternative macrophage activation is essential for survival during schistosomiasis and downmodulates T helper 1 responses and immunopathology." Immunity **20**(5): 623-635.
- Hernandez-Pando, R., H. Orozco, et al. (2000). "Treatment with BB-94, a broad spectrum inhibitor of zinc-dependent metalloproteinases, causes deviation of the cytokine profile towards type-2 in experimental pulmonary tuberculosis in Balb/c mice." Int J Exp Pathol **81**(3): 199-209.
- Heseler, K., K. Spekker, et al. (2008). "Antimicrobial and immunoregulatory effects mediated by human lung cells: role of IFN-gamma-induced tryptophan degradation." FEMS Immunol Med Microbiol **52**(2): 273-281.
- Higashitani, K., T. Kanto, et al. (2012). "Association of enhanced activity of indoleamine 2,3-dioxygenase in dendritic cells with the induction of regulatory T cells in chronic hepatitis C infection." J Gastroenterol.
- Higgins, D. M., J. Sanchez-Campillo, et al. (2008). "Relative levels of M-CSF and GM-CSF influence the specific generation of macrophage populations during infection with *Mycobacterium tuberculosis*." J Immunol **180**(7): 4892-4900.
- Hilkens, C. M., A. Snijders, et al. (1996). "Modulation of T-cell cytokine secretion by accessory cell-derived products." Eur Respir J Suppl **22**: 90s-94s.
- Hoffmann, J. A., F. C. Kafatos, et al. (1999). "Phylogenetic perspectives in innate immunity." Science **284**(5418): 1313-1318.
- Howard, M. and W. E. Paul (1983). "Regulation of B-cell growth and differentiation by soluble factors." Annu Rev Immunol **1**: 307-333.
- Huang, J. T., J. S. Welch, et al. (1999). "Interleukin-4-dependent production of PPAR-gamma ligands in macrophages by 12/15-lipoxygenase." Nature **400**(6742): 378-382.
- Hucke, C., C. R. MacKenzie, et al. (2004). "Nitric oxide-mediated regulation of gamma interferon-induced bacteriostasis: inhibition and degradation of human indoleamine 2,3-dioxygenase." Infect Immun **72**(5): 2723-2730.
- Hutchinson, J. A., P. Riquelme, et al. (2011). "Cutting Edge: Immunological consequences and trafficking of human regulatory macrophages administered to renal transplant recipients." J Immunol **187**(5): 2072-2078.
- Inaba, K., M. Inaba, et al. (1992). "Generation of large numbers of dendritic cells from mouse bone marrow cultures supplemented with granulocyte/macrophage colony-stimulating factor." J Exp Med **176**(6): 1693-1702.
- Iwasaki, A. and R. Medzhitov (2010). "Regulation of adaptive immunity by the innate immune system." Science **327**(5963): 291-295.
- Izzo, A. A., L. S. Izzo, et al. (2004). "A matrix metalloproteinase inhibitor promotes granuloma formation during the early phase of *Mycobacterium tuberculosis* pulmonary infection." Tuberculosis (Edinb) **84**(6): 387-396.
- Janeway, C., Jr. and R. Medzhitov (2000). "Viral interference with IL-1 and toll signaling." Proc Natl Acad Sci U S A **97**(20): 10682-10683.

- Janeway, C. A., Jr. and R. Medzhitov (2002). "Innate immune recognition." *Annu Rev Immunol* **20**: 197-216.
- Jenkins, S. J., D. Ruckerl, et al. (2011). "Local macrophage proliferation, rather than recruitment from the blood, is a signature of TH2 inflammation." *Science* **332**(6035): 1284-1288.
- Jenner, R. G. and R. A. Young (2005). "Insights into host responses against pathogens from transcriptional profiling." *Nat Rev Microbiol* **3**(4): 281-294.
- Jonuleit, H., E. Schmitt, et al. (2000). "Induction of interleukin 10-producing, nonproliferating CD4(+) T cells with regulatory properties by repetitive stimulation with allogeneic immature human dendritic cells." *J Exp Med* **192**(9): 1213-1222.
- Joseph, B., K. Przybilla, et al. (2006). "Identification of *Listeria monocytogenes* genes contributing to intracellular replication by expression profiling and mutant screening." *J Bacteriol* **188**(2): 556-568.
- Kalinski, P. (2012). "Regulation of immune responses by prostaglandin E2." *J Immunol* **188**(1): 21-28.
- Kalinski, P., C. M. Hilkens, et al. (1997). "IL-12-deficient dendritic cells, generated in the presence of prostaglandin E2, promote type 2 cytokine production in maturing human naive T helper cells." *J Immunol* **159**(1): 28-35.
- Kalinski, P., P. L. Vieira, et al. (2001). "Prostaglandin E(2) is a selective inducer of interleukin-12 p40 (IL-12p40) production and an inhibitor of bioactive IL-12p70 heterodimer." *Blood* **97**(11): 3466-3469.
- Kawai, T. and S. Akira (2006). "TLR signaling." *Cell Death Differ* **13**(5): 816-825.
- Keane, J., S. Gershon, et al. (2001). "Tuberculosis associated with infliximab, a tumor necrosis factor alpha-neutralizing agent." *N Engl J Med* **345**(15): 1098-1104.
- Kemp, T. J., B. D. Elzey, et al. (2003). "Plasmacytoid dendritic cell-derived IFN-alpha induces TNF-related apoptosis-inducing ligand/Apo-2L-mediated antitumor activity by human monocytes following CpG oligodeoxynucleotide stimulation." *J Immunol* **171**(1): 212-218.
- Kernbauer, E., V. Maier, et al. (2012). "Conditional Stat1 ablation reveals the importance of interferon signaling for immunity to *Listeria monocytogenes* infection." *PLoS Pathog* **8**(6): e1002763.
- Kessler-Becker, D., S. Smola, et al. (2004). "High plasminogen activator inhibitor type 2 expression is a hallmark of scleroderma fibroblasts in vitro." *Exp Dermatol* **13**(11): 708-714.
- Kessler, M., J. Zielecki, et al. (2012). "Chlamydia trachomatis disturbs epithelial tissue homeostasis in fallopian tubes via paracrine Wnt signaling." *Am J Pathol* **180**(1): 186-198.
- Khallou-Laschet, J., A. Varthaman, et al. (2010). "Macrophage plasticity in experimental atherosclerosis." *PLoS One* **5**(1): e8852.
- Klein, I., J. C. Cornejo, et al. (2007). "Kupffer cell heterogeneity: functional properties of bone marrow derived and sessile hepatic macrophages." *Blood* **110**(12): 4077-4085.
- Knubel, C. P., F. F. Martinez, et al. (2011). "3-Hydroxy kynurenine treatment controls *T. cruzi* replication and the inflammatory pathology preventing the clinical symptoms of chronic Chagas disease." *PLoS One* **6**(10): e26550.
- Knubel, C. P., F. F. Martinez, et al. (2010). "Indoleamine 2,3-dioxygenase (IDO) is critical for host resistance against *Trypanosoma cruzi*." *FASEB J* **24**(8): 2689-2701.
- Kobayashi, K. S., M. Chamillard, et al. (2005). "Nod2-dependent regulation of innate and adaptive immunity in the intestinal tract." *Science* **307**(5710): 731-734.
- Krausgruber, T., K. Blazek, et al. (2011). "IRF5 promotes inflammatory macrophage polarization and TH1-TH17 responses." *Nat Immunol* **12**(3): 231-238.
- Kurihara, T., G. Warr, et al. (1997). "Defects in macrophage recruitment and host defense in mice lacking the CCR2 chemokine receptor." *J Exp Med* **186**(10): 1757-1762.
- Lacey, D. C., A. Achuthan, et al. (2012). "Defining GM-CSF- and macrophage-CSF-dependent macrophage responses by in vitro models." *J Immunol* **188**(11): 5752-5765.

- Lang, R., D. Patel, et al. (2002). "Shaping gene expression in activated and resting primary macrophages by IL-10." *J Immunol* **169**(5): 2253-2263.
- Lawrence, T. and D. W. Gilroy (2007). "Chronic inflammation: a failure of resolution?" *Int J Exp Pathol* **88**(2): 85-94.
- Lawrence, T. and G. Natoli (2011). "Transcriptional regulation of macrophage polarization: enabling diversity with identity." *Nat Rev Immunol* **11**(11): 750-761.
- Leber, J. H., G. T. Crimmins, et al. (2008). "Distinct TLR- and NLR-mediated transcriptional responses to an intracellular pathogen." *PLoS Pathog* **4**(1): e6.
- Legler, D. F., P. Krause, et al. (2006). "Prostaglandin E2 is generally required for human dendritic cell migration and exerts its effect via EP2 and EP4 receptors." *J Immunol* **176**(2): 966-973.
- Lenzo, J. C., A. L. Turner, et al. (2012). "Control of macrophage lineage populations by CSF-1 receptor and GM-CSF in homeostasis and inflammation." *Immunol Cell Biol* **90**(4): 429-440.
- Lindqvist, C. A., L. H. Christiansson, et al. (2010). "T regulatory cells control T-cell proliferation partly by the release of soluble CD25 in patients with B-cell malignancies." *Immunology* **131**(3): 371-376.
- Loughman, J. A. and D. A. Hunstad (2012). "Induction of indoleamine 2,3-dioxygenase by uropathogenic bacteria attenuates innate responses to epithelial infection." *J Infect Dis* **205**(12): 1830-1839.
- Lutz, M. B., N. A. Kukutsch, et al. (2000). "Culture of bone marrow cells in GM-CSF plus high doses of lipopolysaccharide generates exclusively immature dendritic cells which induce alloantigen-specific CD4 T cell anergy in vitro." *Eur J Immunol* **30**(4): 1048-1052.
- Lutz, M. B. and G. Schuler (2002). "Immature, semi-mature and fully mature dendritic cells: which signals induce tolerance or immunity?" *Trends Immunol* **23**(9): 445-449.
- Macey, M. G. (2007). *Flow cytometry principles and applications*, Humana Press.
- Mackness, G. B. (1962). "Cellular resistance to infection." *J Exp Med* **116**: 381-406.
- MacKenzie, C. R., U. Hadding, et al. (1998). "Interferon-gamma-induced activation of indoleamine 2,3-dioxygenase in cord blood monocyte-derived macrophages inhibits the growth of group B streptococci." *J Infect Dis* **178**(3): 875-878.
- MacKenzie, C. R., D. Worku, et al. (2003). "Regulation of IDO-mediated bacteriostasis in macrophages: role of antibiotics and anti-inflammatory agents." *Adv Exp Med Biol* **527**: 67-76.
- Mackler, A. M., E. M. Barber, et al. (2003). "Indoleamine 2,3-dioxygenase is regulated by IFN-gamma in the mouse placenta during *Listeria monocytogenes* infection." *J Immunol* **170**(2): 823-830.
- Magalhaes, E. S., C. N. Paiva, et al. (2009). "Macrophage migration inhibitory factor is critical to interleukin-5-driven eosinophilopoiesis and tissue eosinophilia triggered by *Schistosoma mansoni* infection." *FASEB J* **23**(4): 1262-1271.
- Makala, L. H., B. Baban, et al. (2011). "Leishmania major attenuates host immunity by stimulating local indoleamine 2,3-dioxygenase expression." *J Infect Dis* **203**(5): 715-725.
- Manicassamy, S. and B. Pulendran (2011). "Dendritic cell control of tolerogenic responses." *Immunol Rev* **241**(1): 206-227.
- Mantovani, A., A. Sica, et al. (2004). "The chemokine system in diverse forms of macrophage activation and polarization." *Trends Immunol* **25**(12): 677-686.
- Marquis, H., H. G. Bouwer, et al. (1993). "Intracytoplasmic growth and virulence of *Listeria monocytogenes* auxotrophic mutants." *Infect Immun* **61**(9): 3756-3760.
- Martens, S. and J. Howard (2006). "The interferon-inducible GTPases." *Annu Rev Cell Dev Biol* **22**: 559-589.
- Martinez, F. O., S. Gordon, et al. (2006). "Transcriptional profiling of the human monocyte-to-macrophage differentiation and polarization: new molecules and patterns of gene expression." *J Immunol* **177**(10): 7303-7311.

- Martinez, F. O., L. Helming, et al. (2009). "Alternative activation of macrophages: an immunologic functional perspective." *Annu Rev Immunol* **27**: 451-483.
- McGuirk, P., C. McCann, et al. (2002). "Pathogen-specific T regulatory 1 cells induced in the respiratory tract by a bacterial molecule that stimulates interleukin 10 production by dendritic cells: a novel strategy for evasion of protective T helper type 1 responses by *Bordetella pertussis*." *J Exp Med* **195**(2): 221-231.
- Mellor, A. L. and D. H. Munn (2004). "IDO expression by dendritic cells: tolerance and tryptophan catabolism." *Nat Rev Immunol* **4**(10): 762-774.
- Mengaud, J., C. Braun-Breton, et al. (1991). "Identification of phosphatidylinositol-specific phospholipase C activity in *Listeria monocytogenes*: a novel type of virulence factor?" *Mol Microbiol* **5**(2): 367-372.
- Merad, M., M. G. Manz, et al. (2002). "Langerhans cells renew in the skin throughout life under steady-state conditions." *Nat Immunol* **3**(12): 1135-1141.
- Mezrich, J. D., J. H. Fechner, et al. (2010). "An interaction between kynurenine and the aryl hydrocarbon receptor can generate regulatory T cells." *J Immunol* **185**(6): 3190-3198.
- Minty, A., P. Chalon, et al. (1993). "Interleukin-13 is a new human lymphokine regulating inflammatory and immune responses." *Nature* **362**(6417): 248-250.
- Moldenhauer, L. M., S. N. Keenihan, et al. (2010). "GM-CSF is an essential regulator of T cell activation competence in uterine dendritic cells during early pregnancy in mice." *J Immunol* **185**(11): 7085-7096.
- Mook, P., B. Patel, et al. (2011). "Risk factors for mortality in non-pregnancy-related listeriosis." *Epidemiol Infect*: 1-10.
- Moore, K. W., R. de Waal Malefyt, et al. (2001). "Interleukin-10 and the interleukin-10 receptor." *Annu Rev Immunol* **19**: 683-765.
- Moss, E. G. (2001). "RNA interference: it's a small RNA world." *Curr Biol* **11**(19): R772-775.
- Mosser, D. M. (2003). "The many faces of macrophage activation." *J Leukoc Biol* **73**(2): 209-212.
- Mosser, D. M. and J. P. Edwards (2008). "Exploring the full spectrum of macrophage activation." *Nat Rev Immunol* **8**(12): 958-969.
- Mraheil, M. A., A. Billion, et al. (2011). "Adaptation of *Listeria monocytogenes* to oxidative and nitrosative stress in IFN-gamma-activated macrophages." *Int J Med Microbiol* **301**(7): 547-555.
- Munn, D. H. and A. L. Mellor (2004). "IDO and tolerance to tumors." *Trends Mol Med* **10**(1): 15-18.
- Munn, D. H., M. Zhou, et al. (1998). "Prevention of allogeneic fetal rejection by tryptophan catabolism." *Science* **281**(5380): 1191-1193.
- Murai, M., P. Krause, et al. (2010). "Regulatory T-cell stability and plasticity in mucosal and systemic immune systems." *Mucosal Immunol* **3**(5): 443-449.
- Murray, P. J. and T. A. Wynn (2011). "Protective and pathogenic functions of macrophage subsets." *Nat Rev Immunol* **11**(11): 723-737.
- Muthuswamy, R., J. Mueller-Berghaus, et al. (2010). "PGE(2) transiently enhances DC expression of CCR7 but inhibits the ability of DCs to produce CCL19 and attract naive T cells." *Blood* **116**(9): 1454-1459.
- Narui, K., N. Noguchi, et al. (2009). "Anti-infectious activity of tryptophan metabolites in the L-tryptophan-L-kynurenine pathway." *Biol Pharm Bull* **32**(1): 41-44.
- Nathan, C. F., H. W. Murray, et al. (1983). "Identification of interferon-gamma as the lymphokine that activates human macrophage oxidative metabolism and antimicrobial activity." *J Exp Med* **158**(3): 670-689.
- Natoli, G. (2010). "Maintaining cell identity through global control of genomic organization." *Immunity* **33**(1): 12-24.
- Nau, G. J., J. F. Richmond, et al. (2002). "Human macrophage activation programs induced by bacterial pathogens." *Proc Natl Acad Sci U S A* **99**(3): 1503-1508.



- Neuenhahn, M., K. M. Kerksiek, et al. (2006). "CD8alpha+ dendritic cells are required for efficient entry of *Listeria monocytogenes* into the spleen." *Immunity* **25**(4): 619-630.
- Nickol, A. D. and P. F. Bonventre (1977). "Anomalous high native resistance to athymic mice to bacterial pathogens." *Infect Immun* **18**(3): 636-645.
- O'Reilly, M., D. E. Newcomb, et al. (1999). "Endotoxin, sepsis, and the primrose path." *Shock* **12**(6): 411-420.
- O'Shea, J. J. and P. J. Murray (2008). "Cytokine signaling modules in inflammatory responses." *Immunity* **28**(4): 477-487.
- Oberdorfer, C., O. Adams, et al. (2003). "Role of IDO activation in anti-microbial defense in human native astrocytes." *Adv Exp Med Biol* **527**: 15-26.
- Onomoto, K., S. Morimoto, et al. (2011). "Dysregulation of IFN system can lead to poor response to pegylated interferon and ribavirin therapy in chronic hepatitis C." *PLoS One* **6**(5): e19799.
- Pallotta, M. T., C. Orabona, et al. (2011). "Indoleamine 2,3-dioxygenase is a signaling protein in long-term tolerance by dendritic cells." *Nat Immunol* **12**(9): 870-878.
- Pamer, E. G. (2004). "Immune responses to *Listeria monocytogenes*." *Nat Rev Immunol* **4**(10): 812-823.
- Pfefferkorn, E. R. (1984). "Interferon gamma blocks the growth of *Toxoplasma gondii* in human fibroblasts by inducing the host cells to degrade tryptophan." *Proc Natl Acad Sci U S A* **81**(3): 908-912.
- Pichlmair, A. and C. Reis e Sousa (2007). "Innate recognition of viruses." *Immunity* **27**(3): 370-383.
- Pixley, F. J. and E. R. Stanley (2004). "CSF-1 regulation of the wandering macrophage: complexity in action." *Trends Cell Biol* **14**(11): 628-638.
- Plain, K. M., K. de Silva, et al. (2011). "Indoleamine 2,3-dioxygenase, tryptophan catabolism, and *Mycobacterium avium* subsp. *paratuberculosis*: a model for chronic mycobacterial infections." *Infect Immun* **79**(9): 3821-3832.
- Popov, A., Z. Abdullah, et al. (2006). "Indoleamine 2,3-dioxygenase-expressing dendritic cells form suppurative granulomas following *Listeria monocytogenes* infection." *J Clin Invest* **116**(12): 3160-3170.
- Popov, A., J. Driesen, et al. (2008). "Infection of myeloid dendritic cells with *Listeria monocytogenes* leads to the suppression of T cell function by multiple inhibitory mechanisms." *J Immunol* **181**(7): 4976-4988.
- Porta, C., M. Rimoldi, et al. (2009). "Tolerance and M2 (alternative) macrophage polarization are related processes orchestrated by p50 nuclear factor kappaB." *Proc Natl Acad Sci U S A* **106**(35): 14978-14983.
- Raes, G., R. Van den Bergh, et al. (2005). "Arginase-1 and Ym1 are markers for murine, but not human, alternatively activated myeloid cells." *J Immunol* **174**(11): 6561; author reply 6561-6562.
- Ramakrishnan, L. (2012). "Revisiting the role of the granuloma in tuberculosis." *Nat Rev Immunol* **12**(5): 352-366.
- Randolph, G. J., J. Ochando, et al. (2008). "Migration of dendritic cell subsets and their precursors." *Annu Rev Immunol* **26**: 293-316.
- Rani, R., M. B. Jordan, et al. (2012). "IFN-gamma-driven IDO production from macrophages protects IL-4Ralpha-deficient mice against lethality during *Schistosoma mansoni* infection." *Am J Pathol* **180**(5): 2001-2008.
- Rayamajhi, M., J. Humann, et al. (2010). "Induction of IFN- $\alpha$  enables *Listeria monocytogenes* to suppress macrophage activation by IFN- $\gamma$ ." *J Exp Med* **207**(2): 327-337.
- Reis e Sousa, C. (2006). "Dendritic cells in a mature age." *Nat Rev Immunol* **6**(6): 476-483.

- Robb, R. J. and R. M. Kutny (1987). "Structure-function relationships for the IL 2-receptor system. IV. Analysis of the sequence and ligand-binding properties of soluble Tac protein." *J Immunol* **139**(3): 855-862.
- Roffe, E., A. G. Rothfuchs, et al. (2012). "IL-10 limits parasite burden and protects against fatal myocarditis in a mouse model of *Trypanosoma cruzi* infection." *J Immunol* **188**(2): 649-660.
- Rothe, J., W. Lesslauer, et al. (1993). "Mice lacking the tumour necrosis factor receptor 1 are resistant to TNF-mediated toxicity but highly susceptible to infection by *Listeria monocytogenes*." *Nature* **364**(6440): 798-802.
- Sakai, H., I. Okafuji, et al. (2012). "The CD40-CD40L axis and IFN-gamma play critical roles in Langhans giant cell formation." *Int Immunol* **24**(1): 5-15.
- Sallusto, F., M. Cella, et al. (1995). "Dendritic cells use macropinocytosis and the mannose receptor to concentrate macromolecules in the major histocompatibility complex class II compartment: downregulation by cytokines and bacterial products." *J Exp Med* **182**(2): 389-400.
- Sallusto, F. and A. Lanzavecchia (1994). "Efficient presentation of soluble antigen by cultured human dendritic cells is maintained by granulocyte/macrophage colony-stimulating factor plus interleukin 4 and downregulated by tumor necrosis factor alpha." *J Exp Med* **179**(4): 1109-1118.
- Sanchez-Sanchez, N., L. Riol-Blanco, et al. (2006). "The multiple personalities of the chemokine receptor CCR7 in dendritic cells." *J Immunol* **176**(9): 5153-5159.
- Sander, L. E., M. J. Davis, et al. (2011). "Detection of prokaryotic mRNA signifies microbial viability and promotes immunity." *Nature* **474**(7351): 385-389.
- Satoh, T., O. Takeuchi, et al. (2010). "The Jmjd3-Irf4 axis regulates M2 macrophage polarization and host responses against helminth infection." *Nat Immunol* **11**(10): 936-944.
- Sauer, J. D., K. Sotelo-Troha, et al. (2011). "The N-ethyl-N-nitrosourea-induced Goldenticket mouse mutant reveals an essential function of Sting in the in vivo interferon response to *Listeria monocytogenes* and cyclic dinucleotides." *Infect Immun* **79**(2): 688-694.
- Scandella, E., Y. Men, et al. (2002). "Prostaglandin E2 is a key factor for CCR7 surface expression and migration of monocyte-derived dendritic cells." *Blood* **100**(4): 1354-1361.
- Schaefer, M. (2009). Charakterisierung von regulatorischen Makrophagen und ihre Beziehung zu klassisch und alternativ aktivierten Makrophagen im humanen System, Rheinischen Friedrich-Wilhelms-Universität Bonn.
- Schmidt, S. V., A. C. Nino-Castro, et al. (2012). "Regulatory dendritic cells: there is more than just immune activation." *Front Immunol* **3**: 274.
- Schnupf, P. and D. A. Portnoy (2007). "Listeriolysin O: a phagosome-specific lysin." *Microbes Infect* **9**(10): 1176-1187.
- Schroder, K., P. J. Hertzog, et al. (2004). "Interferon-gamma: an overview of signals, mechanisms and functions." *J Leukoc Biol* **75**(2): 163-189.
- Schroder, W. A., T. T. Le, et al. (2010). "A physiological function of inflammation-associated SerpinB2 is regulation of adaptive immunity." *J Immunol* **184**(5): 2663-2670.
- Schulz, C., E. Gomez Perdiguero, et al. (2012). "A lineage of myeloid cells independent of Myb and hematopoietic stem cells." *Science* **336**(6077): 86-90.
- Seki, E., H. Tsutsui, et al. (2002). "Critical roles of myeloid differentiation factor 88-dependent proinflammatory cytokine release in early phase clearance of *Listeria monocytogenes* in mice." *J Immunol* **169**(7): 3863-3868.
- Serbina, N. V., T. P. Salazar-Mather, et al. (2003). "TNF/iNOS-producing dendritic cells mediate innate immune defense against bacterial infection." *Immunity* **19**(1): 59-70.
- Seveau, S., J. Pizarro-Cerda, et al. (2007). "Molecular mechanisms exploited by *Listeria monocytogenes* during host cell invasion." *Microbes Infect* **9**(10): 1167-1175.

- Shaughnessy, L. M. and J. A. Swanson (2007). "The role of the activated macrophage in clearing *Listeria monocytogenes* infection." *Front Biosci* **12**: 2683-2692.
- Shen, Y., I. Kawamura, et al. (2010). "Toll-like receptor 2- and MyD88-dependent phosphatidylinositol 3-kinase and Rac1 activation facilitates the phagocytosis of *Listeria monocytogenes* by murine macrophages." *Infect Immun* **78**(6): 2857-2867.
- Sica, A. and A. Mantovani (2012). "Macrophage plasticity and polarization: in vivo veritas." *J Clin Invest* **122**(3): 787-795.
- Siewe, L., M. Bollati-Fogolin, et al. (2006). "Interleukin-10 derived from macrophages and/or neutrophils regulates the inflammatory response to LPS but not the response to CpG DNA." *Eur J Immunol* **36**(12): 3248-3255.
- Silk, B. J. and B. E. Mahon (2011). "Comment on "Listeriosis in human pregnancy: a systematic review"." *J Perinat Med* **39**(6): 749-750.
- Silva Miranda, M., A. Breiman, et al. (2012). "The tuberculous granuloma: an unsuccessful host defence mechanism providing a safety shelter for the bacteria?" *Clin Dev Immunol* **2012**: 139127.
- Sindrilaru, A., T. Peters, et al. (2011). "An unrestrained proinflammatory M1 macrophage population induced by iron impairs wound healing in humans and mice." *J Clin Invest* **121**(3): 985-997.
- Sonderregger, F. L., Y. Ma, et al. (2012). "Localized production of IL-10 suppresses early inflammatory cell infiltration and subsequent development of IFN-gamma-mediated Lyme arthritis." *J Immunol* **188**(3): 1381-1393.
- Souza, A. L., E. Roffe, et al. (2005). "Potential role of the chemokine macrophage inflammatory protein 1alpha in human and experimental schistosomiasis." *Infect Immun* **73**(4): 2515-2523.
- Stavrum, R., H. Valvatne, et al. (2012). "Mycobacterium tuberculosis Mce1 protein complex initiates rapid induction of transcription of genes involved in substrate trafficking." *Genes Immun* **13**(6): 496-502.
- Steinman, R. M. and Z. A. Cohn (1973). "Identification of a novel cell type in peripheral lymphoid organs of mice. I. Morphology, quantitation, tissue distribution." *J Exp Med* **137**(5): 1142-1162.
- Stetson, D. B. and R. Medzhitov (2006). "Recognition of cytosolic DNA activates an IRF3-dependent innate immune response." *Immunity* **24**(1): 93-103.
- Stritzker, J., J. Janda, et al. (2004). "Growth, virulence, and immunogenicity of *Listeria monocytogenes* aro mutants." *Infect Immun* **72**(10): 5622-5629.
- Sugimoto, H., S. Oda, et al. (2006). "Crystal structure of human indoleamine 2,3-dioxygenase: catalytic mechanism of O<sub>2</sub> incorporation by a heme-containing dioxygenase." *Proc Natl Acad Sci U S A* **103**(8): 2611-2616.
- Swaminathan, B. and P. Gerner-Smidt (2007). "The epidemiology of human listeriosis." *Microbes Infect* **9**(10): 1236-1243.
- Szanto, A., B. L. Balint, et al. (2010). "STAT6 transcription factor is a facilitator of the nuclear receptor PPARgamma-regulated gene expression in macrophages and dendritic cells." *Immunity* **33**(5): 699-712.
- Takayama, K., G. Garcia-Cardena, et al. (2002). "Prostaglandin E2 suppresses chemokine production in human macrophages through the EP4 receptor." *J Biol Chem* **277**(46): 44147-44154.
- Takeda, K. and S. Akira (2004). "TLR signaling pathways." *Semin Immunol* **16**(1): 3-9.
- Takeda, K., B. E. Clausen, et al. (1999). "Enhanced Th1 activity and development of chronic enterocolitis in mice devoid of Stat3 in macrophages and neutrophils." *Immunity* **10**(1): 39-49.
- Takeda, K., T. Kaisho, et al. (2003). "Toll-like receptors." *Annu Rev Immunol* **21**: 335-376.
- Takeuchi, O. and S. Akira (2009). "Innate immunity to virus infection." *Immunol Rev* **227**(1): 75-86.

- Tassiulas, I., X. Hu, et al. (2004). "Amplification of IFN-alpha-induced STAT1 activation and inflammatory function by Syk and ITAM-containing adaptors." *Nat Immunol* **5**(11): 1181-1189.
- Taylor, J. L., J. M. Hattle, et al. (2006). "Role for matrix metalloproteinase 9 in granuloma formation during pulmonary Mycobacterium tuberculosis infection." *Infect Immun* **74**(11): 6135-6144.
- Terness, P., T. M. Bauer, et al. (2002). "Inhibition of allogeneic T cell proliferation by indoleamine 2,3-dioxygenase-expressing dendritic cells: mediation of suppression by tryptophan metabolites." *J Exp Med* **196**(4): 447-457.
- Theofilopoulos, A. N., R. Baccala, et al. (2005). "Type I interferons (alpha/beta) in immunity and autoimmunity." *Annu Rev Immunol* **23**: 307-336.
- Thomas, S. R., A. C. Terentis, et al. (2007). "Post-translational regulation of human indoleamine 2,3-dioxygenase activity by nitric oxide." *J Biol Chem* **282**(33): 23778-23787.
- Toller, I. M., I. Hitzler, et al. (2010). "Prostaglandin E2 prevents Helicobacter-induced gastric preneoplasia and facilitates persistent infection in a mouse model." *Gastroenterology* **138**(4): 1455-1467, 1467 e1451-1454.
- Tripp, C. S., M. K. Gately, et al. (1994). "Neutralization of IL-12 decreases resistance to Listeria in SCID and C.B-17 mice. Reversal by IFN-gamma." *J Immunol* **152**(4): 1883-1887.
- Unanue, E. R. and J. A. Carrero (2012). "Studies with Listeria monocytogenes lead the way." *Adv Immunol* **113**: 1-5.
- Vance, R. E., R. R. Isberg, et al. (2009). "Patterns of pathogenesis: discrimination of pathogenic and nonpathogenic microbes by the innate immune system." *Cell Host Microbe* **6**(1): 10-21.
- Vazquez, N., S. Rekka, et al. (2012). "Modulation of Innate Host Factors by Mycobacterium avium Complex in Human Macrophages Includes Interleukin 17." *J Infect Dis* **206**(8): 1206-1217.
- Velten, F. W., F. Rambow, et al. (2007). "Enhanced T-cell activation and T-cell-dependent IL-2 production by CD83+, CD25high, CD43high human monocyte-derived dendritic cells." *Mol Immunol* **44**(7): 1544-1550.
- Vermi, W., R. Bonecchi, et al. (2003). "Recruitment of immature plasmacytoid dendritic cells (plasmacytoid monocytes) and myeloid dendritic cells in primary cutaneous melanomas." *Journal of Pathology* **200**(2): 255-268.
- Verreck, F. A., T. de Boer, et al. (2004). "Human IL-23-producing type 1 macrophages promote but IL-10-producing type 2 macrophages subvert immunity to (myco)bacteria." *Proc Natl Acad Sci U S A* **101**(13): 4560-4565.
- Vila-del Sol, V., C. Punzon, et al. (2008). "IFN-gamma-induced TNF-alpha expression is regulated by interferon regulatory factors 1 and 8 in mouse macrophages." *J Immunol* **181**(7): 4461-4470.
- von Bergwelt-Baildon, M. S., A. Popov, et al. (2006). "CD25 and indoleamine 2,3-dioxygenase are up-regulated by prostaglandin E2 and expressed by tumor-associated dendritic cells in vivo: additional mechanisms of T-cell inhibition." *Blood* **108**(1): 228-237.
- Waddell, S. J., S. J. Popper, et al. (2010). "Dissecting interferon-induced transcriptional programs in human peripheral blood cells." *PLoS One* **5**(3): e9753.
- Werling, D., J. C. Hope, et al. (2004). "Differential production of cytokines, reactive oxygen and nitrogen by bovine macrophages and dendritic cells stimulated with Toll-like receptor agonists." *Immunology* **111**(1): 41-52.
- Williams, L., L. Bradley, et al. (2004). "Signal transducer and activator of transcription 3 is the dominant mediator of the anti-inflammatory effects of IL-10 in human macrophages." *J Immunol* **172**(1): 567-576.
- Witte, C. E., K. A. Archer, et al. (2012). "Innate immune pathways triggered by Listeria monocytogenes and their role in the induction of cell-mediated immunity." *Adv Immunol* **113**: 135-156.

- Wong, S. C., A. L. Puaux, et al. (2010). "Macrophage polarization to a unique phenotype driven by B cells." *Eur J Immunol* **40**(8): 2296-2307.
- Wood, K. J., A. Bushell, et al. (2012). "Regulatory immune cells in transplantation." *Nat Rev Immunol* **12**(6): 417-430.
- Woodruff, P. G., H. A. Boushey, et al. (2007). "Genome-wide profiling identifies epithelial cell genes associated with asthma and with treatment response to corticosteroids." *Proc Natl Acad Sci U S A* **104**(40): 15858-15863.
- Woodward, J. J., A. T. Iavarone, et al. (2010). "c-di-AMP secreted by intracellular *Listeria monocytogenes* activates a host type I interferon response." *Science* **328**(5986): 1703-1705.
- Wuest, S. J., M. Crucet, et al. (2012). "Expression and regulation of 12/15-lipoxygenases in human primary macrophages." *Atherosclerosis* **225**(1): 121-127.
- Wurtzel, O., N. Sesto, et al. (2012). "Comparative transcriptomics of pathogenic and non-pathogenic *Listeria* species." *Mol Syst Biol* **8**: 583.
- Wynn, T. A. (2003). "IL-13 effector functions." *Annu Rev Immunol* **21**: 425-456.
- Xanthoulea, S., M. Pasparakis, et al. (2004). "Tumor necrosis factor (TNF) receptor shedding controls thresholds of innate immune activation that balance opposing TNF functions in infectious and inflammatory diseases." *J Exp Med* **200**(3): 367-376.
- Yamamoto, S. and O. Hayaishi (1967). "Tryptophan pyrrolase of rabbit intestine. D- and L-tryptophan-cleaving enzyme or enzymes." *J Biol Chem* **242**(22): 5260-5266.
- Yang, P., H. An, et al. (2010). "The cytosolic nucleic acid sensor LRRFIP1 mediates the production of type I interferon via a beta-catenin-dependent pathway." *Nat Immunol* **11**(6): 487-494.
- Ylostalo, J. H., T. J. Bartosh, et al. (2012). "Human Mesenchymal Stem/Stromal Cells (hMSCs) Cultured as Spheroids are Self-activated to Produce Prostaglandin E2 (PGE2) that Directs Stimulated Macrophages into an Anti-inflammatory Phenotype." *Stem Cells*.
- Yuasa, H. J., M. Takubo, et al. (2007). "Evolution of vertebrate indoleamine 2,3-dioxygenases." *J Mol Evol* **65**(6): 705-714.
- Zhou, J., P. C. Tang, et al. (2010). "CXCR3-dependent accumulation and activation of perivascular macrophages is necessary for homeostatic arterial remodeling to hemodynamic stresses." *J Exp Med* **207**(9): 1951-1966.
- Zou, W., J. H. Kim, et al. (2007). "Microarray analysis reveals that Type I interferon strongly increases the expression of immune-response related genes in Ubp43 (*Usp18*) deficient macrophages." *Biochem Biophys Res Commun* **356**(1): 193-199.

# Curriculum Vitae

**Andrea Cecilia Niño Castro**

## PERSONAL INFORMATION

## EDUCATION

Magister in Biochemistry, Universidad Nacional de Colombia. 2004-2007.

B.A. in Biology. Universidad Nacional de Colombia. 1998- 2003

## PUBLICATIONS

Nino-Castro A, Abdullah A, Popov A, Thabet Y, Beyer M, Knolle P, Domann E, Chakraborty T, Schmidt S, Schultze JL. The IDO1-induced kynurenines play major role in the antimicrobial effect of human myeloid cells against *Listeria monocytogenes*. Submitted to *Innate immunity*.

Beyer M, Mallmann MR, Xue J, Staratschek-Jox A, Vorholt D, Krebs W, Sommer D, Sander J, Mertens C, **Nino-Castro A**, Schmidt SV & Schultze JL. *High-Resolution Transcriptome of Human Macrophages*. *PLoS ONE* **7**: e45466 (2012)

Schmidt SV, **Nino-Castro A** & Schultze JL. *Regulatory dendritic cells: there is more than just immune activation*. *Front. Immunol.* **3**: 274 (2012)

Abdullah Z, Geiger S, **Nino-Castro A**, Böttcher JP, Muraliv E, Gaidt M, Schildberg FA, Riethausen K, Flossdorf J, Krebs W, Chakraborty T, Kurts C, Schultze JL, Knolle PA & Klotz L. *Lack of PPAR $\gamma$  in myeloid cells confers resistance to *Listeria monocytogenes* infection*. *PLoS ONE* **7**: e37349 (2012)

Hoyos M, **Niño A**, Camargo M, Días JC, León S & Camacho M. *Separation of Leishmania-infected macrophages by step-SPLITT fractionation*. J. Chromatogr. B. **877**: 3712 (2009)

M. Camacho M, Forero ME, Fajardo C, **Niño A** & Morales P. *Leishmania amazonensis infection may affect the ability of the host macrophage to be activated by altering their outward potassium currents*. Exp. Parasitol. **120**: 50 (2008)

**Niño A** & Camacho M. *Leishmania (Viannia) braziliensis growth in vitro culture relies more on folic acid availability than Leishmania (Leishmania) amazonensis*. Memorias do Instituto Oswaldo Cruz. **100**: 309 (2005)